



DEPARTMENT OF CIVIL, CHEMICAL, ENVIRONMENTAL AND MATERIALS ENGINEERING (DICAM) INSTITUTE FOR ECOPRENEURSHIP (IEC)

Second Cycle - Double Degree Program

HYBRID MOVING BED BIOFILM REACTOR UNDER DIFFERENT CONDITIONS FOR INCREASED DICLOFENAC REMOVAL FROM WASTEWATER

Dissertation in Environmental Engineering

Supervisors Defended by

Prof. Dr. Michael Thomann

Prof. Dr. Fabio Fava

Matteo Rizzato

Co-Supervisors

Prof. Dr. Dario Frascari Bartosz Kawecki

Graduation Session: October 6, 2025

Academic Year: 2024/2025

Abstract

Pharmaceutical micropollutants, such as diclofenac (DCF), are mainly released through civil wastewater. Since conventional wastewater treatment plants (WWTPs) cannot fully degrade them, these compounds may be discharged into aquatic ecosystems, posing environmental risks due to their biological activity and potential harm to aquatic organisms. Stringent regulations, including Switzerland's Water Protection Ordinance (Waters Protection Ordinance (WPO), 1998, which limits DCF concentrations in surface waters to 0.05 μ g L⁻¹, and the new EU Directive (Directive (EU) 2024/3019 concerning urban wastewater treatment, 2024 requiring at least 80% removal for certain pharmaceuticals, emphasize the need for advanced treatment solutions. This thesis investigates a pilot-scale Hybrid Moving Bed Biofilm Reactor (HMBBR) as a retrofittable, biologically-based technology for enhanced DCF removal, focusing on whether clean carriers can develop biofilms under real civil wastewater conditions and how sludge retention time (SRT) influences early-stage biofilm growth and DCF elimination.

A three-line pilot plant was operated continuously with real wastewater under SRTs of 2, 3, and 5 days. Complementary batch tests were conducted to evaluate DCF degradation by carrier-attached biofilms and to compare their performance with suspended activated sludge from the pilot plant and full-scale WWTPs. It is hypothesized that shorter SRTs promote rapid biofilm colonization on clean carriers, enhancing early-stage DCF removal, and that carrier-attached biofilm contributes more to degradation than suspended biomass.

Results indicate that Line 1, operated at a 2-day SRT, achieved DCF removal of up to 80%, while Lines 2 and 3 reached 74% and 71%, respectively. Batch tests confirm that carrier-attached biofilms have higher degradation capacity than activated sludge alone. These findings support the hypothesis that HMBBRs with clean carriers can be used to start up a plant without relying on pre-colonized carriers, and suggest that biological treatments like HMBBRs can provide an effective strategy for DCF removal, as also demonstrated by Jewell et al. (2016).

Acknowledgments

I would like to sincerely thank my supervisor, Prof. Dr. Michael Thomann, for his guidance, helpful advice, and for sharing his knowledge throughout this work. I am very grateful for the opportunity to carry out my thesis under his supervision and to be part of his research group. I also thank Prof. Dr. Fabio Fava from the University of Bologna for making it possible for me

to participate in the double-degree program, and Prof. Dr. Dario Frascari for agreeing to serve as an expert for this thesis.

I am especially thankful to Bartosz Kawecki for his close guidance and for teaching me how to approach research with care and rigor. His support in data interpretation and modeling was very important for this study.

Thanks go to all members of the UWT group for their support in the laboratory. In particular, Roman Schäfer, Patrik Eckert, and Sebastian Hedwig helped greatly with organizing and running the pilot plant. I also thank Philipp Meier for his work on the plant layout, Luca Loreggian for sharing his experience, and my desk colleague Enrico Temellini for his constant support and advice. Special thanks to Benjamin Gygax and Albin Sofjani for their help with diclofenac analysis, which was essential, especially under tight deadlines.

I would like to thank the WWTPs in Bad Ragaz, Lenzburg, and Roderstorf for providing samples and introducing me to their facilities. I am also grateful to Raphael Stolz for providing the clean carriers used in this study.

Special thanks to the workshop team, especially Pavel Dagorov, for always providing the tools and technical help needed to build and improve the pilot plant.

Finally, I am deeply thankful to my family, Angela, and my new and old friends for their constant encouragement and support. Their care and belief in me gave me the strength to face challenges and enjoy this experience.

With the knowledge and skills gained through this work, I hope to continue in environmental engineering and contribute to protecting our planet. Caring for the environment is both a scientific challenge and a responsibility we all share.

Declaration of Authenticity

I hereby declare

- that I have written this performance record independently and on my own;
- that I have correctly cited all text passages not originating from myself according to common scientific citation rules and that I have clearly mentioned the sources used;
- that I have declared in an index all aids used (e.g. AI tools such as chatbots [e.g. ChatGPT], translation/paraphrasing tools) or programming applications [e.g. Github Copilot] and have indicated their use;
- that I have acquired all intangible rights to any materials I may have used, such as images or graphics, or that these materials were created by me;
- that the topic, the paper or parts of it have not been used in a performance record of another module, unless this has been expressly agreed with the lecturer in advance and is indicated in the paper;
- that I am aware that my work may be checked for plagiarism and for third-party authorship of human or technical origin (artificial intelligence);
- that I am aware that the School of Life Sciences FHNW will pursue a violation of this declaration of authenticity or its underlying obligations of the study and examination regulations of the School of Life Sciences FHNW and that disciplinary consequences (reprimand or expulsion from the study program) may result.

Basel, 08.09.2025

Patrant

Contents

1	Intr	roduction	1	
2	Ma	terial and Methods	9	
2.1 Pilot Plant				
		2.1.1 Operational Conditions and Monitored Parameters	19	
	2.2	Modeling Approaches	22	
		2.2.1 ASM3 Modeling Framework	22	
		2.2.2 Kinetic Models for Diclofenac Elimination	23	
		2.2.3 Simulation of Diclofenac Behaviour in Pilot Reactors	24	
	2.3	Tracer Experiment	25	
	2.4	Batch Test Setup	26	
		2.4.1 Nitrification Experiments	27	
		2.4.2 Diclofenac Removal Experiments	28	
	2.5	Analytics	29	
		2.5.1 Reagents and Analytical Equipment	29	
		2.5.2 Monitoring of Standard Parameters	30	
		2.5.3 Determination of Carrier-Attached Biomass	32	
		2.5.4 Fluorescence Microscopy for Biofilm Observation	33	
		2.5.5 Diclofenac Concentrations	33	
3	Res	sults and Discussion	35	
	3.1	Performance of the Pilot Plant	36	
		3.1.1 Standard Parameters	36	
		3.1.2 ASM3 Simulations	39	
		3.1.3 Biofilm Development in Relation to SRT	40	
	3.2	Tracer Experiment	42	
	3.3	Batch Tests	44	
		3.3.1 Nitrification Performance	44	
		3.3.2 Diclofenac Removal	45	
	3.4	Diclofenac Removal in the Pilot Plant	51	
		3.4.1 Simulations	51	
		3.4.2 Continuous Flow Conditions	51	
4	Cor	nclusion	53	
	4.1	Key Findings	54	

4.2 Future Developments	55
Bibliography	56
Appendix	61
A Calculations	61
A.1 Ammonium Dosage for Batch Tests	61
A.2 Nitrification for batch Tests	61
A.3 Coagulant Dosage for the Pilot Plant	62
A.4 Tracer Concentration	62
A.5 PH Adjustment Solutions	63
A.6 Diclofenac Dosage in Batch Tests and Pilot Plant	63
A.7 Area-Normalized Diclofenac Biodegradation	65
B Project Planning	67
C Operational Challenges During Pilot Plant Operation	70
D Standard Operating Procedure (SOP) for LC-MS Analysis	72
E Risk Assessment	81
F Laboratory and Operational Logbook (LVO)	98

List of Figures

Figure 1.0.1 -	- Molecular structure of diclofenac ($C_{14}H_{11}Cl_2NO_2$) (Vieno & Sillanpää, 2014).	2
Figure 1.0.2 -	Possible Formation of TPs from Diclofenac (Jewell et al., 2016). This figure	
	illustrates the formation of transformation products (TPs) from Diclofenac	
	(DCF). The arrows indicate pathways of transformation. Abbreviations used	
	for the postulated reaction types are: [m] mono-oxygenation, [o] oxidation	
	(dehydrogenation), [a] amidation, [d] decarboxylation, [s] sulfate conjuga-	
	tion, [r] ring-opening reactions, [c] reductive dechlorination, [h] amide hy-	
	drolysis.	3
Figure 1.0.3 -	-General schematic diagram of a HMBBR (Leyva-Díaz et al., 2017)	6
Figure 2.1.1 -	-P&ID layout of the pilot plant (PP) with three lines	11
	General view of the pilot plant (PP)	12
Figure 2.1.3 -	-Front view of MBBR reactor, position of the aeration stone and conseguent	
	movement of the carriers.	15
Figure 2.1.4 -	Overview of the pilot plant in the PTC during operations.	19
Figure 2.1.5 -	Sampling points across the pilot plant	22
Figure 2.2.1 -	Process diagram of the simulated biological wastewater treatment plant in	
	$SIMBA^{\#}$, showing the main components, volumes, and flow rates of the three	
	treatment lines.	23
Figure 2.4.1 -	-Map of Switzerland with the locations of the Wastewater Treatment Plants	
	(WWTPs) and the Pilot plant used for batch tests (Swiss Confederation &	
	swisstopo, 2025).	27
Figure 2.4.2 -	-Batch test setup for diclofenac removal experiments. In the picture Carriers	
	from full-scale plants were used: from left to right, Roderstorf, Lenzburg,	
	and Bad Ragaz.	29
Figure 2.5.1 -	-Biomass-attached versus cleaned carriers from left to right: Real Plants	
	(Lenzburg, Bad Ragaz, Roderstorf) and the Pilot Plant (Line 1, Line 2,	
	Line 3).	33
Figure 3.1.1 -	-Time series of total suspended solids (TSS), phosphorus concentration, dis-	
	solved oxygen concentration, and chemical oxygen demand (COD) measured	
	in the reactors over the experimental period	37
Figure 3.1.2 -	-Time series of nitrogen species: total nitrogen (TN), ammonium (NH_4^+) ,	
	nitrate (NO_3^-) , and nitrite (NO_2^-) concentrations in influent and effluents	
	over the experimental period.	38
Figure 3.1.3 -	Time series of MBBR reactor temperature and pH in influent, sludge, and	
	MBBR effluent over the experimental period.	39

Figure 3.1.4 -	-Comparison of biomass attached on carriers from pilot-scale and full-scale	
	systems. Biofilm Chip M is shown, with live ecosystems highlighted in green.	
	The full-scale WWTP carriers show a well-stratified and thicker biomass	
	layer, whereas the pilot plant carriers exhibit a thinner biofilm	41
Figure 3.2.1 -	Breakthrough curves from tracer experiments for each pilot plant line (Line	
	1, Line 2, and Line 3), comparing measured tracer concentrations against	
	theoretical profiles for the Sludge 1, Sludge 2, and MBBR reactor sections.	
	The data illustrates the residence time distribution (RTD) and hydraulic	
	behavior of each reactor.	43
Figure 3.3.1 -	-Nitrate production during batch tests for the three pilot plant lines. Linear	
	models: Line 1 $(y = 0.64x + 0.12, R^2 = 0.96)$, Line 2 $(y = 0.46x + 0.06,$	
	$R^2 = 0.98$), and Line 3 ($y = 0.20x + 0.006$, $R^2 = 0.99$)	45
Figure 3.3.2 -	-Diclofenac degradation kinetics for activated sludge from three different WWTP	's.
	The plot show normalized DCF concentrations over time fitted with pseudo-	
	first-order degradation models (Section 2.2.2)	46
Figure 3.3.3 -	Diclofenac degradation kinetics for carriers from three full-scale WWTPs.	
	Normalized DCF concentrations over time are fitted with pseudo-first-order	
	degradation models (Section 2.2.2).	47
Figure 3.3.4 -	Diclofenac degradation kinetics for the three lines from the Pilot Plant. Nor-	
	malized DCF concentrations over time were fitted with pseudo-first-order	
	degradation models (Section 2.2.2).	49
Figure 3.4.1 -	Temporal profiles of diclofenac (DCF) concentrations in the wastewater treat-	
	ment system. The left graph shows modelled values using literature kinetic	
	constants for reactors S1 and S2, the MBBR, and the clarifier. The right	
	graph shows estimated values based on experimental data	52
T: D 0 1		0.7
	-Gantt chart of the project timeline	67
	-Inventory of materials and equipment.	68
Figure B.0.3	-Laboratory analysis plan	69
Figure C.0.1	Overview of operational issues encountered in the pilot plant: a) Stop of	
0 1 2 212	the main pump before start-up; b) Temporary shutdown of the main plant	
	causing pH drop; c) Clogs and stuck carriers in the MBBR and sludge; d)	
	Floating gludge accumulation in the clariform	71

List of Tables

Table 1.0.1 –	- Physico-chemical properties of diclofenac (Vieno & Sillanpää, 2014)	4
Table 1.0.2 –	- Estimated cost and micropollutant removal efficiency for different treatment	
	technologies (Matos et al., 2019)	7
m 11 0 1 1		10
	Overview of flows and pump setup.	13
	Overview over the Reactors and Containers used	13
	List of other components used	13
Table 2.1.4 –	- Carriers technical information	15
Table 2.1.5 –	Operational parameters of the pilot plant.	20
Table 2.1.6 –	- Influent wastewater characterization.	20
Table 2.2.1 -	- Model parameters used for simulating DCF concentration profiles in the pilot	
	plant under continuous-flow conditions. Identical parameters are reported	
	once; kinetic constants differ between batch-test and literature values	25
Table 2.3.1 -	Calibration Curve Measurements for Lines 1, 2, and 3.	26
Table 2.3.2 -	- Calibration Curve Parameters for each Line, following $Y = \text{Slope} \cdot X + \text{Intercept}$.	26
Table 2.4.1 -	Carriers Technical Information (Z. Zhang et al., 2022).	27
Table 2.5.1 –	Overview of the main devices used in the laboratory	29
Table 2.5.2 –	Overview of all test-kits used in the laboratory	30
Table 2.5.3 –	Overview of chemical compounds used in the laboratory	30
Table 2.5.4 -	Overview over important consumables used in the laboratory	30
Table 2.5.5 -	- Retention times, MS1 and MS2 m/z ratios of precursor and fragment ions,	
	as well as detection of DCF in LC-MS/MS measurement	34
	· · · · · · · · · · · · · · · · · · ·	
Table 3.1.1 –	Predicted activated sludge and nutrient concentrations in the MBBR reactors	
	(influent to the reactors).	40
Table 3.1.2 –	Predicted effluent concentrations for the three simulated lines (ASM3 only).	40
Table 3.3.1 –	Nitrification rates of carriers in the pilot plant lines derived from batch tests.	
	The rates R_v are normalized by the estimated surface area of the carriers,	
	allowing comparison with literature-reported surface-related nitrification rates.	45
Table 3.3.2 –	Summary of measured and literature values for X_{TSS} and K_{biol} from sludge	
	batch tests.	46
Table 3.3.3 –	Measured and literature values for X_{TSS} , K_{biol} , and area-normalized K_{biol}	
	from real WWTP carrier batch tests.	48
Table 3.3.4 -	Measured values for X_{TSS} , K_{biol} , and area-normalized K_{biol} from Pilot Plant	
	Carriers Batch Tests.	49
Table 3.4.1 -	Diclofenac removal efficiencies under continuous-flow conditions at different	
	influent concentrations	52

List of Abbreviations

Abbreviation	Meaning
AOB	Ammonia-Oxidizing Bacteria
AO	Anaerobic/Oxic
AS	Activated Sludge
A.S.	Analytical Standard
С	Carbon
CBZ	Carbamazepine
Cl	Chlorine
cm	centimetre
CO_2	Carbon Dioxide
COD	Chemical Oxygen Demand
C-OMP	Conventional Organic Micropollutant
d	Diameter or day
DCF	Diclofenac
DO	Dissolved Oxygen
DOC	Dissolved Organic Carbon
DSVI	Diluted Sludge Volume Index
E-OMP	Emerging Organic Micropollutant
EU	European Union
g	gram
GSchV	Water Protection Ordinance
h	hour
H	Hydrogen
HMBBR	Hybrid Moving Bed Biofilm Reactor
HRT	Hydraulic Retention Time
IEC	Institute for Ecopreneurship
IFAS	Integrated Fixed-film Activated Sludge
kg	kilogram
kW	kilowatt
Kubuk	Name of FHNW Building
$L \min^{-1}$	litre per minute
LC-MS	Liquid Chromatography-Mass Spectrometry
LOD	Limit of Detection
LOQ	Limit of Quantification
LVO	Laboratory and Operational Logbook
$\mathrm{m}^3\mathrm{d}^{\text{-}1}$	cubic metre per day
mg	milligram
$ m mgL^{-1}$	milligram per litre
min	minute

MLE Modified Ludzack-Ettinger MBBR Moving Bed Biofilm Reactor

MBR Membrane Bioreactor

mm millimetre

mS cm⁻¹ milliSiemens per centimetre

N Nitrogen ng nanogram NH_4^+ Ammonium nm nanometre NO_2^- Nitrite NO_3^- Nitrate

NOB Nitrite-Oxidizing Bacteria

 O_2 Oxygen

OMP Organic Micropollutant

ORP Oxidation-Reduction Potential

P Phosphorous

PAC Powdered Activated Carbon

PE Population Equivalent

pH pH

PP Pilot Plant

PTC Process Technology Centre
RAS Returned Activated Sludge
RBC Rotating Biological Contactor
RTD Residence Time Distribution

s Second S Sulphur

SC Secondary Clarifier

SND Simultaneous Nitrification-Denitrification

SOP Standard Operating Procedure

SRT Solid Retention Time SVI Sludge Volume Index SMX Sulfamethoxazole

TDS Total Dissolved Solids

TDP Total Dissolved Phosphorus

TOC Total Organic Carbon

TP Total Phosphorus

TS Total Solids

TSS Total Suspended Solids

T-OMP Total Organic Micropollutant
UASB Upflow Anaerobic Sludge Blanket

 $\begin{array}{cc} \text{UV} & \text{Ultraviolet} \\ \mu \text{g} & \text{microgram} \end{array}$

 $\mu \mathrm{g}\,\mathrm{L}^{\text{-}1}$ microgram per litre

 $\,\mu{\rm m}$ micrometre

VSS Volatile Suspended Solids WAS Waste Activated Sludge

WW Wastewater

WWTP Wastewater Treatment Plant

XA Autotrophic Bacteria XH Heterotrophic Bacteria

°C Degree Celsius

List of AI and Software Tools

The following section provides a summary of all artificial intelligence and software tools used throughout this thesis. While these tools are not explicitly mentioned in every paragraph, this summary reflects their application and importance in the research, analysis, and writing process.

Artificial Intelligence Tools

This thesis project utilized several artificial intelligence tools as productivity and writing aids. The primary tools included **ChatGPT** (**OpenAI**), **Perplexity**, **Gemini**, and **Paper Digest**. Their main uses were:

- Brainstorming initial ideas for the theoretical framework.
- Refining the stylistic quality of the text.
- Assisting in proofreading.
- Providing suggestions for language refinement and text structuring.
- Troubleshooting in R and Latex code.
- Summarizing scientific literature (Paper Digest).
- Supporting literature search and answering research questions (*Perplexity, Gemini*).

Importantly, these AI tools did not generate any of the core research, arguments, or data analysis. All scholarly ideas, interpretations of sources, and conclusions are the sole product of the author, with all sources independently verified and cited.

Software Tools

The following software tools were essential during the development of this thesis:

- RStudio for data processing, statistical analysis, and visualization.
- Excel for organizing datasets, preliminary calculations, and tabular presentations.
- PowerPoint for preparing and structuring thesis presentations.
- Latex for typesetting the manuscript, ensuring professional formatting and reference management.
- **Zotero** for collecting, organizing, and citing references efficiently.
- Simba for ASM3 modeling.
- Fusion for 3D drawing and design project.

The combination of these tools significantly supported the research process, improved efficiency, and contributed to the clear presentation of the results.

Chapter 1

Introduction

This chapter introduces the challenge of micropollutants in wastewater, with a focus on diclofenac due to its widespread occurrence, continuous input, and incomplete removal in conventional treatment processes. It reviews current regulatory frameworks and highlights the limitations of conventional treatment technologies in eliminating such contaminants. The chapter then presents hybrid biological treatment systems, including moving bed bioreactors combined with activated sludge, as promising alternatives. Finally, it defines the aim of the study and formulates the research questions that guide the experimental and modeling investigations presented in this thesis.

Micropollutants in Wastewater

Micropollutants, also known as contaminants of emerging concern (CECs) or trace organic contaminants, are a diverse group of synthetic or naturally occurring substances present in water at very low concentrations, typically ranging from nanograms per liter ($\mu g L^{-1}$) to micrograms per liter ($\mu g L^{-1}$) (Schwarzenbach et al., 2006). These compounds encompass a wide array of chemical classes, including pharmaceuticals, personal care products, pesticides, industrial chemicals, and hormones. Despite their small concentrations, many micropollutants are biologically active and can exert adverse effects on aquatic organisms and potentially human health. These effects are primarily associated with compounds that exhibit environmental persistence, the potential for bioaccumulation in food chains, or endocrine disrupting properties (Bonvin et al., 2016). Their widespread presence in natural aquatic systems across Europe is a growing environmental concern, impacting water quality and organisms even at trace levels, with findings also noted in drinking water resources in Switzerland (Wittmer et al., 2014). The recalcitrant nature of many of these compounds to conventional wastewater treatment processes means they are continuously discharged into the environment, necessitating advanced treatment solutions (Eggen et al., 2014).

Diclofenac

Diclofenac (DCF) is a widely used non-steroidal anti-inflammatory drug (NSAID), globally recognized for its potent analysis and anti-inflammatory properties. The molecular structure of diclofenac ($C_{14}H_{11}Cl_2NO_2$) is presented in Figure [1.0.1], and its physico-chemical properties are detailed in Table [1.0.1]. Due to its extensive consumption and incomplete metabolism in the human body, a significant portion of administered DCF is excreted and subsequently detected in municipal wastewater.

Figure 1.0.1: Molecular structure of diclofenac (C₁₄H₁₁Cl₂NO₂) (Vieno & Sillanpää, 2014).

Diclofenac poses significant environmental risks due to its potential hazard to aquatic organisms and the low removal efficiency of conventional treatment processes. Even at trace concentrations in the microgram per liter range, it can cause severe harm to aquatic organisms, such as kidney and liver damage in fish ("Quality Criteria for Surface Waters", 2020; Vieno & Sillanpää, 2014). To protect aquatic ecosystems, Switzerland has established a stringent environmental quality standard (EQS) of $0.05\,\mu\mathrm{g}\,\mathrm{L}^{-1}$ for diclofenac in surface waters. This standard requires that treated wastewater effluent, after dilution in receiving bodies, remains below this concentration.

Meeting this limit is challenging because diclofenac's physico-chemical properties make it difficult to remove through conventional activated sludge (AS) treatment, which forms the backbone

of most wastewater treatment plants (WWTPs). Although diclofenac is moderately hydrophobic with a logKow of 4.51, its relatively low logKd values (ranging from 1.2 to 2.7) indicate that it does not readily adsorb to sludge particles. As a result, diclofenac remains mostly dissolved in the water phase and passes through AS systems with removal rates typically between 0 and 30% (Kawecki & Thomann, 2024) Linge et al., 2015). Additionally, its pKa of 4.15 means that at neutral pH, diclofenac exists primarily as a negatively charged ion, which further reduces its affinity for the negatively charged sludge surfaces. This combination of properties explains its persistence in treated wastewater.

Beyond its persistence, diclofenac can undergo biotransformation in wastewater treatment systems, leading to the formation of various transformation products (TPs) (Alvarino et al., 2018; Jewell et al., 2016). The presence of these TPs complicates the accurate detection and quantification of DCF, as conventional analytical methods may not capture all relevant metabolites. Therefore, advanced techniques such as LC–MS/MS or high-resolution mass spectrometry are required to reliably monitor both DCF and its TPs (Gómez-Maldonado et al., 2021) (Figure 1.0.2).

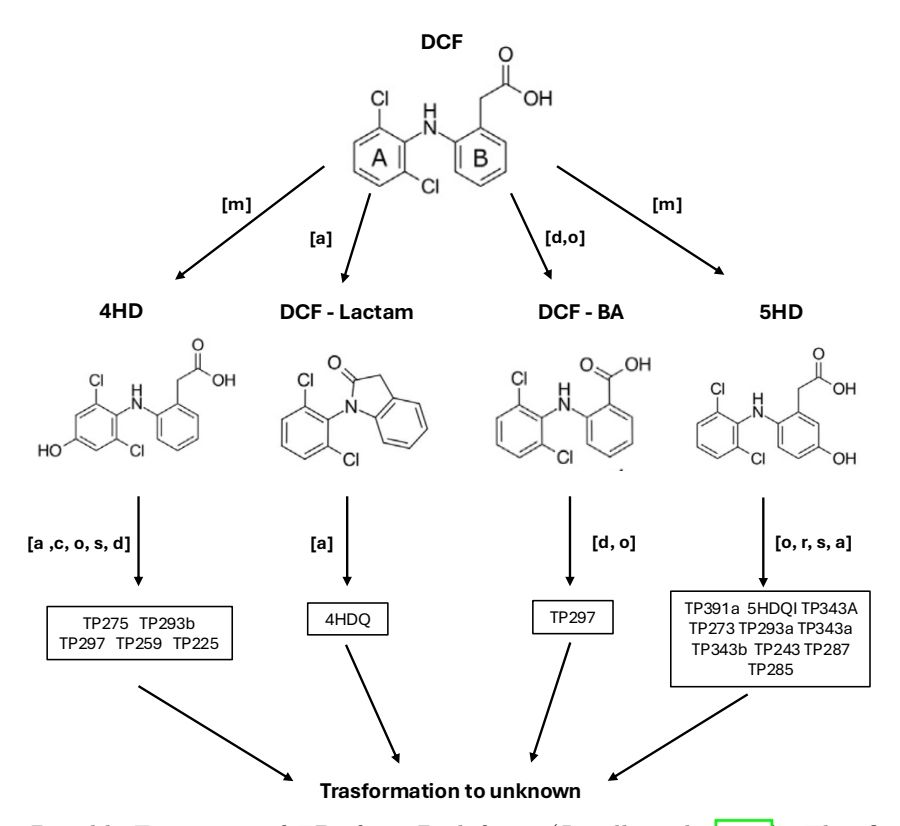


Figure 1.0.2: Possible Formation of TPs from Diclofenac (Jewell et al., 2016). This figure illustrates the formation of transformation products (TPs) from Diclofenac (DCF). The arrows indicate pathways of transformation. Abbreviations used for the postulated reaction types are: [m] mono-oxygenation, [o] oxidation (dehydrogenation), [a] amidation, [d] decarboxylation, [s] sulfate conjugation, [r] ring-opening reactions, [c] reductive dechlorination, [h] amide hydrolysis.

This inadequacy leads to a substantial and continuous discharge of diclofenac and other organic micropollutants (OMPs) into aquatic systems, raising significant concerns about their long-term ecological effects, which are still largely unknown (Bonvin et al., 2016). The cumulative impact of these compounds on aquatic ecosystems underscores the urgency for both regulatory

measures and the development of advanced treatment technologies that go beyond conventional methods to effectively reduce OMP concentrations in effluents.

Table 1.0.1: Physico-chemical properties of diclofenac (Vieno & Sillanpää, 2014).

Parameter	Value
Chemical formula	$\mathrm{C}_{14}\mathrm{H}_{10}\mathrm{Cl}_2\mathrm{NO}_2^-$
CAS no	15307-86-5
	15307-79-6 (disodium salt)
Water solubility	$2.37\mathrm{mg/L}$
pKa	4.15
$\log Kow$	4.51
logKd,primary sludge	2.7
	2.3
logKd,secondary sludge	1.2
	2.1
logKd, MBR	2.3 – 2.5
$\log \mathrm{Kd}, \mathrm{digested}$ sludge	1.3-2.2

Regulatory Frameworks

Wastewater across Europe, including Switzerland, serves as a major pathway for the release of diverse organic micropollutants (OMPs) into the environment. These trace substances, originating from pharmaceuticals, personal care products, and industrial chemicals, pose ecological risks even at low concentrations. As awareness of their environmental and public health impacts has grown, both Switzerland and the European Union have strengthened regulatory frameworks to mitigate their discharge.

Switzerland has been a pioneer in addressing the issue of micropollutants in wastewater. The Waters Protection Ordinance (GSchV) (Waters Protection Ordinance (WPO), 1998) defines detailed requirements for monitoring and discharging treated wastewater. A significant milestone was the 2014 revision of the Water Protection Act (Eggen et al., 2014), which mandated that selected wastewater treatment plants (WWTPs) implement advanced treatment stages to reduce OMP loads. To evaluate the performance of these upgrades, the 2016 DETEC Ordinance (Ordinance of the DETEC on the review of purification effect of measures for the elimination of organic trace substances in wastewater treatment plants, 2016) introduced a list of 12 indicator substances used to assess treatment effectiveness. This structured and targeted approach ensures that technological interventions are both efficient and verifiable, and it reflects Switzerland's long-standing commitment to proactive environmental protection.

In parallel, the European Union has strengthened its regulatory framework through the recast Directive (EU) 2024/3019 on urban wastewater treatment (Directive (EU) 2024/3019 concerning urban wastewater treatment, [2024]). This updated directive extends beyond traditional pollutants, such as BOD, nitrogen, and phosphorus, by mandating removal targets for pharmaceutical residues and other micropollutants. A key requirement is the implementation of a fourth treatment stage for WWTPs serving more than 150,000 population equivalents (p.e.) by 2045, with a mandated minimum of 80% removal efficiency for a defined list of pharmaceutical compounds.

Additionally, WWTPs serving more than 10,000 p.e. that discharge into sensitive water bodies are subject to the same requirements. These legislative developments mark a significant shift toward comprehensive wastewater management across the EU, emphasizing the need for scalable and effective treatment technologies.

Switzerland and the European Union are aligned in their efforts to tackle micropollutants in wastewater, sharing key regulatory principles while differing in mechanisms of implementation:

- Shared Objectives and Targeted Pollutants: Both jurisdictions mandate the removal of micropollutants as an additional treatment objective, alongside conventional pollutants. Each identifies specific indicator substances to evaluate treatment performance, with considerable overlap in the substances selected. These are typically classified by their removability in advanced treatment processes (Joss et al., 2006; Löffler et al., 2011), reflecting a shared scientific consensus on priority compounds.
- Implementation Mechanisms and Funding: Switzerland finances WWTP upgrades via a national fund supported by a small surcharge on wastewater fees (Baresel et al., 2016; Grandjean et al., 2017), ensuring a consistent financial basis for implementation. In contrast, the EU introduces an Extended Producer Responsibility (EPR) scheme, whereby pharmaceutical and cosmetic producers are financially accountable for part of the upgrade costs. Both systems adhere to the "polluter pays" principle but differ in operationalization. Additionally, both apply phased implementation strategies to facilitate long-term planning and infrastructure development.

These parallel developments reflect a broader shift toward stringent environmental protection in the wastewater sector. The evolving frameworks emphasize the urgent need for technological innovation and cross-sector collaboration to ensure effective and sustainable micropollutant removal across Europe.

Wastewater Treatment Processes

Conventional wastewater treatment plants (WWTPs) based on the activated sludge (AS) process often operate near their design capacity. Increasingly stringent effluent standards require higher treatment performance, particularly for the removal of organic micropollutants (OMPs) such as diclofenac (DCF), carbamazepine (CBZ), sulfamethoxazole (SMX), and atenolol (Guibaud, 2010; Leyva-Díaz et al., 2017). While AS is effective for removing organic matter and nutrients, it generally exhibits limited efficiency for OMPs due to their recalcitrant nature and the relatively short biological retention times applied in conventional systems (Di Biase et al., 2019).

Advanced physicochemical processes, including ozonation, activated carbon adsorption, and membrane-based treatments, achieve high micropollutant removal efficiencies. However, these technologies are associated with high operational costs, increased energy demand, and complex infrastructure, limiting their full-scale implementation in municipal WWTPs (Matos et al., 2019; Wolff & colleagues, 2021). Consequently, cost-efficient biological solutions that can be retrofitted into existing plants are of increasing interest.

Among these, Moving Bed Biofilm Reactors (MBBRs) and Hybrid MBBRs (HMBBRs) are particularly promising. MBBRs employ free-floating carriers that provide surfaces for biofilm growth, enhancing retention of slow-growing microorganisms such as nitrifiers and supporting the biodegradation of selected OMPs (Di Biase et al., 2019; Leyva-Díaz et al., 2017). Developed in Norway in the late 1980s and commercialized in the early 1990s (Odegaard, 2006), MBBR technology has been applied worldwide, primarily in small to medium-sized WWTPs or for industrial effluents. Its large-scale municipal adoption has been limited partly due to uncertainties about long-term stability, scaling, and cost-benefit considerations.

Optimized MBBR and HMBBR systems can achieve high OMP removal, with diclofenac removal reported up to 88 % (Jewell et al., 2016). The WWTP at ARA Bad Ragaz (Switzerland) demonstrates successful HMBBR operation, achieving enhanced DCF removal through biofilm-associated microbial communities on the carriers (Jewell et al., 2016).

From an engineering perspective, HMBBRs combine suspended activated sludge with biofilm-attached biomass, increasing effective biomass concentration and enabling stable operation under higher loading conditions (Leyva-Díaz et al., 2017). They can be retrofitted into existing basins without major infrastructure modifications, providing a compact and modular solution (Di Biase et al., 2019).

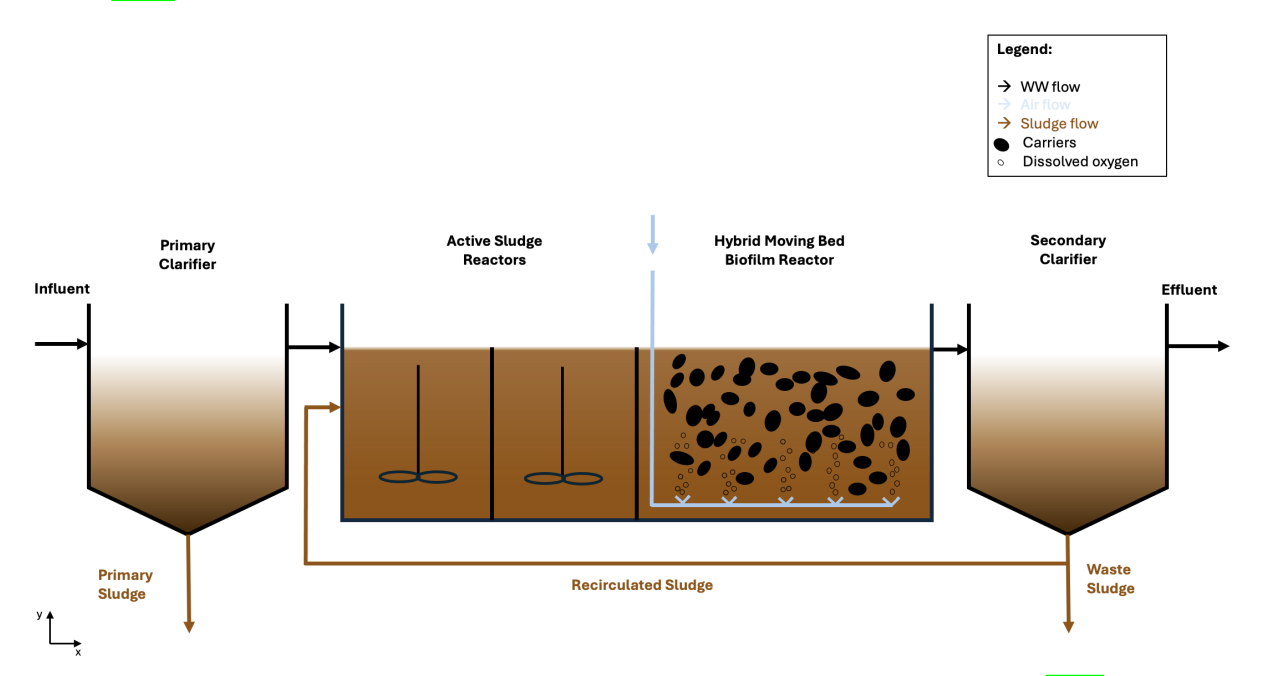


Figure 1.0.3: General schematic diagram of a HMBBR (Leyva-Díaz et al., 2017).

Despite these advantages, several engineering challenges remain. Carrier movement driven by aeration enhances substrate transport and maintains an active biofilm layer (Leyva-Díaz et al., 2017; Odegaard, 2006), but also increases energy demand, potentially accounting for up to 50% of a WWTP's total energy use (Jiménez et al., 2015). Operational risks include stagnation zones, clogging, or carrier loss (Fux et al., 1999). System performance depends on design and operational parameters such as mixing, filling fraction (typically 30–70% of reactor volume), and carrier characteristics, which influence biofilm development and stability (Di Biase et al., 2019).

Regarding costs, conventional AS systems are generally the least expensive, with moderate energy demand and well-established maintenance routines, typically around ≤ 0.20 m⁻³ of

treated wastewater (Matos et al., 2019; Wolff & colleagues, 2021). MBBRs and HMBBRs involve higher capital and operational costs due to carriers, additional aeration, and more complex control systems, with estimated costs of €0.35–0.50 m⁻³, but remain more cost-effective than advanced physicochemical treatments (Di Biase et al., 2019; Leyva-Díaz et al., 2017; Matos et al., 2019). Ozonation, activated carbon adsorption, and other quaternary steps can exceed €1.00 m⁻³, mainly due to energy consumption, chemical use, and additional infrastructure, limiting their widespread implementation in municipal WWTPs (Matos et al., 2019; Wolff & colleagues, 2021). Overall, HMBBRs offer a compromise between improved OMP removal and reasonable operational costs, making them attractive for retrofitting existing plants (Table 1.0.2).

Table 1.0.2: Estimated cost and micropollutant removal efficiency for different treatment technologies (Matos et al., 2019)

Technology	Approx. Cost (€ m ⁻³)	OMP Removal
Activated Sludge (AS)	0.20	Low
MBBR	0.35	Moderate
Hybrid MBBR (HMBBR)	0.50	Moderate-High
Ozonation	1.20	High
Powdered/Granular Activated Carbon	1.50	High
Other Quaternary Steps	1.00 - 1.80	High

HMBBRs, with their compact design, operational flexibility, and effective OMP removal, represent a viable strategy for upgrading existing AS-based WWTPs to meet stricter effluent standards.

Aim and Research Questions

The primary goal of this study is to investigate the efficacy of a pilot-scale Hybrid Moving Bed Biofilm Reactor (HMBBR) system for removing the pharmaceutical micropollutant diclofenac (DCF) from municipal wastewater. The research, conducted at the Process Technology Center (PTC) of the FHNW in Muttenz, Switzerland, focuses on understanding how operational parameters, particularly sludge retention time (SRT), influence biofilm development on carriers and the resulting DCF degradation kinetics.

Key objectives include:

- Evaluating the colonization and biological activity of clean Biofilm Chip M carriers under real wastewater conditions.
- Determining whether these carriers can establish sufficient biofilm activity to contribute significantly to DCF removal.
- Assessing HMBBR performance under short hydraulic retention times (HRT), simulating compact or decentralized wastewater treatment scenarios with variable influent DCF concentrations.
- Investigating how steady-state conditions can be achieved and identifying strategies to reach high performance during plant start-up and early operation.

- Exploring the relationship between biological performance metrics, such as nitrification activity, and diclofenac degradation.
- Providing data-informed guidance for optimizing HMBBR design and operation to achieve effective micropollutant removal in compliance with Swiss and EU regulations.

These objectives frame the study to evaluate HMBBR performance under conditions relevant to practical applications, emphasizing biofilm-driven DCF removal.

The study is guided by the following research questions:

- 1. How does sludge retention time (SRT) influence biofilm formation on clean carriers in a pilot-scale HMBBR system?
- 2. To what extent can clean carriers contribute to diclofenac removal over time, and how does biofilm growth affect removal efficiency?
- 3. How does the biological performance of the HMBBR, particularly nitrification activity and nutrient availability, relate to diclofenac degradation, especially during early operational stages?
- 4. Can HMBBR technology achieve effective micropollutant removal under short hydraulic retention times and compact reactor configurations?
- 5. How do HMBBR results compare to findings from other studies (e.g., Jewell et al.), and can this technology be flexibly implemented in different scenarios? Specifically, can it provide a cost-effective, space-efficient alternative to quaternary treatment steps in WWTPs with limited budgets and footprint?

These research questions are designed to establish a clear connection between operational conditions, biofilm dynamics, and diclofenac removal, while leaving the specific outcomes to be determined through experimental analysis.

Chapter 2

Material and Methods

This chapter describes the materials, experimental setups, and analytical methods employed to investigate nitrification, biofilm development, and diclofenac removal. It begins with the pilot plant, presenting its main components, including the coagulant and aeration systems, sludge and biofilm reactors, secondary clarifiers, waste sludge handling, diclofenac dosing, autosampler, and supporting electrical and safety systems. The following section details the operational conditions and monitored parameters, covering startup, operational strategies, maintenance, sampling, and shutdown procedures.

Modeling approaches are then introduced, including the Activated Sludge Model No. 3 (ASM3) and kinetic models for diclofenac elimination, followed by the tracer experiment and its calibration procedure. Batch test setups are subsequently described, outlining experiments for both nitrification and diclofenac removal. Finally, the analytical framework is presented, covering reagents, equipment, monitoring of standard parameters (e.g., phosphorus, COD, nitrogen, TSS, pH, dissolved oxygen, and temperature), biomass quantification on carriers, biofilm observation via fluorescence microscopy, and diclofenac concentration analysis. Together, these methods provide the foundation for the interpretation of results presented in the subsequent chapter.

2.1 Pilot Plant

A pilot plant (PP) was constructed at the FHNW Process Technology Center (PTC) in Muttenz to replicate a full-scale wastewater treatment plant (WWTP) with a focus on biological treatment (Figure 2.1.2). The PP integrates both activated sludge (AS) processes and hybrid moving bed biofilm reactors (HMBBRs) and is fed with pretreated wastewater from the on-site WWTP, which treats wastewater from the Kubuk-FHNW building.

The PP comprises three identical treatment lines, each including the following sequential stages:

- Activated Sludge Reactors (Types 1 and 2)
- Moving Bed Biofilm Reactors (Type 3)
- Secondary Clarifiers (Type 4)

Figure 2.1.1 shows a Piping and Instrumentation Diagram (P&ID) of the PP, illustrating the main components and flow paths.

The PP operates as a free-flow system, with gravity facilitating movement between stages.

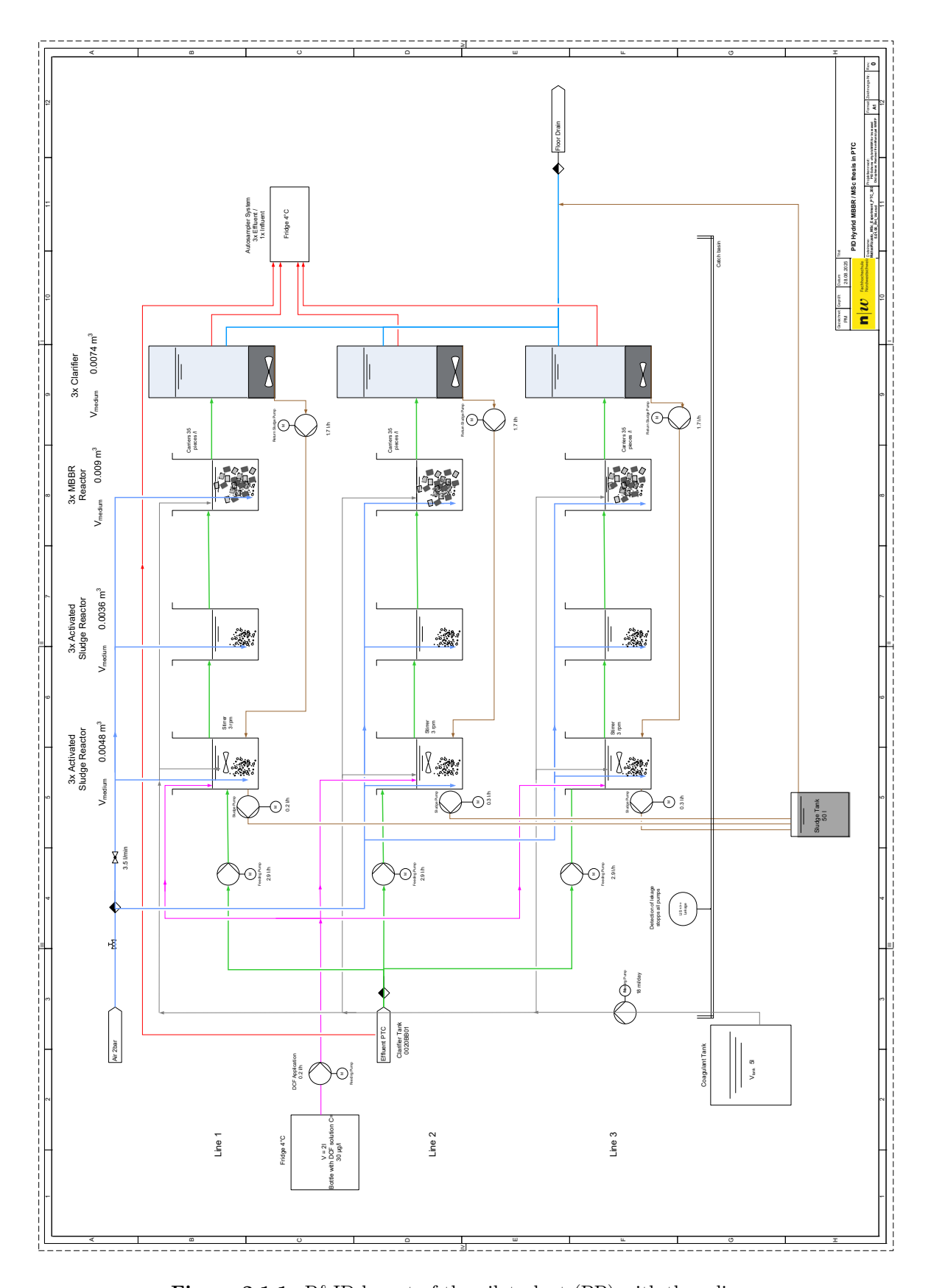
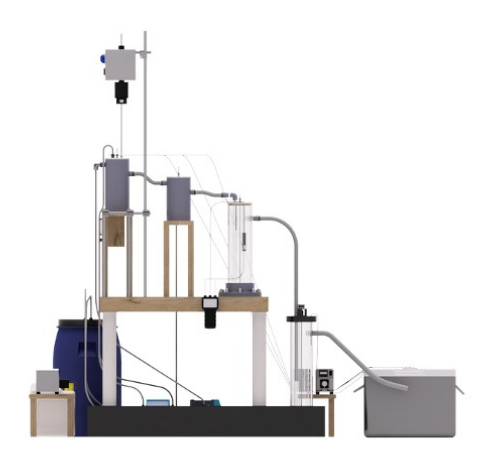


Figure 2.1.1: P&ID layout of the pilot plant (PP) with three lines.



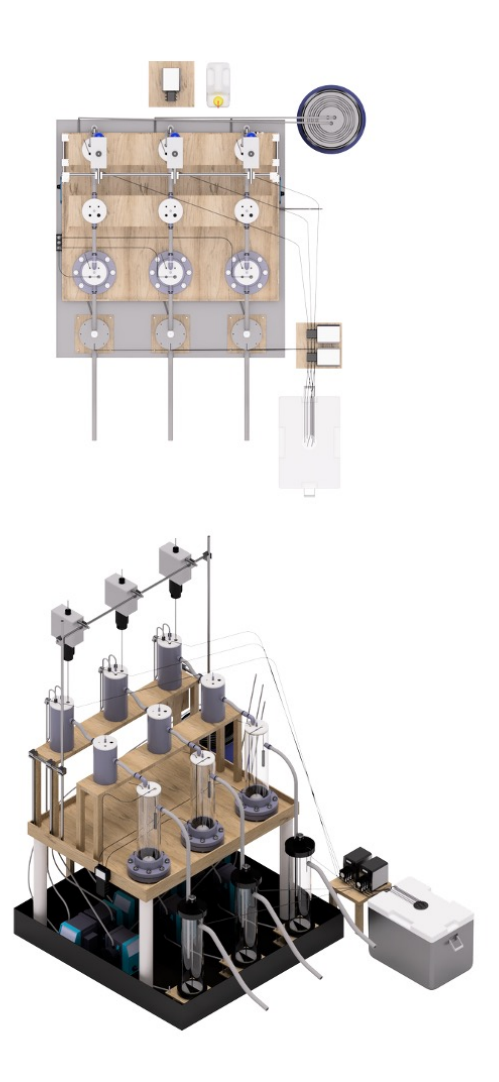


Figure 2.1.2: General view of the pilot plant (PP).

Pilot Plant Components

A detailed overview of the pumps, tubing specifications, and other components of the pilot plant is presented in Table 2.1.1 Table 2.1.2, and Table 2.1.3 while their functions and roles are discussed in the following section.

Table 2.1.1: Overview of flows and pump setup.

Type of pump	Flow rate $[L h^{-1}]$	Remarks
3x Watson Marlow Qdos60	6 - 120	Waste sludge
3x Watson Marlow Qdos60	6 - 120	Sludge recirculation
3x Watson Marlow Qdos60	6 - 120	Influent
1x Ismatec BVP 6 lines	$6 \cdot 10^{-5} - 4.08$	Coagulant dosing system (FeCl ₃)
1x Ismatec Reglo ICC 3 lines	$6 \cdot 10^{-5} - 4.08$	Diclofenac dosing system
1x Ismatec Reglo ICC 2 lines	$6 \cdot 10^{-5} - 4.08$	Autosampler (Effluent)
1x Masterflex Ismatec Reglo ICC 2 lines	$6 \cdot 10^{-5} - 4.08$	Autosampler (Influent/Effluent)

Table 2.1.2: Overview over the Reactors and Containers used.

Type of Reactor/Container	Volume [L]	Material
3x Sludge Reactor Type 1	4.8	HDPE
3x Sludge Reactor Type 2	3.6	HDPE
3x MBBR	9	HDPE
3x Secondary Clarifier	7.4	HDPE
1x Waste Sludge Tank	50	HDPE
1x Coagulant Tank (FeCl ₃)	5	HDPE
1x Diclofenac bottle	2	Glass
4x Autosampler bottles (influent/effluent)	1	Glass

Table 2.1.3: List of other components used.

Components	Quantity
Sludge stirrers	3 units
Secondary clarifiers stirrers	3 units
Y aeration stones	6 units
Semi-sphere aeration stones	3 units
Portatile Fridge at 4°C	1 unit
Tygon LMT Tube $(d = 3 \text{ mm}, f = 12)$	5 m
Tygon LMT Tube ($d = 1.52 \text{ mm}, f = 8$)	$5 \mathrm{m}$
Tygon LMT Tube ($d = 0.95 \text{ mm}, f = 5$)	$25 \mathrm{m}$
Norprene Tube ($d = 4.8 \text{ mm}, f = 3$)	$25 \mathrm{m}$
Sylicon Tube ($d = 4.8 \text{ mm}, f = 3$)	$15 \mathrm{m}$

Coagulant System

For the dosage system setup (Figure 2.1.1), a total of 9.3 mL of iron chloride (FeCl₃) solution (2.5.3) was dosed per day across the Pilot Plant. Specifically, 4.65 mL per day was dosed into Reactor Type 1, and 4.65 mL per day was dosed into Reactor Type 3. The total 9.3 mL of coagulant was distributed across six dosing points, with three dosing points allocated to each reactor (Appendix A.3). The coagulant solution was continuously mixed using a magnetic stirrer to ensure uniformity before dosing. Dosing was precisely controlled by a six-way Ismatec BVP pump (Table 2.1.1), with each treatment line dosed separately to maintain accurate control over the system. The coagulant was stored at room temperature in a 5 liter high density polyethylene container (Table 2.1.2), which is suitable for containing acidic solutions. The dosage of FeCl₃ was based on a molar ratio of iron to phosphorus (β) of 1.5 $mol_{Fe} mol_P^{-1}$, ensuring a sufficient amount of iron was available to precipitate the phosphorus (Y. Zhang et al., 2005).

Aeration System

Continuous aeration was supplied to all reactors at a nominal flow rate of 3.5 L min⁻¹, ensuring sufficient oxygen availability. Compressed air, delivered at a maximum pressure of 2 bar, was provided via control valves, which maintained the flow rate. Reactor Types 1 and 2 utilized two fine-bubble aerator stones, while Reactor Type 3 featured a semi-spherical stone system for enhanced oxygen dissolution. Dissolved oxygen (DO) levels in MBBRs reactors were continuously monitored using dedicated sensors, and all data were recorded by a MultiLine Multi 3510 IDS (Table 2.5.1).

Sludge Reactors

In the initial two stages of the treatment process (Figure 2.1.1), identical Activated Sludge (AS) systems were operated sequentially. These reactors (Table 2.1.2) were characterized by biomass suspended in sludge flocs within both compartments. Both Reactor Type 1 and Reactor Type 2 were continuously aerated. Additionally, Reactor Type 1 was also mixed to prevent sludge accumulation. The primary objective of these stages was the efficient removal of organic matter.

Moving Bed Biofilm Reactors

The Moving Bed Biofilm Reactors (MBBRs) were integrated to facilitating biofilm-based treatment. Each MBBR was filled with 2.7 L of clean Biofilm Chip M carriers (Table 2.1.4), corresponding to an approximate filling fraction of 30%, a value consistent with established literature (Eddy, 2003; Jewell et al., 2016).

Airflow to each MBBR was controlled by individual flow controllers, as further explained in Section 2.1 to ensure sufficient mixing and prevent the formation of stagnation zones (Rusten et al., 2006), (Di Biase et al., 2019). However, the internal geometry of the MBBRs presented operational challenges. These reactors were not optimally designed for the comparatively large Biofilmchip M carriers. Furthermore, the presence of submerged pipes, the inserted aerator pipe, and the Dissolved Oxygen (DO) sensors created additional obstacles within the reactor. Due to these structural limitations, carriers often became stagnant or entrapped in poorly mixed

Table 2.1.4: Carriers technical information

Parameters	characteristics
Model	Biofilm Chip M
Company	Veolia / AnoxKaldnes
Material	HDPE
Length [mm]	2.2
Diameter [mm]	45
Surface area $[m^2 m^{-3}]$	1200

zones, compromising overall reactor performance. Despite these challenges, a daily check and adjustment of the airflow permitted regular flotation of the carriers within the MBBRs, as visually represented in Figure 2.1.3.

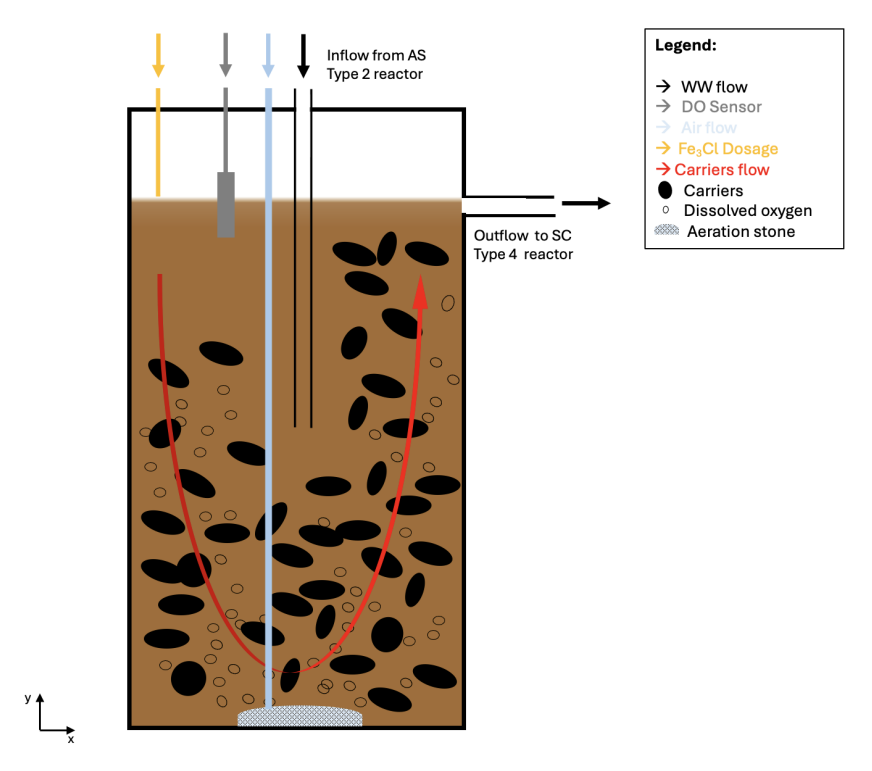


Figure 2.1.3: Front view of MBBR reactor, position of the aeration stone and consequent movement of the carriers.

Secondary Clarifier Reactors

The final stage of the wastewater treatment system consisted of a secondary clarifier (SC) where solids separation took place (Figure 2.1.1). In the secondary clarifier, the wastewater flow was slowed down, allowing for the sedimentation of activated sludge (AS) from the treated wastewater. To facilitate efficient sludge settling, a scraper was installed on the lid of the clarifier and set to 1.5 RPM (table 2.1.3). This scraper directed the settled sludge toward the center of the SC bottom for efficient collection. The collected sludge was then recirculated back to the first reactor as returned activated sludge (RAS) (table 2.1.1). The RAS flow rate was set at 3 L h⁻¹, ensuring proper biomass retention within the system. Three clarifiers, each with a volume of 7.4 L, were utilized for the sedimentation process. The residual effluent passed through the clarifier and was

discharged directly into the floor drain (Gujer & Henze, 2008).

Waste Sludge System

Waste sludge management for each operational line involved extracting sludge from Reactor Type 1 and transferring it to Reactor Type 5 (Figure 2.1.1). The primary control parameter for these operations was the Solids Retention Time (SRT), which was adjusted by varying the waste sludge flow rate. A higher waste rate resulted in a lower SRT (Eddy, 2003).

Crucially, before setting the operational SRTs, the minimum SRT (SRT_{min}) for effective nitrification was determined. This SRT_{min} represents the lowest SRT at which nitrifying bacteria can be maintained in the system without being washed out, thereby ensuring stable nitrification. Its calculation is vital, as a lower SRT can lead to the loss of these sensitive organisms, especially under unfavorable conditions like low temperatures or higher ammonia concentrations.

The SRT_{min} for nitrification is calculated based on the kinetic parameters of the nitrifying bacteria, specifically their maximum specific growth rate $(\mu_{ANO,max})$ and decay coefficient $(b_{ANO,T})$. For the purposes of this study, typical values of $\mu_{ANO,max} = 0.55 \text{ d}^{-1}$ and $b_{ANO,T} = 0.04 \text{ d}^{-1}$ were used for nitrifying bacteria. The general formula for SRT_{min} , derived from a mass balance for nitrifying bacteria in the reactor (Henze et al., [2008]), is given by:

$$SRT_{min} = \frac{1}{(1 + K_{ANO,I})\mu_{ANO,max} - b_{ANO,T}}$$
(2.1.1)

where $K_{ANO,I}$ is the inhibition constant for ammonia. Both $\mu_{ANO,max}$ and $b_{ANO,T}$ are temperature-dependent. The relationship between ammonia concentration and the specific growth rate of nitrifying bacteria has been extensively studied in the literature (Henze et al., 2008). It is important to note that the actual specific growth rate, μ_{ANO} , is also governed by the ammonia concentration (S_{NHx}) and described by the Monod equation:

$$\mu_{ANO} = \mu_{ANO,max} \frac{S_{NHx}}{K_{ANO} + S_{NHx}} \tag{2.1.2}$$

where K_{ANO} is the half-saturation constant for ammonia. This kinetic relationship is fundamental to understanding nitrification dynamics (Henze et al., $\boxed{2008}$). Once the strain of nitrifying bacteria was established and the theoretical SRT_{min} was determined, the operational SRTs for the experimental lines were set significantly above this minimum to ensure stable nitrification. The theoretical daily waste sludge flow rate (Q_{WAS}) required to maintain these desired SRTs was determined using the mass balance equation:

$$Q_{WAS} = \frac{V_R}{SRT} \tag{2.1.3}$$

where V_R is the Total Reactor Volume of 17.4 L. The flow was precisely controlled using

three peristaltic pumps Watson Marlow Qdos60 (Table 2.1.1). Based on this methodology, the calculated daily waste sludge volumes for the experimental lines were as follows:

- For SRT Line 1, with a target SRT of 2d, the required Q_{WAS} was calculated to be $\approx 8.70 \,\mathrm{L\,d^{-1}}$.
- For SRT Line 2, with a target SRT of 3d, the required Q_{WAS} was calculated to be $\approx 5.80 \,\mathrm{L\,d^{-1}}$.
- For SRT Line 3, with a target SRT of 5d, the required Q_{WAS} was calculated to be $\approx 3.48 \,\mathrm{L\,d^{-1}}$.

These values guided the operational strategy for waste sludge removal, ensuring the desired biomass retention times within the pilot plant's bioreactor (Gujer & Henze, 2008). Maintaining an SRT at or above SRT_{min} is essential to ensure stable nitrification, as it prevents the washout of the slow-growing nitrifying bacteria and sustains the system's ammonia removal capacity.

For this reason, one line was operated at an SRT of 2 days, corresponding to the estimated SRT_{\min} . The other two lines were set at 3 and 5 days, respectively, to provide a broader range of SRT conditions across the pilot plant. This variation allowed the study to assess the effect of biomass retention time on biofilm development, nitrification, and diclofenac removal, offering insights into system performance under different operational strategies.

Diclofenac Dosing System

Diclofenac, after steady-state conditions, was continuously dosed into Reactor Type 1 from a refrigerated glass reservoir using a multiline peristaltic Ismatec Reglo ICC pump (Table 2.1.1). The required stock concentration was calculated from:

$$C_{\text{stock}} = \frac{C_{\text{target }}Q_{\text{in}}}{Q_{\text{d}}} \tag{2.1.4}$$

 $C_{\text{stock}} = \text{DCF}$ concentration in the dosing reservoir;

 $C_{\text{target}} = \text{target DCF concentration in the reactor influent};$

 $Q_{\rm in}$ = influent flow rate to the reactor;

 $Q_{\rm d}$ = volumetric dosing rate.

For $C_{\text{target}} = 5$ and $10 \,\mu\text{g L}^{-1}$, $Q_{\text{in}} = 1.5 \,\text{L h}^{-1}$, and $Q_{\text{d}} = 10 \,\text{mL h}^{-1}$, the stock concentrations were 0.75 and 1.50 mg L⁻¹ (Annex A.6).

Autosampler System

An automated sampling system, comprising four autosamplers (Figure 2.1.1), was implemented to monitor various points within the pilot plant. These autosamplers were controlled by two separate pumps: one Ismatec Reglo ICC pump equipped with two lines, and one Masterflex Ismatec Reglo ICC Digital Pump also with two lines (Table 2.1.1). Sampling points were strategically located to ensure comprehensive data collection (Figure 2.1.1). Three autosampling lines were dedicated to Reactor Type 4, positioned at the surface to collect effluent samples. The fourth autosampler was placed at the influent line, drawing samples from the primary clarifier of the PTC.

Samples were collected continuously over a 24-hour period. This continuous sampling was regulated by a timer socket, programmed to activate the autosamplers every 15 minutes. Each collected sample was directed into a glass bottle and stored in a fridge maintained at 4°C to preserve sample integrity. Automated sampling was performed once per week (Section 2.5.2).

Electrical and Safety System

The pilot plant is equipped with a containment structure and containers that are directly connected to the main sewage system, ensuring safe discharge in case of leaks or overflow. In addition, the installation is complemented by a dedicated safety and control system. The electrical setup is protected by residual current devices (RCDs) and circuit breakers to prevent short circuits or accidental contact. An emergency stop switch is located near the reactors, allowing operators to immediately shut down the entire system if necessary. The overflow sensor is directly linked to the secure socket, ensuring automatic power cut-off to all pumps in case of abnormal operation, thereby minimizing the risk of flooding, equipment damage, or chemical leakage (Appendix E, F).

2.1.1 Operational Conditions and Monitored Parameters

Startup

The pilot plant began operation on April 4, 2025. For startup, the system was inoculated with clean Biofilmchip M carriers (Table 2.1.4), along with wastewater and activated sludge sourced from the FHNW Process Technology Center (PTC). After filling, the General Electric control system, stirrers, pumps, and aeration units were started to initiate operation.



Figure 2.1.4: Overview of the pilot plant in the PTC during operations.

Parameters

The operational conditions of the pilot plant were carefully monitored and verified daily to maintain stable performance throughout the experimental period. The pH remained within the range of 7.5 ± 0.5 , which is considered optimal for biological processes in wastewater treatment (Henze et al., 2008). The temperature of the wastewater in the reactors was maintained at 20.5 ± 0.5 °C.

Hydraulic Retention Times (HRTs) and Sludge Retention Times (SRTs) were set according to the experimental design to provide an appropriate balance between treatment efficiency and biomass retention. The SRTs imposed in the three lines were 2, 3, and 5 days, respectively. The HRT for each line was calculated using the reactor volume and the net flow leaving the reactor, taking into account the influent flow rate $(Q_{\rm in}=1.5~{\rm L\,h^{-1}})$ and the withdrawal flow of waste sludge $(Q_{\rm WS,line})$ as:

$$HRT_{line} = \frac{V_{reactor}}{Q_{in} - Q_{WS,line}}$$
 (2.1.5)

This ensures that the retention time reflects the actual residence of wastewater in the reactor while accounting for biomass removal. The resulting HRTs for lines 1, 2, and 3 were 15.3 h, 13.8 h, and 12.8 h, respectively, providing conditions conducive to biofilm development and nitrification activity.

Tables 2.1.5 and 2.1.6 summarize the main characteristics of influent wastewater and key operational parameters of the pilot plant, which guided the design and operation of the system throughout the study.

Parameter	Value	Unit
Reactor Volume	17.4	L
HRT Line 1	15.3	h
HRT Line 2	13.8	h
HRT Line 3	12.8	h
Influent Flow	1.5	${ m L}{ m h}^{-1}$
RAS Ratio ^a	2	_
RAS Flow	3	${ m L}{ m h}^{-1}$
WS Flow Line 1	0.36	${ m L}{ m h}^{-1}$
WS Flow Line 2	0.24	${ m L}{ m h}^{-1}$
WS Flow Line 3	0.145	${ m L}{ m h}^{-1}$
SRT Line 1	2	d
SRT Line 2	3	d
SRT Line 3	5	d
Aeration Rate MBBRs	3.5	$L \mathrm{min}^{-1}$
рН	7.5 ± 0.5	-
Temperature	21 ± 0.5	$^{\circ}\mathrm{C}$

Table 2.1.5: Operational parameters of the pilot plant.

Table 2.1.6: Influent wastewater characterization.

Influent Wastewater	$\frac{\mathbf{COD}}{[\mathrm{mg}\mathrm{L}^{-1}]}$	$\mathbf{N_{tot}}$ $[\mathrm{mg}\mathrm{L}^{-1}]$	$\frac{\mathbf{P_{tot}}}{[\mathrm{mg}\mathrm{L}^{-1}]}$
Raw	576 ± 159	84 ± 29	12 ± 6
After primary clarifier	460 ± 120	130 ± 30	8 ± 3

Operation and Maintenance

Stable operation of the pilot plant required regular maintenance to ensure reproducibility of the experimental results. Dosing pumps (Table 2.1.1) were periodically recalibrated due to tubing deformation, which caused declining flow rates. Biofilm accumulation on pump channels and tubing occasionally led to clogging; these sections were therefore replaced monthly or manually cleaned when necessary. A weekly maintenance routine included scrubbing the reactors to limit biofilm buildup, flushing influent tubing and connecting pipes with pressurised air, and rinsing influent and pump tubing to minimise clogging. Pump heads and sludge pipes showing wear were replaced to maintain hydraulic performance and dosing accuracy. It should be noted that during the initial weeks of operation, the system was subject to modifications and adjustments necessary

to stabilise the pilot plant. Additionally, temporary shutdowns occurred due to construction activities within the PTC facility. These interruptions meant that operating conditions were not fully stable during the entire experimental period.

Sampling Procedures

To assess the operational stability of the system, key performance parameters were monitored once per week throughout the experimental period. The monitoring was based on multiple sampling points located across the pilot system (Figure 2.1.5). Samples were collected using 20 mL syringes, filtered (except for TSS and COD analyses) through syringe filters (Table 2.5.4), and stored at -20° C until laboratory analysis. Laboratory checks confirmed that the use of different filter materials did not influence the sample composition or measured concentrations; when available, polypropylene (PP) filters were primarily used. This monitoring strategy served two main objectives: (i) to verify that the three treatment lines operated under comparable conditions, and (ii) to ensure compliance with the effluent quality requirements established by the Gewässerschutzverordnung (GSchV) (Waters Protection Ordinance (WPO), $\boxed{1998}$). The analysis procedures are listed on Section $\boxed{2.5}$ and the results presented on Section $\boxed{3.1.1}$.

Samples for Diclofenac detection were performed once steady-state conditions were achieved, approximately three months after start-up, when sufficient biofilm growth on the carriers had been visually and biologically confirmed (Section 2.5.3). After six days of continuous DCF dosing (Section 2.1), corresponding to approximately ten hydraulic retention times (HRTs), the system was considered equilibrated. The main sampling campaign lasted ten days, during which influent and effluent samples were collected daily from each of the three treatment lines at different times of the day to account for temporal variations. All samples were immediately filtered to remove suspended solids and stored at $-20\,^{\circ}$ C until analysis (Table 2.5.4). The quantification of DCF concentrations is described in Section 2.5.5. Diclofenac removal in the operating pilot plant was evaluated under continuous-flow conditions through systematic sampling at both influent and effluent points (Section 3.4.2). Removal efficiency was calculated by comparing measured DCF concentrations at these points under steady-state operation, reflecting the combined performance of biological and physicochemical processes in real time.

Shutdown

After 112 days of operations, on July 25, 2025, the pilot plant was dismantled at the end of the experimental campaign. All equipment was carefully disassembled, thoroughly cleaned, and properly stored for potential future use. The procedure was carried out in accordance with safety and laboratory protocols to ensure proper handling of biological materials and chemical residues.

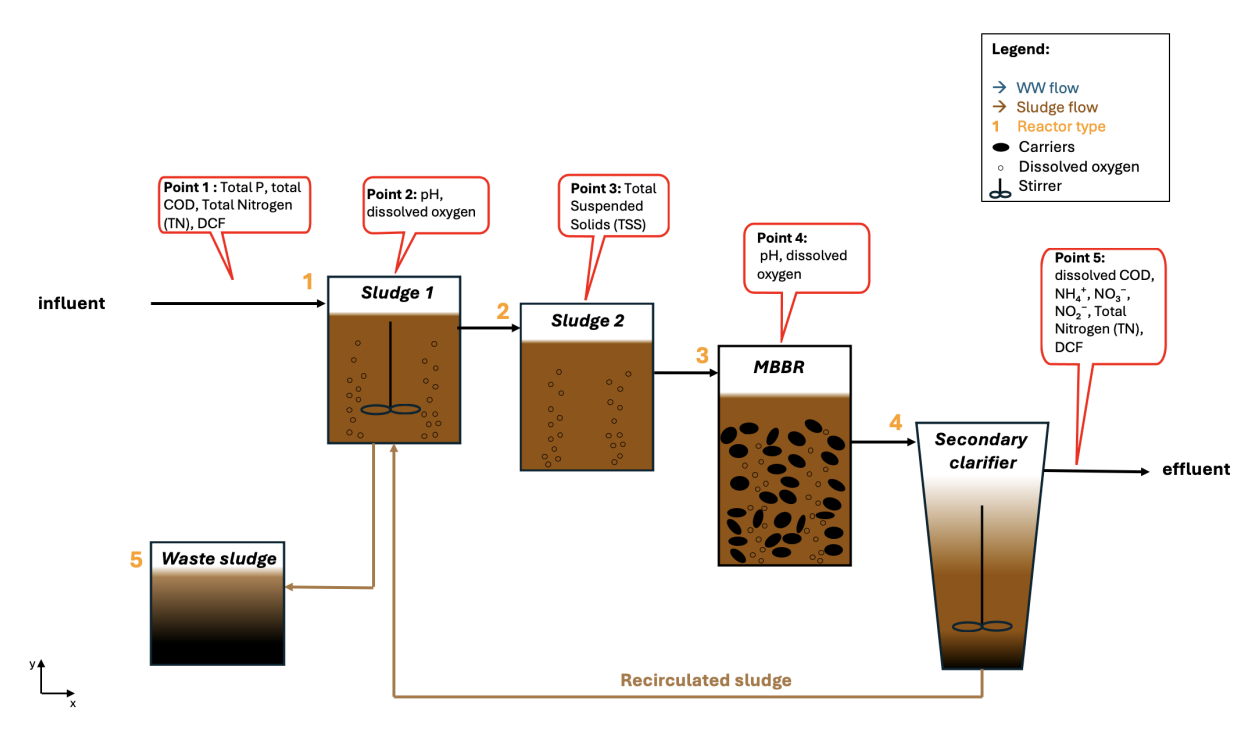


Figure 2.1.5: Sampling points across the pilot plant.

2.2 Modeling Approaches

To support the experimental investigation of diclofenac (DCF) removal in the pilot plant, mathematical modeling was employed using approaches directly relevant to the processes studied. Dynamic simulations in SIMBA# with the ASM3 model allowed representation of the biological processes, including oxygen consumption, sludge production, and nutrient dynamics in both activated sludge and MBBR units. Finally, pseudo-first- and pseudo-second-order kinetic models were applied to describe DCF degradation and adsorption in batch and pilot-scale experiments. These models provide quantitative insight into the removal mechanisms and allow estimation of key parameters, such as biodegradation rate constants and adsorption capacities.

2.2.1 ASM3 Modeling Framework

Dynamic simulations of the pilot plant were performed using SIMBA[#] (Ifak, Institut für Automation und Kommunikation e.V.) to evaluate effluent quality, oxygen demand, and sludge production under varying influent and operational conditions (Figure 2.2.1).

Biological treatment processes were modeled using the Activated Sludge Model ASM3 (Gujer et al., 1999), applied to both activated sludge and MBBR reactors. The dedicated SIMBA# biofilm model was not used due to the complexity of defining initial biofilm parameters. ASM3 simulations were run for 30 days until steady state, considering only suspended biomass in the initial phase before biofilm development became significant (Henze et al., 2008).

Simulations were initialized with influent characteristics representative of the pilot plant wastewater (Section 3.1.1): 500 mg COD L⁻¹, 120 mg N L⁻¹, 8 mg P L⁻¹, a flow rate of 1.5 L h⁻¹, and a water temperature of 22 °C. Operational parameters included reactor volumes and configuration matching the pilot plant, as well as sludge retention times (SRTs) corresponding to the

early operational phase (Table 2.1.5, Table 2.1.2).

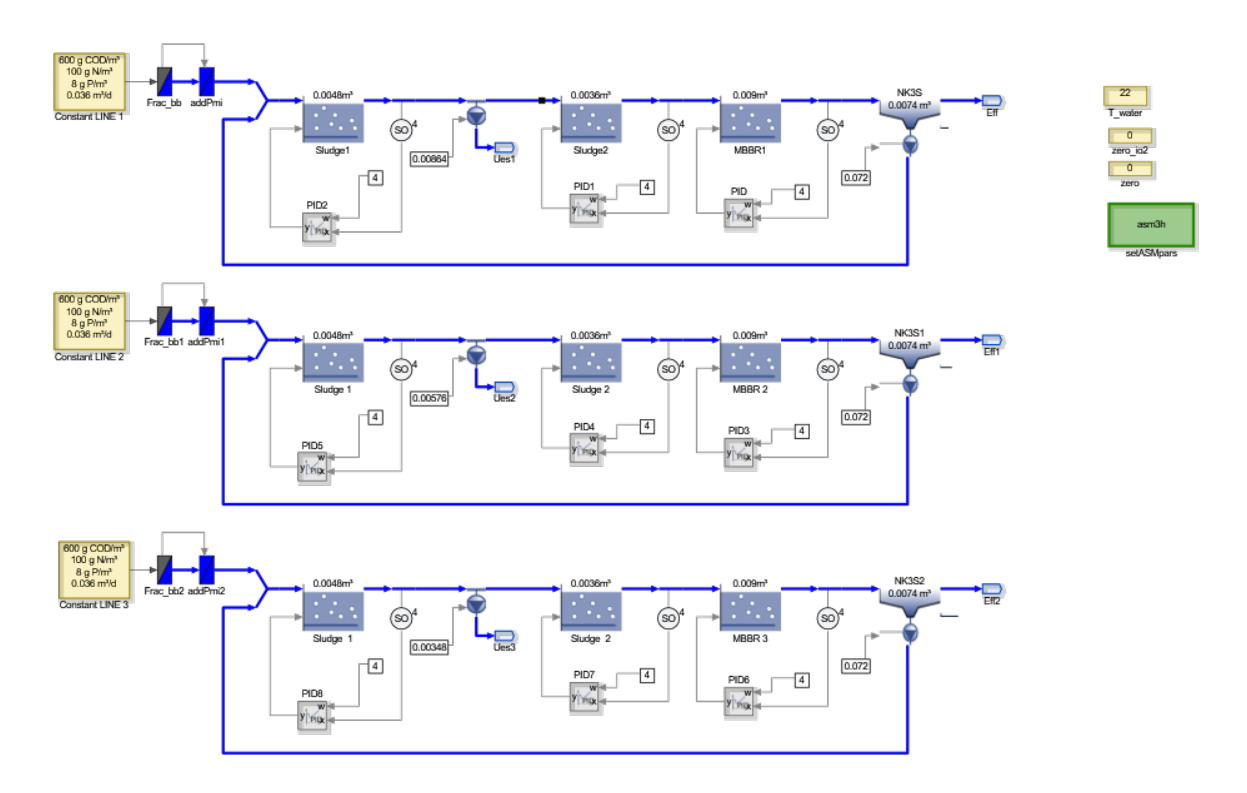


Figure 2.2.1: Process diagram of the simulated biological wastewater treatment plant in SIMBA[#], showing the main components, volumes, and flow rates of the three treatment lines.

2.2.2 Kinetic Models for Diclofenac Elimination

To interpret diclofenac (DCF) elimination in biological experiments, different kinetic models were considered. Pseudo-first-order (PFO) elimination was applied for both activated sludge and carrier-based batch tests, as well as for the overall removal in the pilot plant. In sludge batch tests, adsorption could occur during the initial phase; the pseudo-first-order (PFO) and pseudo-second-order (PSO) adsorption models (Ho & McKay, 1998, 1999) were tested, but they were not the primary focus.

For biological degradation, DCF removal was described using a pseudo-first-order biodegradation model (Jewell et al., 2016):

$$\frac{dC}{dt} = -k_{\text{biol}} \cdot X_{\text{TSS}} \cdot C \tag{2.2.1}$$

Where:

 $C = \text{DCF concentration at time } t \ (\mu \text{g-L}^{-1}),$

 $X_{\rm TSS} = \text{biomass concentration } (g \cdot L^{-1}),$

 $k_{\text{biol}} = \text{pseudo-first-order biodegradation constant } (L \ g_{\text{TSS}}^{-1} \cdot d^{-1}),$

 $C_0 = \text{initial DCF concentration.}$

Integration of Equation 2.2.1 yields:

$$\ln\left(\frac{C}{C_0}\right) = -k_{\text{biol}} \cdot X_{\text{TSS}} \cdot t \tag{2.2.2}$$

Adsorption models were applied only in sludge batch tests to investigate potential initial sorption:

$$Q_t = Q_e \left(1 - e^{-k_1 t} \right), \quad \frac{t}{Q_t} = \frac{1}{k_2 Q_e^2} + \frac{t}{Q_e}$$
 (2.2.3)

Where:

 $Q_t = \text{adsorption capacity at time } t \text{ (mg} \cdot \text{g}^{-1}),$

 $Q_e = \text{equilibrium adsorption capacity } (\text{mg} \cdot \text{g}^{-1}),$

 $k_1 = PFO$ adsorption rate constant (min⁻¹),

 $k_2 = \text{PSO adsorption rate constant } (g \cdot \text{mg}^{-1} \cdot \text{min}^{-1}).$

Overall, pseudo-first-order biodegradation was applied to describe DCF elimination in carrier-based batch tests, sludge batch tests (after the initial phase), and the pilot plant. Model quality was evaluated using R^2 and comparison of experimental and predicted values. This approach allows distinction between rapid initial sorption and slower biological degradation, providing an accurate description of DCF elimination dynamics (Gonzalez-Gil et al., [2016]; Ternes et al., [2004]).

2.2.3 Simulation of Diclofenac Behaviour in Pilot Reactors

A numerical model based on mass balance was developed to simulate DCF concentration dynamics in the four main compartments of the pilot plant: Sludge 1, Sludge 2, MBBR, and the clarifier. A small timestep ($\Delta t = 0.0001$ h) was used for numerical integration.

The general mass balance for a substance in a continuously stirred tank reactor (CSTR) is expressed as (Levenspiel, 1999):

$$V\frac{dC}{dt} = Q_{\rm in}C_{\rm in} - Q_{\rm out}C_{\rm out} + R_{\rm prod} - R_{\rm cons}$$
 (2.2.4)

Where:

V = reactor volume (L),

C = DCF concentration in the reactor ($\mu g L^{-1}$),

t = time (d),

 $Q_{\rm in}, Q_{\rm out} = \text{influent and effluent flow rates (L d}^{-1}),$

 $C_{\rm in}, C_{\rm out} = \text{influent and effluent DCF concentrations } (\mu g L^{-1}),$

 $R_{\text{prod}}, R_{\text{cons}} = \text{production and consumption rates of DCF } (\mu \text{g d}^{-1}).$

For DCF, no in-reactor production occurs ($R_{\text{prod}} = 0$). The consumption term represents biological degradation, modeled as a pseudo-first-order process:

$$R_{\rm cons} = k_{\rm biol} \cdot C_{\rm DCF} \cdot X_{\rm TSS} \cdot V \tag{2.2.5}$$

Where:

 $R_{\rm cons} = {\rm rate} \ {\rm of} \ {\rm DCF} \ {\rm removal} \ {\rm due} \ {\rm to} \ {\rm biodegradation} \ (\mu {\rm g} \ {\rm d}^{-1}),$

 $k_{\text{biol}} = \text{pseudo-first-order biodegradation rate constant (L gTSS}^{-1} d^{-1}),$

 $C_{\rm DCF} = {\rm DCF}$ concentration ($\mu {\rm g~L}^{-1}$),

 $X_{\rm TSS} = {\rm biomass\ concentration\ (gTSS\ L^{-1})},$

V = reactor volume (L).

Values of k_{biol} were obtained from literature and batch experiments. This formulation assumes well-mixed conditions and that DCF removal occurs exclusively through biological degradation.

In the simulation, Sludge 1 receives influent from the feed line and recirculated sludge from the clarifier, with outflow directed to Sludge 2. Sludge 2, an aerobic reactor, discharges to the MBBR, which additionally accounts for DCF removal by biofilm-attached biomass. The MBBR outflow proceeds to the clarifier, where sludge is separated from treated water; two streams are considered: waste sludge and return sludge. Steady-state simulations were performed to assess long-term DCF removal, and modeled concentrations were compared with pilot plant data (Table 2.2.1).

Table 2.2.1: Model parameters used for simulating DCF concentration profiles in the pilot plant under continuous-flow conditions. Identical parameters are reported once; kinetic constants differ between batch-test and literature values.

Parameter	Value	Unit
Sludge 1 volume	4.8	L
Sludge 2 volume	3.6	${ m L}$
MBBR volume	9.0	${ m L}$
Clarifier volume	7.4	${ m L}$
Influent flow rate	36	$L d^{-1}$
Waste sludge flow rate	8.64	$L d^{-1}$
Return sludge flow rate	72	$\mathrm{L}\mathrm{d}^{-1}$
Activated sludge concentration	2.05	$ m gTSSL^{-1}$
Attached biomass concentration	2.67	$ m gTSSL^{-1}$
Initial DCF concentration (reactors)	0	$\mu\mathrm{g}\mathrm{L}^{-1}$
DCF influent concentration	5	$ m \mu gL^{-1}$
k_{biol} (AS, batch-test)	0.02283	$\mathrm{L}\mathrm{d}^{-1}\mathrm{gTSS^{-1}}$
k_{biol} (AS, literature)	0.5	$\mathrm{L}\mathrm{d}^{-1}\mathrm{gTSS^{-1}}$
k_{biol} (attached biomass, batch-test)	0.1357	$L d^{-1} gTSS^{-1}$
k_{biol} (attached biomass, literature)	1.5	$L d^{-1} gTSS^{-1}$

2.3 Tracer Experiment

The Tracer experiments were performed on the pilot plant (Levenspiel, 1999). A known quantity of NaCl solution, serving as the tracer, was prepared with an initial NaCl concentration of 8 g L⁻¹. A total of 38.4 g of this NaCl solution was introduced as a pulse input into the influent of the reactor (Appendix A.4). The electrical conductivity of the reactor's effluent and at various points within the system (Sludge reactor Type 1, Sludge reactor Type 2, and MBBR Type 3) was continuously monitored using conductivity probes. Data was recorded with a MultiLine Multi 3510 IDS (Table 2.5.1) at regular time intervals until the tracer concentration returned to its baseline level.

Calibration Curve

A calibration curve was established that correlates the measured electrical conductivity ($\mu S cm^{-1}$) with the tracer concentration ($g L^{-1}$) to accurately convert the raw conductivity data into meaningful concentration values (Igbokwe et al., 2015). A linear relationship was assumed between conductivity and NaCl concentration, represented by the equation:

$$C = \frac{\kappa - \kappa_0}{m} \tag{2.3.1}$$

 $C = \text{NaCl concentration } (gL^{-1});$

 $\kappa = \text{Measured conductivity } (\mu \text{Scm}^{-1});$

 $\kappa_0 = \text{Intercept of the calibration curve } (\mu \text{Scm}^{-1});$

 $m = \text{Slope of the calibration curve } (\mu \text{Scm}^{-1}(\text{gL}^{-1})^{-1}).$

Calibration curves were developed by adding several NaCl solutions of known concentrations to the different sludges from reactor Type 1 and measuring their conductivity. The raw data for these calibrations are presented in Table 2.3.1 Linear regression was performed to determine the slopes and intercepts for each line. These parameters, used for converting conductivity measurements to tracer concentrations, are summarized in Table 2.3.2 The derived slope and intercept values were then applied to the measured conductivity data from the tests to obtain the tracer concentrations over time.

NaCl Conc. (gL^{-1})	Conductivity Line 1 (μScm^{-1})	Conductivity Line 2 (μScm^{-1})	$\begin{array}{c} \textbf{Conductivity Line 3} \\ (\mu \text{Scm}^{-1}) \end{array}$
0	1000	1070	1036
0.25	1547	1583	1543
0.5	2130	2130	2060
1	3080	3180	3180
2	4840	5120	5090
4	8460	8660	8460
8	16500	15530	14890

Table 2.3.1: Calibration Curve Measurements for Lines 1, 2, and 3.

Table 2.3.2: Calibration Curve Parameters for each Line, following $Y = \text{Slope} \cdot X + \text{Intercept}$.

Reactor Line	Slope	Intercept
	$(\mu Scm^{-1}(gL^{-1})^{-1})$	$(\mu \mathrm{Scm}^{-1})$
Line 1	1915	2000
Line 2	1802	1269
Line 3	1727	1650

2.4 Batch Test Setup

Batch tests were conducted to assess the microbial activity and treatment performance of different carriers under controlled laboratory conditions. These tests allowed precise regulation of operational parameters, including substrate concentration, temperature, pH, and aeration, facilitating the evaluation of specific biological processes such as nitrification and micropollutant removal. Both pilot-scale and full-scale plant carriers were included to directly compare their performance under the same conditions (Figure 2.4.1).

The carriers used in the experiments, along with their technical specifications, are summarized in Table 2.4.1 The pilot plant utilized Biofilm chip M, while the full-scale plants included Bad Ragaz (Biofilm chip M), Lenzburg (BWT15), and Roderstorf (Biofilm chip P). For the pilot plant, carriers were extracted during the last weeks of operation, after completion of all studies

in the continuous pilot system, ensuring that the biofilm had undergone the full operational period before laboratory testing. For carrier-based biofilm experiments, diclofenac removal was normalized to the total carrier surface area to account for differences in carrier number or size, enabling direct comparison of degradation efficiency per unit biofilm surface (see Annex A.7 for calculation details).

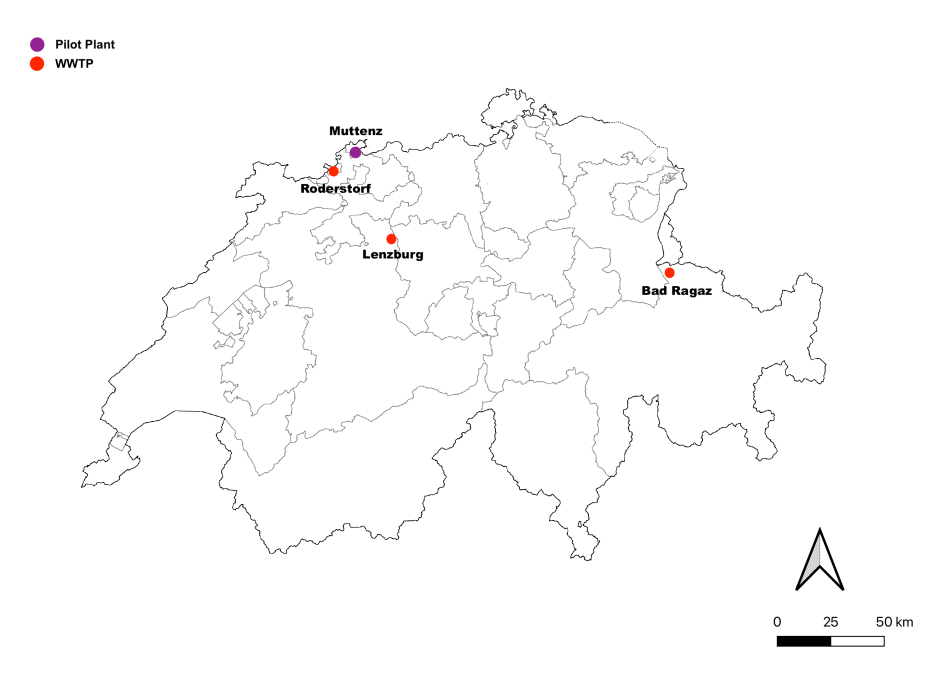


Figure 2.4.1: Map of Switzerland with the locations of the Wastewater Treatment Plants (WWTPs) and the Pilot plant used for batch tests (Swiss Confederation & swisstopo, |2025|).

	Bad Ragaz - PP	Lenzburg	Roderstorf	Unit
Model	Biofilm chip M	BWT15	Biofilm chip P	-
Company	Veolia	Biowater Technology AS	Veolia	-
Material	HDPE	HDPE	HDPE	-
Length	2.2	5	3.1	mm
Diameter	45	14.5×14.5	45.4	mm
Specific Surface	1200	828	900	$\mathrm{m}^2/\mathrm{m}^3$
Openings	small	medium	small	_

Table 2.4.1: Carriers Technical Information (Z. Zhang et al., 2022).

2.4.1 Nitrification Experiments

Nitrification experiments (Gong et al., 2022; Kim et al., 2020) were performed to confirm the presence and activity of nitrifying microorganisms within the carriers. Carriers were obtained from large-scale municipal wastewater treatment plants (Bad Ragaz, Lenzburg, and Roderstorf) as well as from the pilot plant (PP; Line 1, Line 2, Line 3). All batch tests were conducted in reactors filled to a 30% volume ratio with carriers to emulate operational conditions. Pilot plant experiments used 1 L reactors containing 35 carriers from each line (due to the limited availability of carriers), while real plant experiments used 2 L reactors with approximately 70

carriers from Bad Ragaz, 70 from Roderstorf, and 200 from Lenzburg. Continuous aeration at 1 atm was applied to maintain aerobic conditions, and pH was controlled at 7.5 for both pilot plant and real plant tests. Temperature was maintained at 24°C throughout the experiments. Post-membrane filtration wastewater from FHNW PTC was used in pilot plant experiments to reduce the influence of organic matter and other constituents present in raw wastewater. Ammonium was added as NH₄Cl at 158 mg L⁻¹, resulting in an initial NH₄-N concentration of 40 mg L^{-1} (Appendix A.1). Experiments with real plant carriers used raw wastewater from the FHNW PTC Kubuk tank as the matrix (Figure 2.4.2). The surface-related nitrification rate, R_v , normalized to the total carrier surface area, was calculated to compare the nitrification performance of different carriers (Annex A.2).

Sampling was performed at defined intervals of t = 0, 0.5, 1, 2, 4, 6, 8, 10, 24, 48, 60, and 72 hours. Ammonium (NH₄⁺) and nitrate (NO₃⁻) concentrations were determined using Merck test kits (Table 2.5.2). Nitrate accumulation was considered the primary indicator of nitrification, and the volumetric production rate was derived from the temporal change in nitrate concentration.

2.4.2 Diclofenac Removal Experiments

Batch incubation experiments were conducted to compare diclofenac removal between activated sludge and carrier-attached biofilms, and to evaluate pilot plant performance relative to full-scale wastewater treatment plants under comparable conditions. Experiments were carried out in 2-L Schott glass bottles containing either AS or biofilm-coated carriers. Sludge sources included FHNW Process Technology Center (PTC), WWTP Bad Ragaz, and WWTP Lenzburg, while carriers were inoculated with sludge from WWTP Bad Ragaz, WWTP Rodersdorf, WWTP Lenzburg, and the pilot plant.

After inoculation, systems were stabilized for 4 h before spiking DCF to a target concentration of 200 μ g/L (Annex A.6). All incubations were performed in duplicate under continuous aeration to maintain oxic conditions, with pH adjusted as necessary using 2 M HCl or NaOH. Water samples (10 mL) were collected at defined time points, filtered through 25 mm HPLC syringe filters (PP, 0.45 μ m, Table 2.5.4), and stored at (-20 °C) until analysis (Section 2.5.5).

Sampling schedules were tailored to the expected degradation behavior: for carrier-based biofilm systems, samples were collected at 0, 0.5, 0.8, 2, 4, 6, 8, 20, 32, 44, 56, 104, 128, 152, 176 h, while for activated sludge systems, sampling was performed at 0, 2, 4, 6, 8, 10, 24, 36, 48, 60, 72, 84, 204, 216 h. The different sampling strategies reflect the expected kinetics: slower DCF degradation in sludge systems required longer-term monitoring, whereas carrier-based biofilms exhibited faster initial degradation, necessitating more frequent sampling within the first 24 h to capture early dynamics accurately. To ensure comparability, the PTC sludge batch test was repeated at a TSS concentration similar to the other two sludge-based batch tests $(X_{\text{TSS}} \approx 2 \text{ grss} \cdot \text{L}^{-1})$.



Figure 2.4.2: Batch test setup for diclofenac removal experiments. In the picture Carriers from full-scale plants were used: from left to right, Roderstorf, Lenzburg, and Bad Ragaz.

2.5 Analytics

Various analytical techniques were employed to monitor water quality parameters and pollutant concentrations throughout the study. These analyses were essential not only for evaluating treatment performance, but also for verifying the correct setup and operational stability of both the pilot plant and the batch experiments.

2.5.1 Reagents and Analytical Equipment

Several devices and materials were used in the laboratory to carry out the measurements and analyses described in this study. These are listed in the following section.

Table 2.5.1: Overview of the main devices used in the laboratory

Device	Supplier
Photometer DR 6000	Hach Lange GmbH
Cuvette 50 mm High Precision Cell	Hellma Analytics
Thermostat HT 200 S	Hach Lange GmbH
Vacuum oven VD 23	Binder
Muffle furnace L $40/11/B180$	Nabertherm GmbH
Scale XSR105	Mettler Toledo
Scale PES	Kern
Moisture analyzer DBS	Kern
Total Organic Carbon Analyzer TOC	Hach Lange GmbH
Centrifuge	Eppendorf 5804 R
MultiLine Multi 3510 IDS	WTW
Piston pipettes	Accumax
HandyStep Touch S	Brand
Agilent 1260 Infinity LC system $+$ 6460 QQQ-MS	Agilent Technologies
Microscopy Olympus IX83	Olympus

Table 2.5.2:	Overview	of all	test-kits	used in	the	laboratory.
--------------	----------	--------	-----------	---------	-----	-------------

Test-kit	Supplier	Substance measured	$\begin{array}{c} \textbf{Range} \\ (mgL^{-1}) \end{array}$
Merck test	Merck	$NH_4^+ - N$	0.010 – 3.00
Merck test	Merck	$NO_3^ N$	0.3 – 30.0
Merck test	Merck	$NO_2^ N$	0.002 – 1.00
LCK 349	Hach Lange GmbH	P	0.05 - 1.5

Table 2.5.3: Overview of chemical compounds used in the laboratory.

Compound	Formula	Supplier	CAS-number	Description
Sodium chloride	NaCl	Sigma-Aldrich	12125-02-9	ACS reagent
Iron(III) chloride	$FeCl_3$	Thommen-Furler AG	7705-08-0	Solution 40%
Ethanol	C_2H_5OH	Thommen-Furler AG	64-17-5	abs. not denat.
Sodium hydroxide	NaOH	Sigma-Aldrich	1310-73-2	Pellets
Hydrochloric acid	HCl	Sigma-Aldrich	7647-01-0	37% water sol.
Ammonium chloride	$\mathrm{NH_4Cl}$	Sigma-Aldrich	12125-02-9	ACS reagent
Nanopure water	H_2O	Lab U1	-	Various use
Acetonitrile	C_2H_3N	Sigma-Aldrich	75-05-8	A. S.
Formic acid	$\mathrm{CH_2O_2}$	Sigma-Aldrich	64-18-6	A. S.
Diclofenac 13C ₆	$\mathrm{C}_{14}\mathrm{H}_5{}^{13}\mathrm{C}_6\mathrm{Cl}_2\mathrm{NO}_2\mathrm{Na}$	NeoChema	1261393-71-8	A. S.
Sodium diclofenac	$C_{14}H_{10}Cl_2NNaO_2$	Sigma-Aldrich	15307-79-6	A. S.

Table 2.5.4: Overview over important consumables used in the laboratory.

Consumable	Supplier	Description	
Syringe filter	Infochroma	AG 8825Y-P-4, 25 mm Yeti	
		Spritzenfilter, PP, 0.45 μm	
Syringe filter	Infochroma	AG 8825Y-P-4, 25 mm Yeti	
		Spritzenfilter, PVFE, $0.45~\mu m$	
Syringe filter	Infochroma	AG 8825-Y-N-4, 25 mm HPLC	
		Spritzenfilter, Nylon, $0.45~\mu m$	
Syringe	Infochroma	Plastic monouse, 20 mL	
pH test strips	Macherey-Nagel	pH-Fix 0–14, fixed indicator	
Glass vials	WICOM	-	
Caps	Agilent	Plastic monouse	
Pastette plastic pipettes	Agilent	Plastic monouse	
Falcon tube	Infochroma	15 mL Plastic monouse tubes	

2.5.2 Monitoring of Standard Parameters

Standard water quality parameters were monitored throughout the experiments to assess the general performance of the pilot plant and batch tests (Section 3). Measurements were performed at regular intervals to capture temporal variations in the reactors and clarifiers (Section 2.1.1).

Results from these analyses provided information on nutrient removal efficiency and biomass activity, supporting the interpretation of diclofenac degradation data. The use of standardized test kits ensured comparability and reliability of the measurements across different compartments and experimental setups (Table 2.5.2).

Phosphorus Monitoring

Phosphorus (P) concentrations were measured at sampling point 1 (Figure 2.1.5) using commercially available test kits (CK 349, Hach Lange GmbH), with a detection range of $0.05-1.5 \text{ mg L}^{-1}$

(Table 2.5.2). The test kits allowed for reliable quantification of orthophosphate, which was used as an indicator of phosphorus removal efficiency in the treatment lines. The influent phosphorus concentration data served as the basis for calculating the required coagulant dose, allowing the appropriate dosing of iron chloride to achieve efficient phosphorus precipitation (2.1).

COD Monitoring

Total organic carbon (TOC) measurements were performed to indirectly estimate chemical oxygen demand (COD) at sampling points 1 and 5 (Figure 2.1.5). TOC was analyzed using a Total Organic Carbon Analyzer (Table 2.5.1), and the resulting carbon concentrations were converted to COD values using a stoichiometric conversion factor. A ratio of COD/TOC = 2.5 was applied, based on standard correlations for domestic and municipal wastewater matrices (Eddy, 2003). This approach enabled reliable monitoring of the organic load within the reactors while minimizing sample handling time and reagent use. The TOC-based COD estimation was used to evaluate the organic removal efficiency of the different treatment lines and monitor reactor performance over time.

Nitrogen Monitoring

Nitrification performance was assessed by measuring the concentrations of total nitrogen (TN), ammonium (NH_4^+), nitrite (NO_2^-), and nitrate (NO_3^-). These parameters served to evaluate both the removal efficiency of nitrogenous compounds and the microbial activity associated with the nitrification process. Samples were analyzed using Merck test kits for NH_4^+ , NO_2^- , and NO_3^- , or with a Total Organic Carbon Analyzer (TOC, Hach Lange GmbH) for TN (Table 2.5.2). In the initial phase of the experiment, nitrogen concentrations were highly variable, requiring frequent dilution of samples with nanopure water to remain within the detection limits of the test kits.

Total Suspended Solids Monitoring (TSS)

Total suspended solids (TSS) measurements were conducted regularly using the moisture analyzer listed in Table 2.5.1. On each sampling day, a 10 mL sample was taken from the second-stage activated sludge (AS) reactor using a 10 mL plastic syringe. The sample was then placed directly into the moisture analyzer, and TSS concentrations were obtained after approximately two hours. These measurements served two main purposes: to determine the time required for sludge concentrations to stabilize within the pilot system, and to assess the three different biomass solids retention times (SRT) set in the treatment lines. This test was fundamental to continuously verify that the SRT values remained consistently different among the lines and that operational conditions were stable over time. In addition, waste sludge was occasionally sampled and analyzed for TSS to estimate the amount of sludge being removed from the system and to further confirm that the different SRTs were being effectively maintained across the treatment lines.

PH Monitoring

PH measurements were conducted using pH sensors measuring directly from each reactor at sampling points 2 and 4 (Figure 2.1.5). The sensors were connected to a MultiLine Multi 3510 IDS WTW device (Table 2.5.1) and were calibrated regularly following the manufacturer's recommendations to ensure accurate readings over time. The pH was checked daily and monitored to remain within a range of 7.5 to 8.0 at point 2 and between 6.5 and 7.5 at point 4. These data were essential to verify pH stability across the three treatment lines and ensure optimal conditions for biological processes (Henze et al., 2008).

Dissolved Oxygen Monitoring

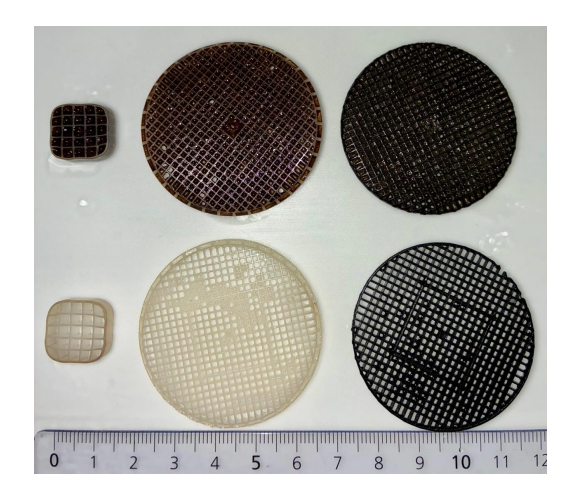
The concentrations of dissolved oxygen (DO) were monitored using in-line optical DO sensors connected to a MultiLine Multi 3510 IDS WTW device (Table 2.5.1). Sensors were installed in moving bed biofilm reactors (MBBR) (Point 4, Figure 2.1.5) to assess whether sufficient oxygen was supplied to carriers. These sensors provided continuous real-time measurements, which were crucial for maintaining aerobic conditions, particularly for effective nitrification. DO concentrations were maintained above 5 mg L^{-1} to ensure adequate oxygen transfer, especially within the biofilm on the carriers. Routine calibration and cleaning were performed to prevent drift and fouling of the sensor. DO data were logged and analyzed to assess oxygen availability in each line, ensuring that comparable aerobic conditions were maintained in all treatment configurations (Gujer, 2007).

Temperature Monitoring

Temperature was monitored using in-line sensors connected to a MultiLine Multi 3510 IDS WTW device (Table 2.5.1) throughout the experimental period to ensure that the reactors operated within a suitable range for biological processes. During the spring months, the water temperature in the system remained stable at approximately 20°C, while in summer it increased slightly to around 22°C. These values fall within the optimal range for microbial activity in conventional biological wastewater treatment systems (Gujer & Henze, 2008).

2.5.3 Determination of Carrier-Attached Biomass

To determine the biomass attached to the carriers, five replicates consisting of five carriers each were dried overnight at $105\,^{\circ}$ C and then weighed. Subsequently, the carriers were soaked in a $2\,\mathrm{mol}\,\mathrm{L}^{-1}$ HCl solution overnight and subjected to a cleaning procedure involving sonication, stirring, and scrubbing. This was followed by two rinses with concentrated $\mathrm{H}_2\mathrm{SO}_4$ (98%) and three rinses with Nano-Pure water over the course of four days, including additional overnight soaking periods. Finally, the cleaned carriers (Figure 2.5.1) were dried overnight and reweighed to determine the biomass mass, following the method described by (Jewell et al., 2016). Five replicates were measured over the course of the batch experiments.



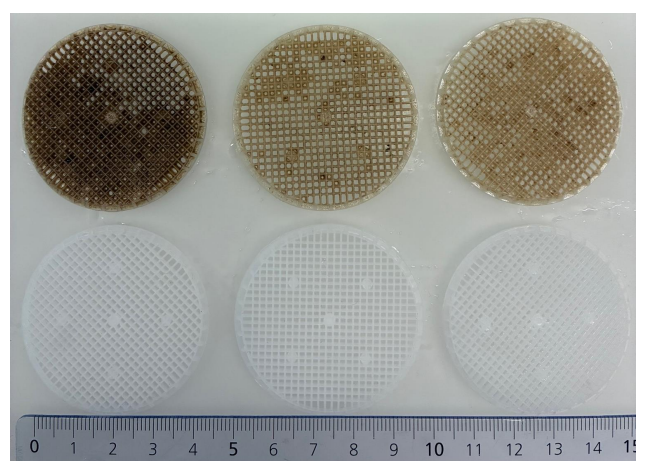


Figure 2.5.1: Biomass-attached versus cleaned carriers from left to right: Real Plants (Lenzburg, Bad Ragaz, Roderstorf) and the Pilot Plant (Line 1, Line 2, Line 3).

2.5.4 Fluorescence Microscopy for Biofilm Observation

Fluorescence microscopy was employed to qualitatively assess biofilm development on carriers during the experimental period. Samples of carriers were collected at defined intervals, gently rinsed with sterile phosphate-buffered saline (PBS) to remove loosely attached particles, and subsequently stained with fluorescent dyes targeting microbial cells and biofilm components. In particular, nucleic acids were visualized using 4',6-diamidino-2-phenylindole (DAPI), which binds strongly to DNA and allows for the detection of both bacterial and eukaryotic cells under UV excitation (Porter & Feig, 1980). In selected samples, additional staining with SYBR Green I was applied to confirm total cell distribution within the biofilm matrix.

Microscopic observations were performed using an epifluorescence microscope (Table 2.5.1) equipped with filter sets for DAPI and SYBR Green. Images were acquired with a high-resolution digital camera and processed for qualitative evaluation of cell distribution and relative biofilm coverage. While not quantitative, fluorescence microscopy provided complementary information to gravimetric biomass measurements and supported the interpretation of biofilm growth dynamics described in Section 3.1.3.

2.5.5 Diclofenac Concentrations

Diclofenac (DCF) concentrations were determined using direct injection liquid chromatography coupled with tandem mass spectrometry (LC-MS/MS). The analytical setup consisted of an Agilent 1260 Infinity liquid chromatography system coupled to an Agilent 6460 triple quadrupole mass spectrometer (QQQ-MS), as listed in Table $\boxed{2.5.1}$. Chromatographic separation was achieved using a gradient high-performance liquid chromatography (HPLC) method with a mobile phase composed of water and acetonitrile, both containing 0.1% formic acid. An ACQUITY HSS T3 UPLC column (1.8 µm, 3.0×100 mm; Waters, Switzerland) was used for compound separation. DCF detection and quantification were performed in positive electrospray ionization mode on the basis of characteristic fragment ions. To account for matrix effects and variability in measurement, a stable isotope-labeled internal standard (Diclofenac- $^{13}C_6$) was added to all samples prior to analysis ($\boxed{2.5.5}$). Sample preparation was conducted in 15 mL Falcon tubes. Each

tube was spiked with 25 μ L of internal standard solution, followed by the addition of 4.5 mL of nanopure water and 0.5 mL of sample. The mixture was homogenized using a vortex mixer before being transferred to LC-MS/MS vials for analysis. The dilution factor was adjusted as necessary to ensure DCF concentrations were within the calibration range. Tests confirmed that the use of different syringe filter types (see Table $\boxed{2.5.4}$) had no measurable influence on DCF concentrations, ensuring consistency across all prepared samples. All analyses were carried out in collaboration with analytics specialists Benjamin Gygax and Albin Sofjani (Appendix \boxed{D}).

Table 2.5.5: Retention times, MS1 and MS2 m/z ratios of precursor and fragment ions, as well as detection of DCF in LC-MS/MS measurement

Substance	ISTD ^a	Rt [min]	MS1 m/z [-]	$\frac{\mathbf{MS2} \ \mathbf{m/z}}{[-]}$
Diclofenac- ¹³ C ₆	Yes	10.32	302.1	220
Diclofenac	No	10.34	296.0	215.1
Diclofenac	No	10.34	296.0	214.1

^aInternal Standard

Chapter 3

Results and Discussion

This chapter presents and discusses the main experimental results. It begins with the performance of the pilot plant, including standard parameters, ASM3 simulations, biofilm development in relation to SRT, and hydraulic characterization through tracer experiments. The focus then shifts to batch tests, starting with nitrification performance, followed by diclofenac removal under controlled conditions using activated sludge, carriers from full-scale plants, and carriers from the pilot plant. Finally, removal in the pilot plant is examined through both model simulations and continuous flow observations.

3.1 Performance of the Pilot Plant

The startup phase of the pilot plant was affected by several operational delays. A blockage of the main influent pump at the PTC temporarily interrupted the flow of raw wastewater, directly impacting the pilot plant schedule. Persistent clogging from sludge and fibrous material required increased maintenance during the first months of operation, and an unexpected pH drop following a temporary stop of the main plant inhibited nitrifiers. These events illustrate the sensitivity of small-scale systems to external disturbances and the challenges inherent to pilot-scale operation (Section 2.1 and Annex C).

Although combined treatment with powdered activated carbon (PAC) was initially considered, it was not implemented due to these unavoidable delays. This allowed the study to focus on evaluating the intrinsic performance of the hybrid MBBR system, providing direct insights into carrier performance and biofilm development under controlled conditions.

The following sections provide a detailed overview of the pilot plant's performance and discuss the main experimental results.

3.1.1 Standard Parameters

The performance of the pilot plant with respect to conventional wastewater parameters is summarized in Figures 3.1.1, 3.1.2 and 3.1.3. The initial 3–4 weeks were characterized by strong variability across all parameters, reflecting start-up dynamics, microbial colonization, and biofilm maturation (Eddy, 2003).

Following stabilization (day 30), influent COD concentrations of approximately 500 mg L^{-1} were consistently reduced to below 100 mg L^{-1} across all effluents during the startup phase, and reached even lower values towards the end of the experiments. This represents a great organic matter removal efficiency, which, although somewhat lower than the typical performance of fullscale systems treating higher-strength wastewater, remains fully consistent with the behavior expected from aerobic HMBBR configurations (Wanner & Gujer, 2006). Effluent TSS values differentiated clearly between the three experimental lines in accordance with the distinct sludge retention times (SRT) applied, confirming effective biomass retention and the maintenance of the intended operational regimes. In Line 3, however, TSS values were higher than expected and also deviated from those predicted by the model (Section 2.2.1), most likely due to the instability of the line and the elevated maintenance requirements encountered throughout the experimental period. Nevertheless, these differences still highlighted the contrast among the three lines and provided a suitable basis for analyzing and comparing their performance (Section 3.1.3) (Andreottola & colleagues, 2000). Dissolved oxygen (DO) levels in the MBBR reactors remained consistently above 6 mg L^{-1} , ensuring sufficient availability for both heterotrophic and nitrifying populations (Tatari et al., 2017). Phosphorus concentrations in the influent were monitored to verify correct coagulant dosing (Appendix A.3). Phosphorus concentrations in the influent were monitored to verify correct coagulant dosing (Appendix A.3). Occasional peaks were observed, attributable to variability in raw wastewater composition, but effluent values remained within ranges comparable to full-scale WWTPs, confirming that the pilot plant achieved effective phosphorus elimination despite its smaller scale. Random spot checks of effluent P indicated

elimination rates exceeding 90%, confirming that removal was actually achieved. Nevertheless, the primary role of phosphorus monitoring in this study was to ensure accurate coagulant dosing, while systematic assessment of P elimination was not within the main scope (Figure 3.1.1).

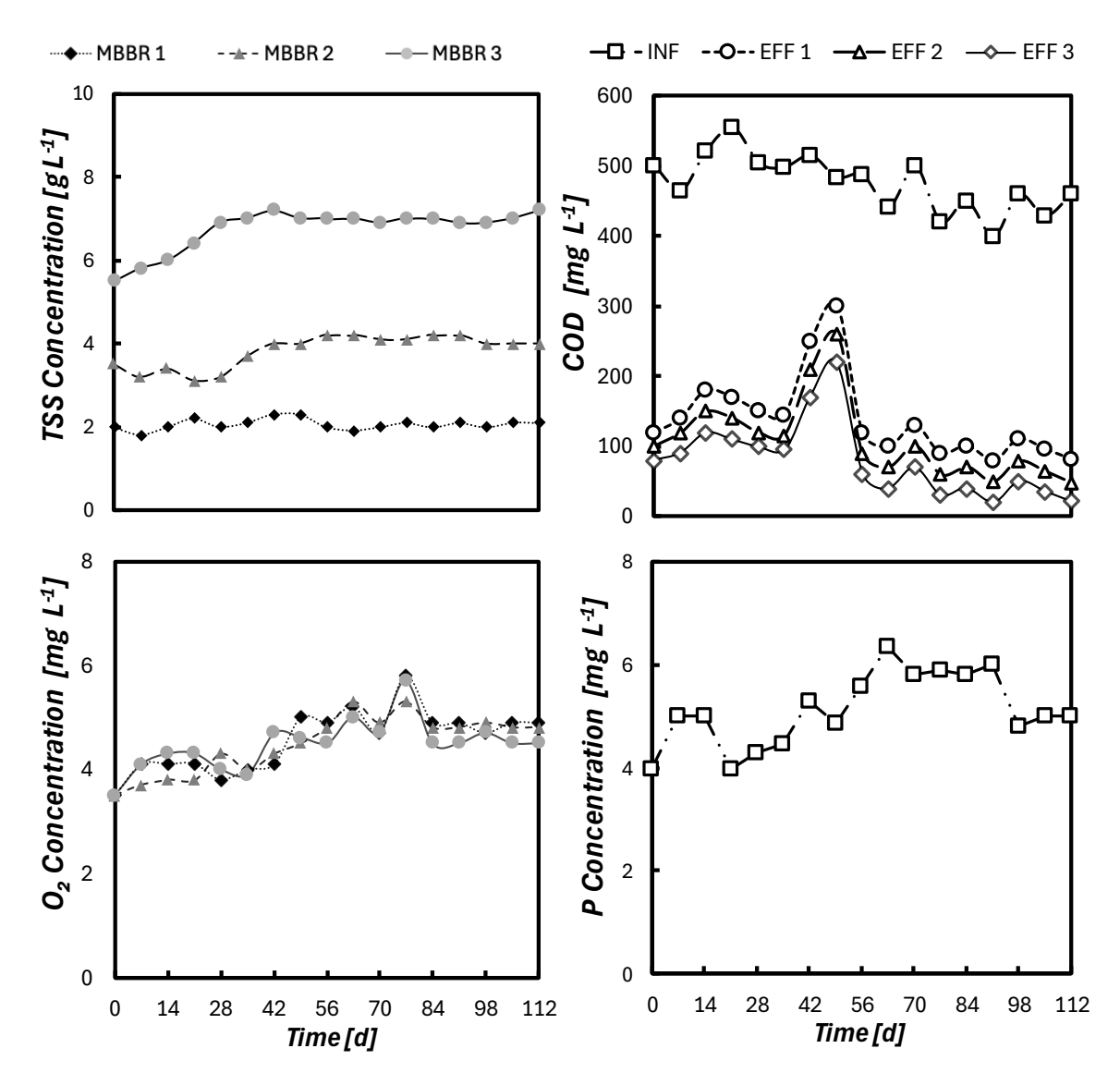


Figure 3.1.1: Time series of total suspended solids (TSS), phosphorus concentration, dissolved oxygen concentration, and chemical oxygen demand (COD) measured in the reactors over the experimental period.

Reactor temperatures were stable at $21 \pm 0.5^{\circ}$ C. In contrast, pH exhibited a sharp decline from neutral (7.5) to acidic conditions after day 35 (Figure 3.1.3). This coincided with a blockage at the PTC, which interrupted the influent wastewater supply, while the coagulant dosing system continued operating. Because the safety system did not detect the absence of outflows from the pilot plant reactors, iron chloride was dosed continuously, leading to rapid acidification through proton release during hydrolysis (Gebbie, 2006). The resulting pH drop strongly inhibited nitrifying microorganisms, consistent with literature describing the sensitivity of ammonia-oxidizing and nitrite-oxidizing bacteria to acidic conditions (Anthonisen et al., 1976). This incident caused a collapse of nitrification with cascading effects on all monitored parameters, and highlighted the vulnerability of pilot-scale systems to external operational disturbances.

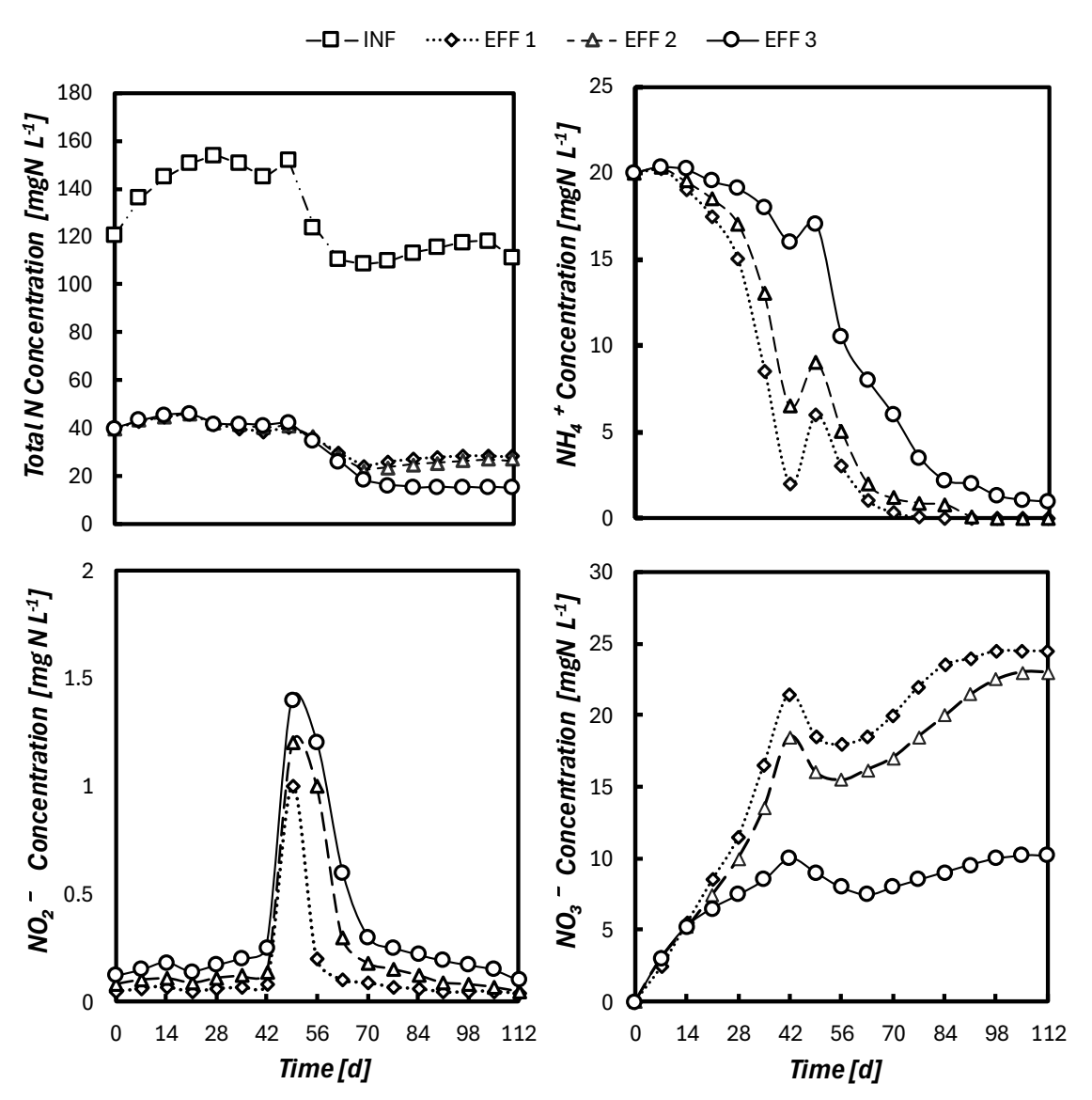


Figure 3.1.2: Time series of nitrogen species: total nitrogen (TN), ammonium (NH₄⁺), nitrate (NO₃⁻), and nitrite (NO₂⁻) concentrations in influent and effluents over the experimental period.

Prior to the incident, ammonium removal was nearly complete, and nitrate accumulation indicated efficient two-step nitrification. Some inconsistencies between influent total nitrogen (TN) and the sum of NH₄⁺, NO₃⁻, and NO₂⁻ in the effluent were observed during the first months, partly attributable to influent variability, analytical sensitivity (Section 2.5.2), and unstable early biofilm development. Following acidification, ammonium concentrations rose sharply (20 mgN L⁻¹), nitrate accumulation decreased drastically, and TN removal efficiency decreased significantly (Figure 3.1.2). Nitrite remained generally low, suggesting strong inhibition of NOB without sustained intermediate accumulation. Recovery of nitrification required several weeks as biofilm communities re-established functional nitrifiers, delaying steady-state conditions and adequate biofilm thickness for stable nutrient removal (Rittmann & McCarty, 2001).

Overall, organic matter removal proved robust even under disturbance, while nutrient removal, particularly nitrogen, was highly sensitive to operational stability and pH control. The incident extended the time required to reach steady state and delayed biofilm maturation on car-

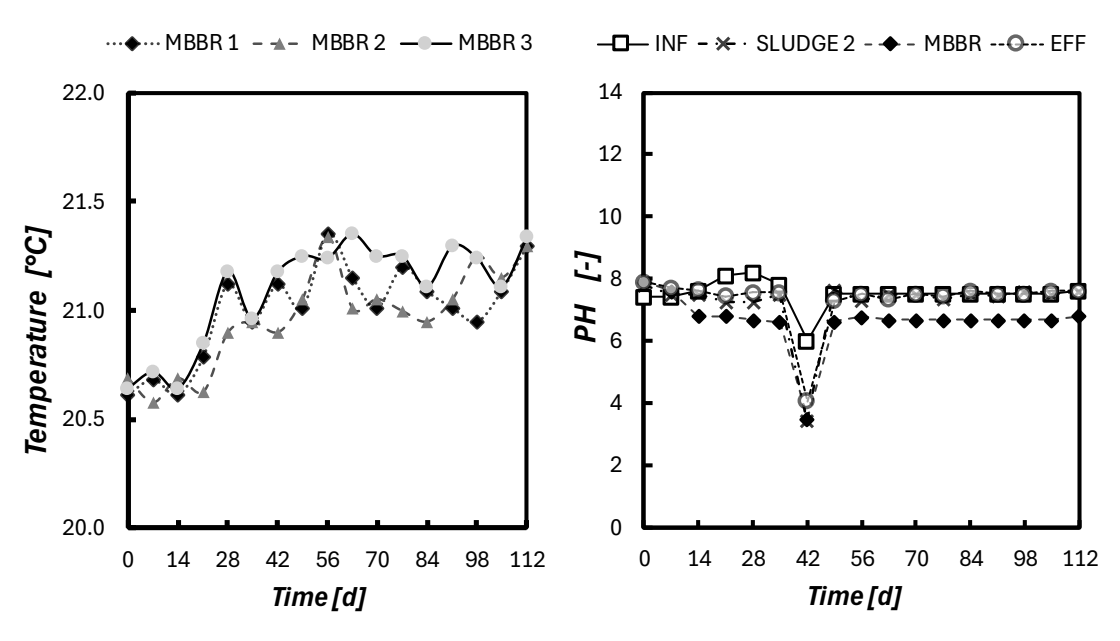


Figure 3.1.3: Time series of MBBR reactor temperature and pH in influent, sludge, and MBBR effluent over the experimental period.

riers. Only after restoring balanced nitrogen conversion could reliable conditions be achieved for the subsequent investigation of micropollutant removal, particularly diclofenac, which critically depends on stable biofilm activity.

3.1.2 ASM3 Simulations

ASM3 simulations were used to provide indicative predictions of activated sludge concentrations and nutrient/COD loading in the MBBR reactors. These results are based on assumptions from the model and may help to explore how substrate and nutrient availability could vary with sludge retention time (SRT), and how such variations might influence biofilm development and micropollutant removal.

The predicted influent concentrations to the MBBRs are reported in Table 3.1.1 TSS, XH, and XA increased with longer SRTs, with the highest values estimated for MBBR 3 (SRT 5 d). This may imply that a higher biomass inventory upstream could increase the amount of suspended material entering the MBBRs. Dissolved COD, on the other hand, decreased from MBBR 1 (SRT 2 d) to MBBR 3, suggesting more extensive substrate removal at longer SRTs. Ammonium followed a similar decreasing trend, while nitrate and nitrite increased. Together, these shifts point to a transition from substrate-rich, nitrogen-reduced influent under short SRTs to more substrate-limited, nitrogen-oxidized conditions under longer SRTs. Such changes in COD and ammonium availability could shape the metabolic environment for carrier biofilms, with shorter SRTs favouring higher substrate supply and longer SRTs potentially promoting conditions where co-metabolic or specialized pathways become more relevant.

The predicted effluent concentrations are shown in Table 3.1.2 These values complete the ASM3 outputs and provide a reference for comparison with the pilot plant monitoring data (Section 3.1.1). In the simulations, COD was consistently reduced to below 40 mg L^{-1} , while ammonium was only partially removed (12–13 mg N L^{-1}). This outcome suggests that nitrifica-

Table 3.1.1: Predicted activated sludge and nutrient concentrations in the MBBR reactors (influent to the reactors).

Parameter	MBBR 1	MBBR 2	MBBR 3	Unit
TSS	1.35	1.89	2.83	$ m gL^{-1}$
XH	0.77	0.97	1.21	$ m gCODL^{-1}$
XA	0.045	0.062	0.085	$ m gCODL^{-1}$
NH_4 - N	21.3	17.7	15.4	$ m mgNL^{-1}$
NO_x -N	56.1	61.0	64.9	$ m mgNL^{-1}$
Dissolved COD	67.8	58.0	38.1	$ m mgCODL^{-1}$

tion was not fully established under the assumed conditions, with residual ammonium persisting despite an increase in oxidized nitrogen species. The slight rise in NO_x -N and TN across the SRTs may indicate that nitrification occurred to some extent, but that autotrophic activity remained a limiting factor. This interpretation is reasonable given that the simulations are based only on the microbiological ASM3 framework, without accounting for any additional nitrification potential or biofilm-related processes in the MBBRs.

Table 3.1.2: Predicted effluent concentrations for the three simulated lines (ASM3 only).

Parameter	Eff 1	Eff 2	Eff 3	Unit
TSS	0.0024	0.0037	0.0054	$ m gL^{-1}$
NH_4 - N	13.4	12.8	13.4	$ m mgNL^{-1}$
NO_x -N	64.1	66.5	68.2	$ m mgNL^{-1}$
TN	77.9	79.8	82.1	$ m mgNL^{-1}$
COD	32.9	34.0	35.5	$ m mgCODL^{-1}$

Overall, the ASM3 simulations outline a shift in loading conditions across SRTs, from higher ammonium and COD supply under short SRTs to lower substrate availability and higher oxidized nitrogen under long SRTs. The predicted effluent values provide a baseline for evaluating how the actual pilot plant responds, particularly in terms of COD polishing and nitrogen removal.

3.1.3 Biofilm Development in Relation to SRT

Sequential monitoring of biofilm development by optical inspection, microscopy, and weight measurements enabled the distinction between early colonization and more advanced growth stages across the three lines (Section 2.5.3 and 2.5.4). During the initial phase, biofilm formation was slow and spatially heterogeneous, reflecting a typical lag phase in which pioneer microorganisms attach to the carrier surface and secrete extracellular polymeric substances (EPS) to facilitate further colonization (Rittmann & McCarty, 2001). At this stage, thin and patchy biofilm structures were observed. As growth progressed, the biofilm became denser and more continuous, with stratified microbial structures emerging. Weight measurements confirmed the gradual accumulation of biomass, while fluorescence staining revealed metabolically active microbial communities (Figure 3.1.4a), supporting the transition from initial attachment to a mature biofilm state.

Biofilm growth was strongly influenced by the suspended sludge SRT. In the experiment, Line 1, operated at the shortest SRT (2 days), developed the most active biofilm and achieved higher nitrification together with the highest diclofenac removal. Lines 2 (3 days) and 3 (5 days)

formed biofilms with lower activity, resulting in reduced removal rates. This pattern reflects the fact that in hybrid MBBRs, the suspended sludge SRT primarily governs the suspended biomass, while biofilm development on carriers proceeds largely independently (Henze et al., 2008). At shorter SRTs, lower suspended biomass concentrations lead to less substrate removal in the earlier reactors, which increases ammonia and COD loading to the subsequent reactors (Section 3.1.2). This higher substrate availability promotes faster colonization and activity of the biofilm on the carriers (Gujer & Henze, 2008).

Comparison with full-scale carriers from real WWTPs highlighted how substrate loading, hydraulic conditions, and SRT influence biofilm development. Pilot plant carriers displayed relatively thin but metabolically active biofilms (Section 3.3.2), whereas full-scale carriers supported thicker, more mature biofilms (Section 3.3.2) (Jewell et al., 2016). In the pilot system, the limited biofilm thickness resulted from lower substrate residence time and higher shear in the shorter SRT lines, which favored rapid substrate diffusion and high specific removal rates but restricted stratification. Complete nitrification required thicker biofilms, particularly after the pH shock, as slow-growing nitrifiers preferentially establish in deeper layers once stratification occurs (Eddy, 2003). Controlled waste sludge removal, corresponding to the calculated Q_{WAS} , maintained SRTs above the minimum for nitrification (SRT_{min}) , preventing washout of slow-growing nitrifiers while supporting ordinary heterotrophic organisms (OHOs) in oxidizing organic matter (Henze et al., 2008). In Line 1, higher substrate loading to the carriers at the shortest SRT promoted faster biofilm growth, resulting in thicker, more diverse biofilms with enhanced transformation potential. Lines 2 and 3, with longer SRTs and lower substrate flux to the carriers, developed thinner biofilms, reducing co-metabolic activity and micropollutant degradation (Rittmann & McCarty, 2001). Additionally, carrier-attached biofilms stabilized nitrification by seeding suspended biomass, particularly in Line 1.

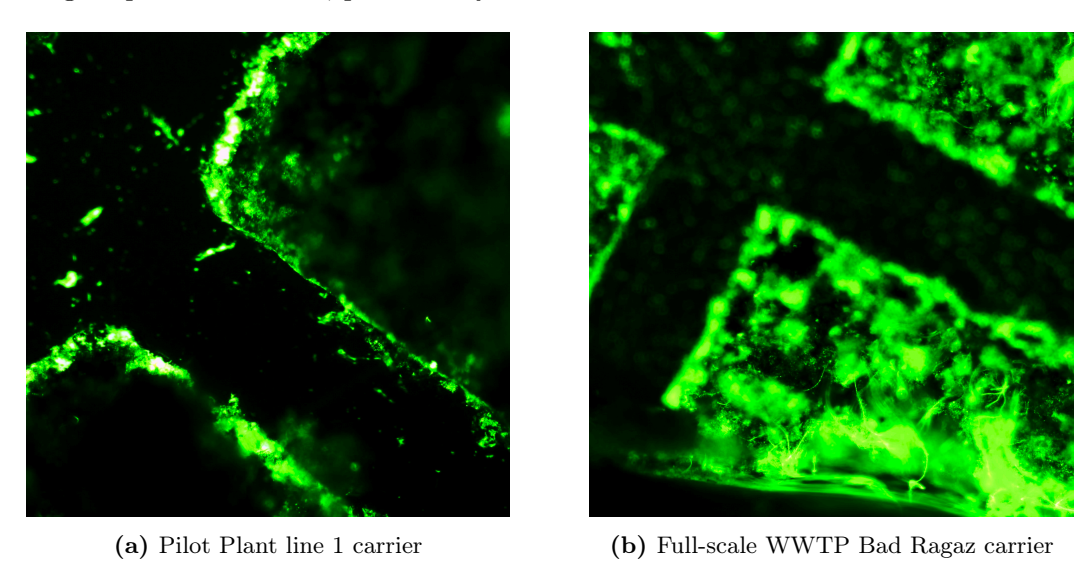


Figure 3.1.4: Comparison of biomass attached on carriers from pilot-scale and full-scale systems. Biofilm Chip M is shown, with live ecosystems highlighted in green. The full-scale WWTP carriers show a well-stratified and thicker biomass layer, whereas the pilot plant carriers exhibit a thinner biofilm.

3.2 Tracer Experiment

The tracer experiment was used to characterize the hydraulic behavior of the pilot plant reactors and to assess the presence of potential hydraulic shortcuts or dead zones that could reduce the effective treatment volume (Eddy, 2003) (Section 2.3). Conductivity measurements, converted to tracer concentrations, yielded breakthrough curves for Sludge 1, Sludge 2, and the MBBR of each pilot plant line. These experimental curves were compared with theoretical profiles calculated assuming ideal CSTR behavior, based on the pilot plant parameters listed in Table 2.1.2 and Table 2.1.5.

The comparison showed that measured and theoretical curves were in close agreement across all three lines, confirming that the reactors provided near-ideal mixing without significant hydraulic losses. The mean residence times and variance of the experimental curves matched the theoretical predictions, indicating that the effective treatment volumes corresponded well to the design values. Minor deviations observed in Line 3, likely related to slight stratification around the conductivity sensor, did not affect the overall hydraulic interpretation. Importantly, the absence of early peaks or long tails in the breakthrough curves suggests that neither short-circuiting or stagnant zones were present.

These results confirm that the observed biological performance of the pilot plant can be attributed to process conditions and biofilm development rather than hydraulic limitations. The validation of ideal hydraulic behavior provides a robust basis for interpreting the treatment data, particularly the diclofenac removal trends and biofilm accumulation on carriers (Figure 3.2.1).

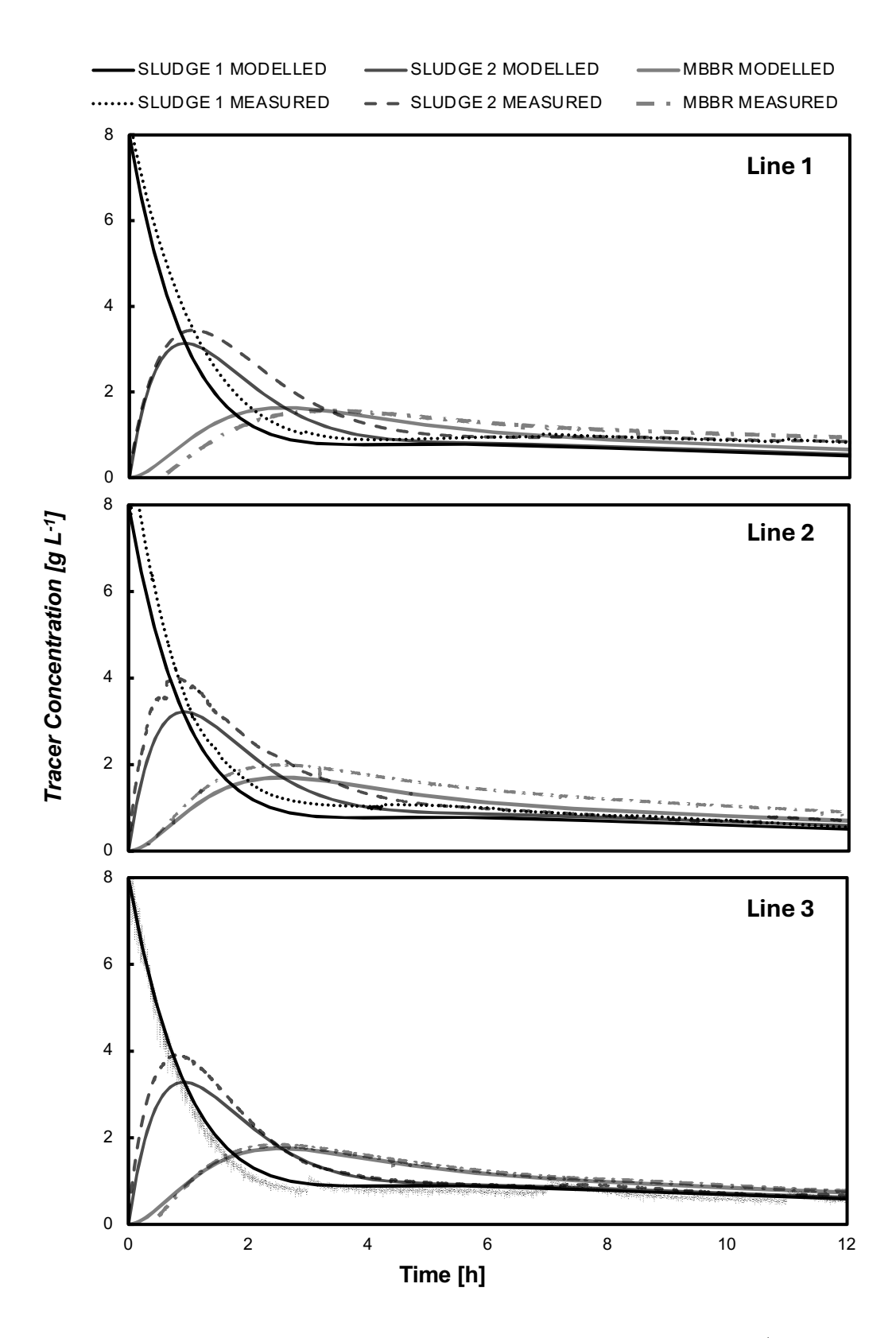


Figure 3.2.1: Breakthrough curves from tracer experiments for each pilot plant line (Line 1, Line 2, and Line 3), comparing measured tracer concentrations against theoretical profiles for the Sludge 1, Sludge 2, and MBBR reactor sections. The data illustrates the residence time distribution (RTD) and hydraulic behavior of each reactor.

3.3 Batch Tests

This section presents the results of the batch experiments designed to compare the biological performance of attached biomass (biofilm) and suspended biomass (AS), and to evaluate the influence of different carrier materials under controlled laboratory conditions (Section 2.4).

The main objective of these experiments was to assess how suspended sludge and carrier-attached biofilms contribute to diclofenac (DCF) removal, to identify potential differences between biomass types, and to determine whether the pilot plant, although in its initial operational phase, can reproduce degradation trends comparable to those observed in full-scale systems (Figure [2.4.1]). By situating the pilot plant results within the broader context of full-scale WWTPs, these experiments provide a basis for evaluating the reliability, representativeness, and transferability of pilot-scale findings to real-world applications and literature benchmarks on DCF elimination (Falås et al., [2012], [2013]; Jewell et al., [2016]).

3.3.1 Nitrification Performance

Nitrification activity showed a clear gradient across the three lines, with Line 1 highest, followed by Line 2 and Line 3. Figure 3.3.1 shows nitrate production kinetics, with linear models fitting well ($R^2 > 0.95$), confirming the reliability of the calculated rates. This trend reflects the different sludge retention times (SRT) in each line. Even at relatively low SRT, the HMBBR promotes the growth of nitrifying bacteria, increasing their abundance in the biofilm even under fast nutrient turnover. However, when compared to literature values $(0.7-3.5\,\mathrm{g\,N\,m^{-2}\,d^{-1}})$ (Di Trapani et al., 2008; Falås et al., 2012, 2013; Levstek & Plazl, 2009), the measured values in the pilot plant were approximately one order of magnitude lower. The maximum observed rate (Line 1: $0.0427\,\mathrm{g\,N\,m^{-2}\,d^{-1}}$) indicates limited nitrifying activity under the tested conditions. Table 3.3.1 summarizes the calculated slopes from the batch tests and the corresponding nitrification rates normalized by the carrier surface area. Normalization by surface area allows for comparison with literature values and highlights the extent of nitrifier colonization on the biofilm carriers (Section 2.4).

The reduced nitrification performance is likely due to incomplete biofilm development. Nitrifying biofilms typically require several months to mature fully, and the relatively short operation in this study probably led to suboptimal colonization of the carriers, reflected in the lower nitrification rates observed (Pellicer-Nàcher et al., 2013). Despite the low absolute rates, the presence of measurable nitrification across all three lines confirms colonization by nitrifying populations. This is a crucial prerequisite for investigating potential links between nitrification activity and Diclofenac removal. Nitrification was also evaluated in the real plant batch tests (as explained in Section 2.4.1). However, due to unstable operational conditions during the experimental period, the results lacked the precision required to establish a reliable correlation or quantifiable removal rate. Consequently, these data are not further discussed here.

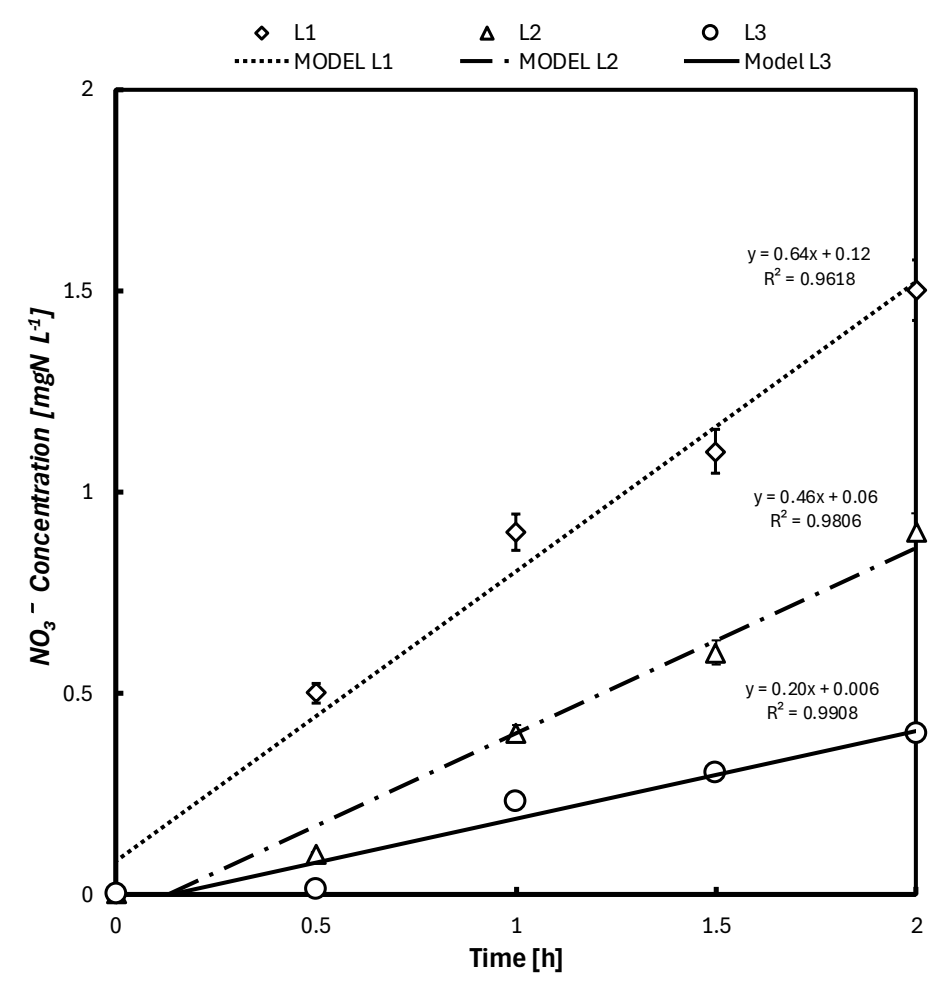


Figure 3.3.1: Nitrate production during batch tests for the three pilot plant lines. Linear models: Line 1 $(y = 0.64x + 0.12, R^2 = 0.96)$, Line 2 $(y = 0.46x + 0.06, R^2 = 0.98)$, and Line 3 $(y = 0.20x + 0.006, R^2 = 0.99)$.

Table 3.3.1: Nitrification rates of carriers in the pilot plant lines derived from batch tests. The rates R_v are normalized by the estimated surface area of the carriers, allowing comparison with literature-reported surface-related nitrification rates.

Parameter	Line 1	Line 2	Line 3
Production rate (slope)	0.64	0.46	0.20
$R_v \text{ NO}_3 \left[\text{gN/m}^2 \cdot \text{d} \right]$	0.0427	0.0280	0.0133

3.3.2 Diclofenac Removal

Diclofenac Removal with Activated Sludge

Diclofenac removal was investigated using activated sludge from Lenzburg, Bad Ragaz, and PTC (Figure 2.4.1). Results (Figure 3.3.2) Table 3.3.2) demonstrate measurable degradation over time (Section 2.5.5). Controlled batch tests with AS-only experiments provide a baseline for comparison.

For PTC sludge, two batch experiments were performed. The first, at $X_{TSS} \approx 7 \, \text{g}_{TSS} \cdot \text{L}^{-1}$,

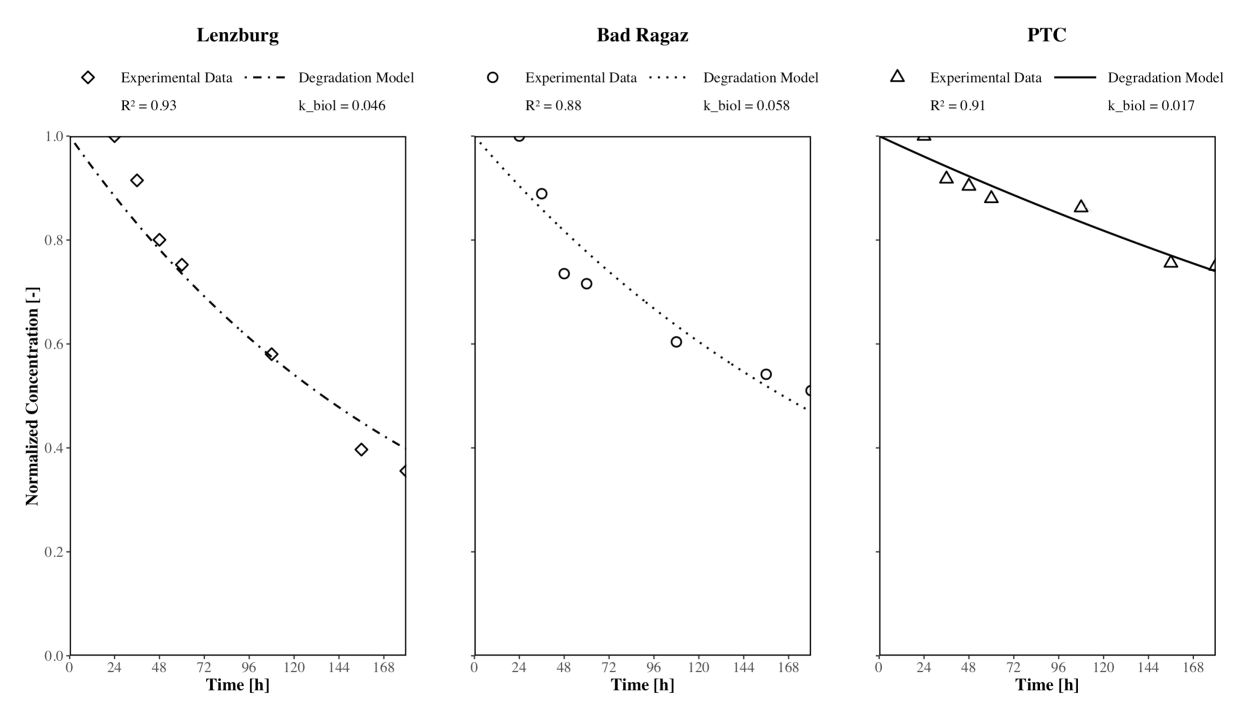


Figure 3.3.2: Diclofenac degradation kinetics for activated sludge from three different WWTPs. The plot show normalized DCF concentrations over time fitted with pseudo-first-order degradation models (Section 2.2.2).

showed pronounced fluctuations during the first 24 h, likely due to adsorption effects at high biomass concentrations. A second batch at $X_{\rm TSS} \approx 2.4\,{\rm g_{TSS}\cdot L^{-1}}$ produced more consistent results and is used for the analysis.

Measured pseudo-first-order biodegradation rates (K_{biol}) ranged from 0.017 to 0.058 $\text{L} \cdot \text{g}_{\text{TSS}}^{-1} \cdot \text{d}^{-1}$, with Bad Ragaz showing the highest rate $(K_{\text{biol}} = 0.057, R^2 = 0.88)$, followed by Lenzburg $(K_{\text{biol}} = 0.046, R^2 = 0.93)$ and PTC $(K_{\text{biol}} = 0.017, R^2 = 0.91)$, all within literature values (Di Trapani et al., [2008]; Falås et al., [2012], [2013]; Jewell et al., [2016]).

The first 24 h were excluded from K_{biol} estimation due to high variability likely related to adsorption. After this phase, pseudo-first-order kinetics confirmed diclofenac degradation in all sludges. Differences between plants indicate variable biodegradation potential, yet conventional AS alone is insufficient for complete removal under the tested conditions (Zając-Woźnialis et al., 2023).

Table 3.3.2: Summary of measured and literature values for X_{TSS} and K_{biol} from sludge batch tests.

		X_{TSS} literature		$K_{\rm biol}$ literature
	$(g_{TSS} \cdot L^{-1})$	$(g_{TSS} \cdot L^{-1})$	$(L \cdot g_{TSS}^{-1} \cdot d^{-1})$	$(L \cdot g_{TSS}^{-1} \cdot d^{-1})$
Lenzburg	2.68	n.a.	0.046	$\leq 0.01-0.1^{a}$
Bad Ragaz	1.74	$1.2 – 2.3^{\mathrm{a,b}}$	0.057	$\leq 0.01 – 0.1^{a,b}$
PTC	2.40	n.a.	0.017	$\leq 0.01 – 0.1^{a,b}$

^a (Falås et al., 2013) ^b (Falås et al., 2012)

Diclofenac Removal with Real Plants Carriers

Batch tests with carriers from the full-scale plants in Lenzburg, Bad Ragaz, and Roderstorf revealed distinct differences in diclofenac degradation capacity (Figure 2.4.1). Degradation followed pseudo-first-order kinetics (Section 2.2.2) with high R^2 values (>0.98), indicating that the model accurately describes the removal dynamics. Calculated K_{biol} values were highest for Lenzburg (0.763 $\text{L}\cdot\text{g}_{\text{TSS}}^{-1}\cdot\text{d}^{-1}$), intermediate for Bad Ragaz (0.527 $\text{L}\cdot\text{g}_{\text{TSS}}^{-1}\cdot\text{d}^{-1}$), and lowest for Roderstorf (0.210 $\text{L}\cdot\text{g}_{\text{TSS}}^{-1}\cdot\text{d}^{-1}$).

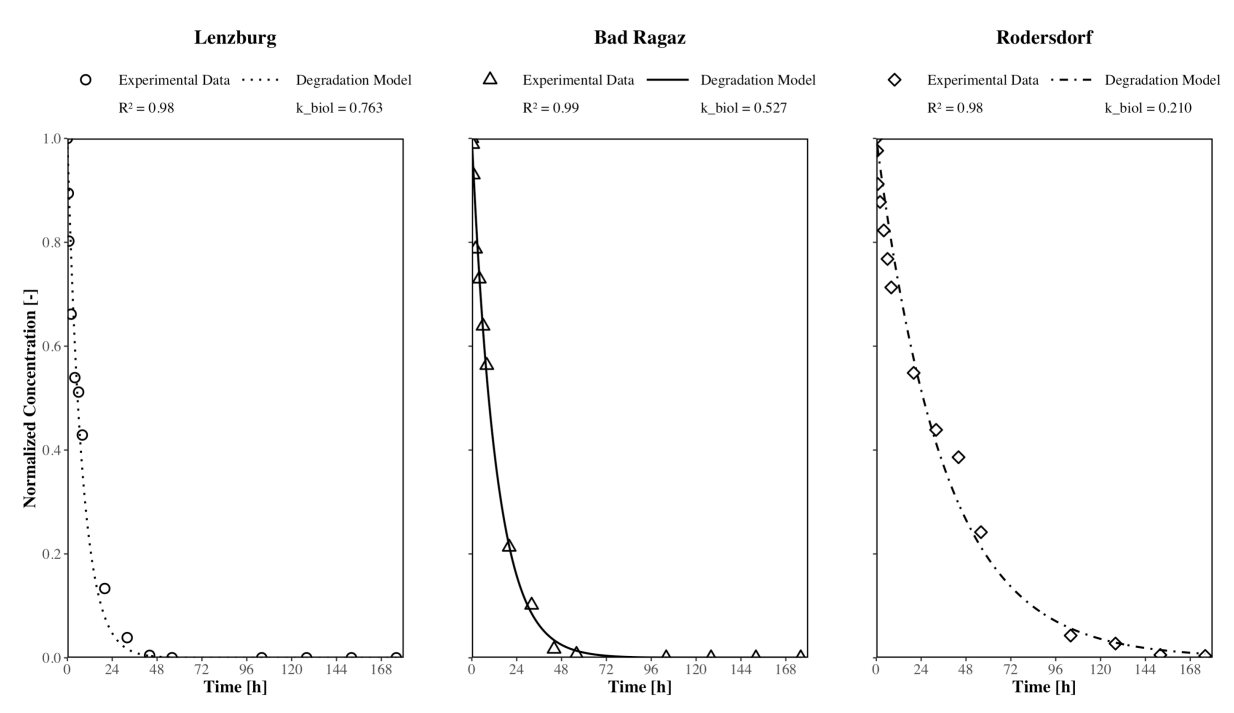


Figure 3.3.3: Diclofenac degradation kinetics for carriers from three full-scale WWTPs. Normalized DCF concentrations over time are fitted with pseudo-first-order degradation models (Section 2.2.2).

Carrier-attached biomass was determined following Jewell et al. (Jewell et al., 2016), but reproducibility was limited (Section 2.5.3). Consequently, X_{TSS} values may include wet biomass fractions or be affected by handling, which could influence the estimated K_{biol} . While Jewell et al. reported near-complete diclofenac removal within 24 h for Bad Ragaz carriers, in this study full elimination required approximately 36 h, likely reflecting differences in carrier sampling and biofilm heterogeneity rather than procedural inconsistencies.

Measured K_{biol} values fall within the ranges reported in the literature (Falås et al., [2012], [2013]) and are consistent with the observed elimination patterns (Figure [3.3.3]). Differences in carrier performance can be attributed to several interrelated factors. High mobility of Lenzburg carriers likely promoted uniform biofilm distribution and enhanced contact between the biofilm and diclofenac. Intermediate mobility of Bad Ragaz carriers and minimal movement of Roderstorf carriers suggest that low carrier mobility creates local stagnation zones, limiting substrate contact and reducing effective diclofenac exposure, which may slow microbial degradation. Well-dispersed biofilms on mobile carriers are expected to improve mass transfer of diclofenac, oxygen, and nutrients into the biofilm, whereas dense or uneven biofilms on poorly moving carriers may restrict substrate diffusion into deeper layers, reducing apparent biodegradation rates. Carrier

motion may also generate local shear forces that prevent excessive biofilm thickness, promote biofilm renewal, and potentially favor the activity of diclofenac-degrading microbial populations. In contrast, heavy and poorly moving carriers such as those from Roderstorf may experience reduced shear, leading to stagnation zones with limited microbial activity. Differences in microbial community composition may further modulate removal efficiency, as mobile carriers likely expose biofilm regions with higher fractions of active diclofenac-degrading bacteria, while poorly mixed carriers may limit microbial induction due to restricted substrate availability.

When normalized by carrier surface area (Table 3.3.3), Lenzburg carriers again displayed the highest area-specific efficiency (1.535 $\text{L} \cdot \text{g}_{\text{biomass}}^{-1} \cdot \text{m}^{-2} \cdot \text{d}^{-1}$), and Roderstorf the lowest (0.291 $\text{L} \cdot \text{g}_{\text{biomass}}^{-1} \cdot \text{m}^{-2} \cdot \text{d}^{-1}$), highlighting the combined influence of biofilm quantity, distribution, and carrier hydrodynamics on diclofenac removal.

Table 3.3.3: Measured and literature values for X_{TSS} , K_{biol} , and area-normalized K_{biol} from real WWTP carrier batch tests.

WWTP	$X_{ m TSS}$ measured	$X_{ extbf{TSS}}$ literature	$K_{ m biol}$ measured	$K_{ m biol}$ literature	$K_{ m biol}$ area-normalized
	$(g_{\rm TSS}{\cdot}L^{-1})$	$(g_{\rm TSS}{\cdot}L^{-1})$	$(L \cdot g_{TSS}^{-1} \cdot d^{-1})$	$(L \cdot g_{TSS}^{-1} \cdot d^{-1})$	$(L \cdot g_{TSS}^{-1} \cdot m^{-2} \cdot d^{-1})$
Lenzburg	4	n.a.	0.763	n.a.	1.535
Bad Ragaz	3.5	$3.2 – 4.7^{a,b}$	0.527	$1.5^{\rm c}$	0.732
Roderstorf	3.15	n.a.	0.210	n.a.	0.291

^a (Falås et al., 2012)

In conclusion, the pseudo-first-order kinetics provide a consistent description of diclofenac removal. The observed differences in degradation efficiency appear to be influenced by carrier mobility, biofilm distribution, and potential microbial activity gradients. Lenzburg carriers, with the highest mobility, exhibited the fastest diclofenac elimination, Bad Ragaz carriers were intermediate, and Roderstorf carriers the slowest. These findings support the hypothesis that hydrodynamics and carrier movement modulate substrate exposure and microbial activity. However, plant-specific factors cannot be completely excluded, and controlled experiments are necessary to quantify the relative contributions of carrier type, biofilm distribution, and microbial composition to diclofenac removal.

Diclofenac Removal with Pilot Plant Carriers

The three pilot plant lines exhibited distinct diclofenac removal dynamics, with pseudo-first-order models providing a reliable description of the kinetics ($R^2 = 0.97$, 0.95, and 0.90 for Lines 1–3, respectively) (Section 2.2.2). The high temporal resolution of sampling allowed precise evaluation of the early degradation phase, enabling a more robust analysis compared to previous studies (Jewell et al., 2016).

To reduce the number of samples, batch tests were stopped after 84 h, as prior experiments

^b (Falås et al., 2013)

^c (Jewell et al., 2016)

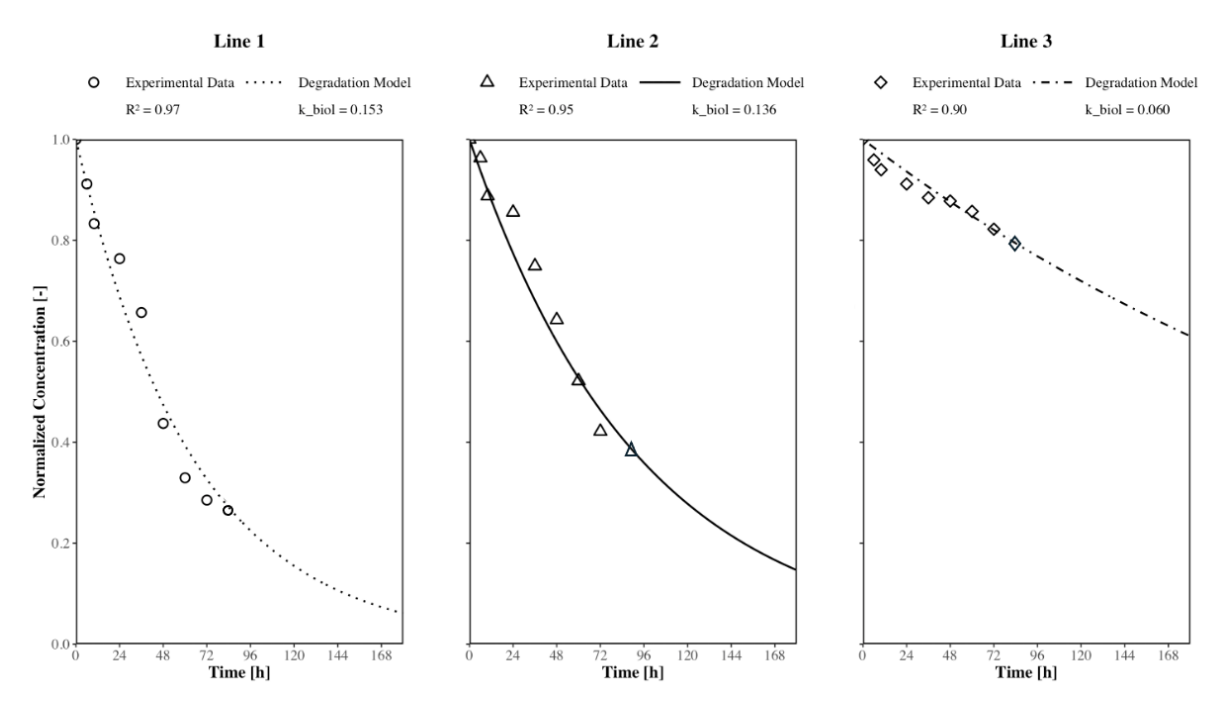


Figure 3.3.4: Diclofenac degradation kinetics for the three lines from the Pilot Plant. Normalized DCF concentrations over time were fitted with pseudo-first-order degradation models (Section 2.2.2).

indicated that most diclofenac degradation occurs within the first 24–48 h. By the end of the run, Line 1 achieved nearly 80% removal, demonstrating that the carriers were able to initiate diclofenac degradation after a relatively short period of operation, although full elimination, as observed with carriers from mature full-scale plants, was not reached (Section 3.3.2). Extending the test beyond 84 h was therefore not expected to substantially increase removal, and the shortened duration still captured the most relevant degradation dynamics. These results indicate that measurable diclofenac removal occurs within the first 48 h, consistent with early microbial activity and biofilm establishment on the carriers. A summary of the fitted parameters is provided in Table 3.3.4

Table 3.3.4: Measured values for X_{TSS} , K_{biol} , and area-normalized K_{biol} from Pilot Plant Carriers Batch Tests.

	X_{TSS} $(g_{TSS} \cdot L^{-1})$	K_{biol} (L · g_{TSS}^{-1} ·d ⁻¹)	$\begin{aligned} K_{\text{biol}} \\ \text{area-normalized} \\ (L \cdot g_{TSS}^{-1} \cdot m^{-2} \cdot d^{-1}) \end{aligned}$
Line 1	2.45	0.153	0.424
Line 2	1.88	0.136	0.378
Line 3	1.09	0.060	0.168

Compared to the real-plant carrier batch tests (Section 3.3.2), the K_{biol} values observed in the pilot plant are substantially lower. This reflects the fact that biofilms were still developing on the clean carriers, resulting in slower degradation trends (Figure 3.3.4). Uncertainties in estimating attached biomass further contribute to variability, as the absolute amount of biofilm in the pilot plant was very small, making gravimetric measurements highly sensitive to error (Section 2.5.3). The method used, following Jewell et al. (Jewell et al., 2016), provides an estimate of carrier-

attached biomass, but alternative approaches could yield more precise quantification, particularly at low biomass concentrations. For example, Line 1 and the Bad Ragaz carriers display similar $X_{\rm TSS}$ values on paper, yet the mature carriers from Bad Ragaz contained visibly denser and more developed biofilms (Section 2.5.4). This highlights the limitations of biomass quantification at low concentrations and helps explain why kinetic constants in the pilot plant remain below those measured in full-scale plants.

Nevertheless, the ability of Line 1 to reach nearly 80% elimination within 84 h under low-SRT conditions demonstrates the effectiveness of the hybrid MBBR even with early-stage biofilms. With further operation time (e.g., 2 to 3 additional months), biofilm accumulation would likely increase two to three times, potentially allowing degradation rates comparable to full-scale systems. The low SRT in these reactors likely contributed to the rapid biofilm development by maintaining higher total concentrations of COD and ammonium, which can promote microbial growth on the clean carriers (Section 3.1.2). In addition, reduced microbial competition under low-SRT conditions may further favor the establishment of active microbial communities. This effect is illustrated by Line 3, which exhibited slower biofilm accumulation and lower diclofenac removal, demonstrating how SRT and early microbial colonization dynamics influence degradation kinetics. While the exact mechanisms cannot be confirmed, the observed results suggest that both higher substrate availability and reduced competition accelerate biofilm development and the onset of diclofenac removal.

3.4 Diclofenac Removal in the Pilot Plant

Diclofenac (DCF) removal in the pilot plant was evaluated through both model simulations and continuous-flow experiments, highlighting the system's effectiveness and the key role of biofilm growth on the carriers.

3.4.1 Simulations

To complement the experimental evaluation, simulations of DCF behaviour along the treatment line were conducted using a simplified mass balance approach with first-order degradation kinetics. The parameter set for these simulations is reported in Table 2.2.1 reflecting the configuration and operating conditions of the pilot plant.

A key limitation of this approach is the definition of representative K_{biol} values for continuous-flow conditions. Batch-derived constants (0.017 L d⁻¹ gTSS⁻¹ for activated sludge and 0.135 L d⁻¹ gTSS⁻¹ for Line 1 attached biomass) were relatively low, resulting in simulated DCF profiles that consistently underestimated removal in the pilot plant. This discrepancy highlights the inherent mismatch between batch kinetics and dynamic pilot-scale conditions, where biofilm heterogeneity, substrate gradients, and continuous flow cannot be fully captured.

To evaluate this sensitivity, simulations were repeated using literature-based $K_{\rm biol}$ values from Jewell et al. (2016), which are roughly one order of magnitude higher. These simulations predicted substantially greater DCF removal, with near-complete elimination already within the MBBR stage. The comparison between batch-calibrated and literature-based scenarios (Figure 3.4.1) illustrates the strong influence of kinetic parameters on model predictions and underscores the need for site-specific calibration when modeling hybrid MBBR systems.

Overall, these simulations provide a framework to interpret removal trends, but their outputs are highly sensitive to the chosen kinetic constants. Since K_{biol} was not measured directly under continuous operation, the results should be regarded as indicative rather than predictive. Future work should focus on deriving pilot-plant-specific kinetic constants under realistic conditions to improve predictive accuracy.

3.4.2 Continuous Flow Conditions

During steady-state operation, the pilot plant achieved diclofenac (DCF) removal efficiencies of 80.2% in Line 1, 74.4% in Line 2, and 71.2% in Line 3. These differences are likely related to variations in biofilm development on the carriers. Line 1, operated at a suspended sludge SRT of 2 days, supported the most active biofilm and showed the highest removal efficiency. Lines 2 and 3 (SRTs of 3 and 5 days, respectively) exhibited lower removal, consistent with batch test results (Section 3.3.2), where biofilm activity was shown to enhance DCF degradation.

Besides biodegradation, adsorption processes may have contributed to removal, particularly in the first two activated sludge reactors of each line (Figure 2.1.1). Transient adsorption onto suspended biomass could explain part of the early decrease in DCF concentrations. Similar effects have been reported in previous studies (Chen et al., 2021; Xu et al., 2024; X. Zhang et al., 2023), although the extent depends on sludge structure and biofilm maturity.

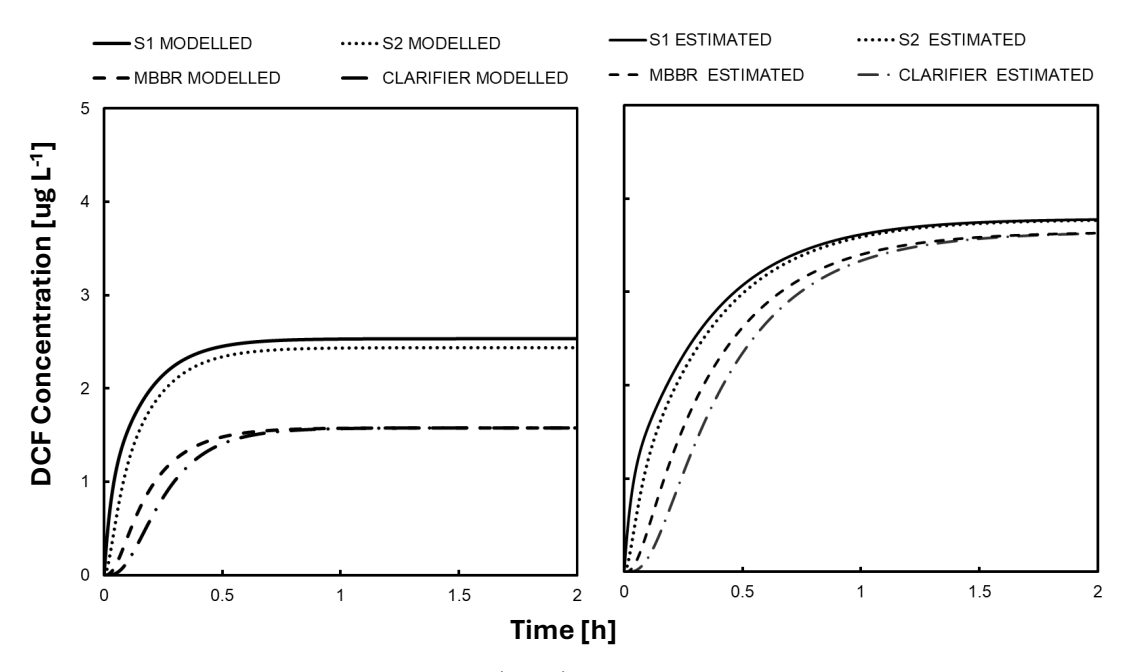


Figure 3.4.1: Temporal profiles of diclofenac (DCF) concentrations in the wastewater treatment system. The left graph shows modelled values using literature kinetic constants for reactors S1 and S2, the MBBR, and the clarifier. The right graph shows estimated values based on experimental data.

Robust performance was also observed when influent concentrations were varied. Continuous-flow experiments were carried out using the pilot plant dosing system (Section 2.1) and sampling protocol (Section 2.1.1). At baseline levels of approximately 1 μ gL⁻¹, lower than typical municipal wastewater, DCF was consistently removed to below detection. When the influent was increased to 5 μ gL⁻¹, removal efficiencies reached 80.3%, 76.5%, and 75.0% in Lines 1–3, respectively. At 10 μ gL⁻¹, simulating hospital wastewater, the system maintained high performance, achieving 80.2%, 72.4%, and 67.3% removal in Lines 1–3.

Table 3.4.1: Diclofenac removal efficiencies under continuous-flow conditions at different influent concentrations.

${\bf Influent}^a$	$\mathbf{Line} 1^b$	$\mathbf{Line} 2^c$	Line 3^d
$1 \mu g L^{-1}$	>99% ^e	>99% ^e	>99% ^e
$5 ext{ μgL}^{-1}$ $10 ext{ μgL}^{-1}$	80.25% $80.19%$	76.48% $72.41%$	75.03% $67.28%$

 $^{^{}a}$ Influent diclofenac concentration.

Overall, these results indicate that the hybrid MBBR maintained high and stable diclofenac removal across a range of influent concentrations. Biofilm activity appeared to play a central role, with shorter SRTs supporting higher substrate loading to the carriers and, consequently, higher degradation rates. Although complete elimination was only achieved at low influent levels, the system consistently achieved 80% removal under all tested conditions in line 1, demonstrating effective mitigation under representative municipal and mixed-source wastewater scenarios.

^b Line 1 (SRT = 2 d).

^c Line 2 (SRT = 3 d).

^d Line 3 (SRT = 5 d).

 $[^]e$ Removal efficiency below detection limit (<LOQ).

Chapter 4

Conclusion

This chapter summarizes the key findings of the study, highlighting insights from both batch tests and pilot plant experiments. It discusses the performance of activated sludge and biofilm carriers in nitrification and diclofenac removal, the dynamics of suspended biomass and biofilm development, and the system's behavior under continuous flow conditions. The chapter also reflects on how operational parameters, particularly sludge retention time (SRT), influence biofilm establishment and diclofenac degradation, thereby linking experimental results to the overall aim of evaluating HMBBR efficacy for pharmaceutical removal. Finally, directions for future research are outlined to support the optimization of hybrid biological treatment systems.

4.1 Key Findings

This study evaluated the potential of a pilot-scale Hybrid Moving Bed Biofilm Reactor (HMBBR) for the removal of diclofenac (DCF) from municipal wastewater, with a particular focus on understanding how operational parameters, biofilm development, and microbial activity influence DCF degradation. Experiments conducted over 112 days of operation demonstrated that short SRTs (2 d) promoted rapid colonization of initially clean Biofilm Chip M carriers, leading to DCF removal efficiencies of up to 80%. In contrast, longer SRTs (5 d) allowed suspended biomass to dominate, limiting substrate availability for biofilm activity and resulting in lower early-stage DCF removal. These findings indicate that SRT plays a central role in balancing suspended and attached-growth biomass, while also highlighting the adaptation period required when introducing clean carriers into a treatment system.

Batch experiments confirmed that DCF degradation follows pseudo-first-order kinetics, with biodegradation constants (k_{biol}) ranging from 0.153 to 0.058 L g_{TSS}^{-1} d⁻¹ depending on sludge source and carrier type. Systems utilizing carriers from full-scale plants (Bad Ragaz, Lenzburg, Roderstorf) exhibited higher area-normalized rates due to their more mature biofilms. Despite initially thin biofilms in the pilot plant, measurable DCF removal occurred within the first months, demonstrating that clean carriers can establish functional biofilm activity rapidly under favorable conditions. These results address the questions regarding how biofilm formation evolves over time and the contribution of carriers to DCF removal, highlighting that even initially clean carriers can significantly enhance micropollutant elimination.

During continuous operation over the 112-day period, the HMBBR maintained reasonable COD, nitrogen, and phosphorus removal while gradually developing biofilms on the carriers. Initially, during the start-up phase, all parameters were highly variable, reflecting the adaptation period as clean carriers were colonized and microbial communities established. Once steady state was reached, diclofenac removal depended on the influent concentration: for an influent of $1 \mu g L^{-1}$, removal exceeded 99% in all lines; at $5 \mu g L^{-1}$, removal reached 80.25% in Line 1, 76.48% in Line 2, and 75.03% in Line 3; and at $10 \mu g L^{-1}$, removal was 80.19% in Line 1, 72.41% in Line 2, and 67.28% in Line 3. These results demonstrate that short SRTs shifted the functional burden from suspended biomass to the biofilm, stabilizing both nitrification and micropollutant removal across a range of influent DCF concentrations. Batch nitrification tests confirmed the presence of active nitrifiers on the carriers, supporting the notion that nitrification activity may correlate with DCF degradation. This insight links biological performance metrics to micropollutant removal, showing how operational conditions such as SRT can be used strategically to enhance treatment efficiency (Di Biase et al., $\boxed{2019}$; Jewell et al., $\boxed{2016}$).

Overall, the experiments demonstrate that a pilot-scale HMBBR with initially clean carriers can achieve substantial diclofenac removal over a 112-day operational period, even under short HRTs and compact reactor configurations. The results highlight the critical influence of SRT and biofilm development dynamics, addressing the study's aim to evaluate HMBBR performance for pharmaceutical removal and answering research questions regarding carrier contribution, biofilm growth, biological performance, and operational feasibility under practical conditions.

4.2 Future Developments

Future research should focus on further improving HMBBR performance and understanding the mechanisms underlying micropollutant removal. Extending pilot plant operation over longer periods would allow observation of biofilm maturation and its effect on DCF degradation, providing insight into temporal changes in both biofilm thickness and microbial activity.

Investigating the relationship between nitrification activity and diclofenac degradation on carriers over time could establish a practical monitoring parameter for real WWTPs, enabling operators to predict DCF removal efficiency based on easily measurable process indicators. Additionally, characterizing microbial community composition in both biofilm and suspended sludge could identify key organisms responsible for DCF degradation and their interactions with nitrifiers and other functional groups. Studying activated sludge from the pilot plant in more detail could further clarify elimination and adoption factors that influence micropollutant removal.

Testing alternative carrier designs, including coated carriers such as activated carbon or other sorptive surfaces, and varying carrier configurations, could enhance biofilm attachment and increase micropollutant removal rates. Long-term monitoring of diclofenac transformation products (TPs) and detecting DCF concentrations in each reactor line would provide critical information on the completeness, safety, and consistency of biodegradation, as well as inform strategies to minimize persistent or toxic byproducts.

Finally, a comprehensive cost analysis should be conducted to evaluate the economic feasibility of HMBBR implementation. This analysis would assess capital and operational expenditures, maintenance requirements, energy demand, and potential savings compared to conventional tertiary treatments, providing practical guidance for utilities considering hybrid biofilm technologies. Integrating technical performance with cost considerations would enable informed decision-making for full-scale adoption and support the development of cost-effective, spaceefficient treatment solutions.

Collectively, these directions would contribute to optimizing HMBBR operation, improving micropollutant removal efficiency, and providing practical guidance for implementing hybrid biological treatment systems in real wastewater treatment facilities. They also address key research questions on steady-state achievement, operational strategies, flexible technology implementation, and economic feasibility as a cost-effective alternative to conventional tertiary treatment.

Bibliography

- Alvarino, T., Torresi, E., Vázquez-Padín, J. R., Garrido, J. M., Plósz, B. G., & Smets, B. F. (2018). Transformation of organic micropollutants in nitrifying moving bed biofilm reactors: Elucidating pathways and microbial communities. *Water Research*, 141, 183–194. https://doi.org/10.1016/j.watres.2018.05.013
- Andreottola, G., & colleagues. (2000). Nitrifier stratification in biofilm systems. Water Research, 34, 4171–4178.
- Anthonisen, A., Loehr, R., Prakasam, T., & Srinath, E. (1976). Inhibition of nitrification by ammonia and nitrous acid. *Journal (Water Pollution Control Federation)*, 48(5), 835–852.
- Baresel, C., Joss, A., Ternes, T. A., von Gunten, U., & Böhler, M. (2016). Ozonation for micropollutant removal in switzerland: State of the art and future perspectives. *Water Science and Technology*, 74(4), 900–909. https://doi.org/10.2166/wst.2016.274
- Bonvin, F., Kohler, M., Bonvin, E., Hollender, J., Schymanski, E. L., Ternes, T. A., & von Gunten, U. (2016). Ozonation for the removal of micropollutants from wastewater: Comparison of ozonation kinetics and transformation products between batch and continuous-flow experiments. Water Research, 94, 30–42. https://doi.org/10.1016/j.watres.2016.02.043
- Chen, Y., et al. (2021). Removal of diclofenac from water by adsorption using activated carbon in batch and fixed-bed column processes. *Journal of Environmental Management*, 280, 111741.
- Di Biase, A., Kowalski, M. S., Devlin, T. R., & Oleszkiewicz, J. A. (2019). Moving bed biofilm reactor technology in municipal wastewater treatment: A review. *Journal of Environmental Management*, 247, 849–866. https://doi.org/10.1016/j.jenvman.2019.06.053
- Di Trapani, D., Mannina, G., Torregrossa, M., & Viviani, G. (2008). Hybrid moving bed biofilm reactors: A pilot plant experiment. Water Science and Technology: A Journal of the International Association on Water Pollution Research, 57, 1539–45. https://doi.org/10.2166/wst.2008.219
- Directive (EU) 2024/3019 concerning urban wastewater treatment, November 27, 2024, https://eur-lex.europa.eu/eli/dir/2024/3019/oj/eng
- Eddy, M. bibinitperiod. (2003). Wastewater engineering: Treatment and reuse. McGraw-Hill.
- Eggen, R. I. L., Hollender, J., Joss, A., Schärer, M., & Stamm, C. (2014). Reducing the discharge of micropollutants in the aquatic environment: The benefits of upgrading wastewater treatment plants. *Environmental Science & Technology*, 48(13), 7688–7696. https://doi.org/10.1021/es500907n

- Falås, P., Baillon-Dhumez, A., Andersen, H., Ledin, A., & La Cour Jansen, J. (2012). Suspended biofilm carrier and activated sludge removal of acidic pharmaceuticals. *Water Research*, 46(4), 1167–1175. https://doi.org/10.1016/j.watres.2011.12.003
- Falås, P., Longrée, P., La Cour Jansen, J., Siegrist, H., Hollender, J., & Joss, A. (2013). Micropollutant removal by attached and suspended growth in a hybrid biofilm-activated sludge process. Water Research, 47(13), 4498–4506. https://doi.org/10.1016/j.watres.2013.05.
- Fux, C., et al. (1999). Operational risks in moving bed biofilm reactors. Water Science and Technology, 39(1), 1–8. https://doi.org/10.1016/S0273-1223(99)00002-3
- Gebbie, P. (2006). The chemistry of alum in water purification. *Chemistry in Australia*, 73(8), 16–19.
- Gómez-Maldonado, J., García-Galán, M. J., Rodríguez-Mozaz, S., & Barceló, D. (2021). Analytical approaches for the detection of transformation products of pharmaceuticals in water:

 A review. TrAC Trends in Analytical Chemistry, 143, 116388. https://doi.org/10.1016/j.trac.2021.116388
- Gong, M., Smith, S. T., & Stensel, H. D. (2022). Methods for measuring nitrifier maximum specific growth rate: Crucial for plant capacity rating. Water Environment Research, 94(4), e10714. https://doi.org/10.1002/wer.10714
- Gonzalez-Gil, L., Papa, M., Feretti, D., & et al. (2016). Biodegradation of pharmaceuticals in moving bed biofilm reactors (mbbrs): Contribution of attached and suspended biomass. Science of the Total Environment, 541, 751–762. https://doi.org/10.1016/j.scitotenv. 2015.09.132
- Grandjean, D., Chèvre, N., Part, F., & Meli, A. (2017). Swiss strategy for micropollutant removal in wastewater treatment plants: Status and challenges. Water Science and Technology, 75(12), 2931–2938. [https://doi.org/10.2166/wst.2017.202]
- Guibaud, G. (2010). Removal of diclofenac from wastewater: A comprehensive review of removal technologies. *Science of the Total Environment*, 408(20), 4445–4463. https://doi.org/10.1016/j.scitotenv.2010.07.015
- Gujer, W., & Henze, M. (2008). Systems analysis and design for wastewater treatment. IWA Publishing.
- Gujer, W., Henze, M., Mino, T., & van Loosdrecht, M. (1999). Activated sludge model no. 3. Water Science and Technology, 39(1), 183–193.
- Gujer, W. (Ed.). (2007). Urban water management (3., bearbeitete Auflage). Springer Berlin Heidelberg. https://doi.org/10.1007/978-3-540-34330-1
- Henze, M., van Loosdrecht, M., Ekama, G., & Brdjanovic, D. (2008). Biological wastewater treatment: Principles, modelling, and design. IWA Publishing.
- Ho, Y. S., & McKay, G. (1998). Sorption of dye from aqueous solution by peat. Chem. Eng. J., 70, 115-124. https://doi.org/10.1016/S0923-0467(98)00076-1
- Ho, Y. S., & McKay, G. (1999). Pseudo-second order model for sorption processes. *Process Biochemistry*, 34(5), 451–465. https://doi.org/10.1016/S0032-9592(98)00112-5
- Igbokwe, P., Okoro, C., & Anomneze, A. (2015). Characterization of a 5 litre continuous stirred tank reactor. *Journal of Modern Physics*, 6(4), 384–390.

- Jewell, K. S., Falås, P., Wick, A., Joss, A., & Ternes, T. A. (2016). Transformation of diclofenac in hybrid biofilm-activated sludge systems and the role of nitrifying activity. Water Research, 105, 559–570. https://doi.org/10.1016/j.watres.2016.09.026
- Jiménez, J., et al. (2015). Energy consumption in moving bed biofilm reactors. Water Research, 85, 1–10. https://doi.org/10.1016/j.watres.2015.08.039
- Joss, A., Keller, M., Alder, A. C., Götz, N., Pomi, R., Ternes, T. A., & Siegrist, H. (2006). Removal of pharmaceuticals and personal care products in biological wastewater treatment plants configured with different sludge retention times. Water Research, 40(17), 3067–3078. https://doi.org/10.1016/j.watres.2006.06.014
- Kawecki, T., & Thomann, M. (2024). Ara-ausbau zur erfüllung der motion 20.4262: Zusätzliche massnahmen zur einhaltung der numerischen anforderungen und deren kosten [Technical Report No. 240620 Bericht zusätzliche Massnahmen Motion 20.4262.pdf].
- Kim, J.-Y., Lee, T.-J., Lee, B.-U., Han, D.-H., & Kang, D.-H. (2020). Evaluation of nitrification effects on bod by batch experiments. *Applied Sciences*, 10(18), 6449. https://doi.org/10.3390/app10186449
- Levenspiel, O. (1999). Chemical reaction engineering (3rd). Wiley.
- Levstek, M., & Plazl, I. (2009). Influence of carrier type on nitrification in the moving-bed biofilm process. Water Science and Technology, 59(5), 875–882. https://doi.org/10.2166/wst. 2009.002
- Leyva-Díaz, J. C., Martín-Pascual, J., & Poyatos, J. M. (2017). Moving bed biofilm reactor to treat wastewater. *Int. J. Environ. Sci. Technol.*, 14(4), 881–910. https://doi.org/10.1007/s13762-016-1169-y
- Linge, K. L., Hollender, J., Buser, H. R., Joss, A., & Ternes, T. A. (2015). Microbial removal of the pharmaceutical compounds ibuprofen and diclofenac from wastewater. *Environmental* Science and Pollution Research, 22(8), 6094–6105. https://doi.org/10.1007/s11356-014-4061-6
- Löffler, D., Meller, M., & Ternes, T. A. (2011). Removal of micropollutants by biological wastewater treatment: Performance and limitations. Water Science and Technology, 63(3), 480–487. [https://doi.org/10.2166/wst.2011.050]
- Matos, J., et al. (2019). Economic assessment of advanced treatment technologies for micropollutant removal. *Journal of Environmental Management*, 231, 457–467.
- Odegaard, H. (2006). Innovations in wastewater treatment: The moving bed biofilm reactor. Water Science and Technology, 53(9), 17–33. https://doi.org/10.2166/wst.2006.331
- Ordinance of the DETEC on the review of purification effect of measures for the elimination of organic trace substances in wastewater treatment plants, 2016, https://micropoll.ch/wp-content/uploads/2025/05/20250502 Micropollutant-Elimination-in-Switzerland.pdf
- Pellicer-Nàcher, C., Domingo-Félez, C., Mutlu, A. G., & Smets, B. F. (2013). Critical assessment of extracellular polymeric substances isolation methods from mixed culture biomass. *Water Research*, 47(15), 5564–5574. https://doi.org/10.1016/j.watres.2013.06.013
- Porter, K., & Feig, Y. (1980). Specific staining of bacteria with fluorochrome-conjugated lectins. Applied and Environmental Microbiology, 39(1), 123–127.

- Quality criteria for surface waters. (2020). Ecotox Centre; Swiss Centre for Applied Ecotoxicology. https://www.ecotoxcentre.ch/expert-service/quality-criteria/quality-criteria-for-surface-waters
- Rittmann, B. E., & McCarty, P. L. (2001). Environmental biotechnology: Principles and applications. McGraw-Hill.
- Rusten, B., Eikebrokk, B., Ulgenes, Y., & Lygren, E. (2006). Design and operations of the kaldnes moving bed biofilm reactors. *Aquacultural Engineering*, 34(3), 322–331. https://doi.org/10.1016/j.aquaeng.2005.04.002
- Schwarzenbach, R. P., Escher, B. I., Fenner, K., Hofstetter, T. B., Johnson, C. A., von Gunten, U., & Wehrli, B. (2006). The challenge of micropollutants in aquatic systems. *Science*, 313(5790), 1072–1077. https://doi.org/10.1126/science.1127291
- Swiss Confederation & swisstopo. (2025). Maps of Switzerland Swiss Confederation map.geo.admin.ch [Accessed 28 August 2025.].
- Tatari, K., Musovic, S., Dechesne, A., Albrechtsen, H.-J., & Smets, B. (2017). Full-scale study on the impact of temperature on nitrification and microbial community structure in mbbr systems. Water Research, 111, 260–269. https://doi.org/10.1016/j.watres.2016.12.045
- Ternes, T. A., Joss, A., & Siegrist, H. (2004). Peer reviewed: Scrutinizing pharmaceuticals and personal care products in wastewater treatment. *Environmental Science & Technology*, 38(20), 392A–399A. https://doi.org/10.1021/es040639t
- Vieno, N., & Sillanpää, M. (2014). Fate of diclofenac in municipal wastewater treatment plant
 a review. *Environment International*, 69, 28–39. https://doi.org/10.1016/j.envint.
 [2014.03.021]
- Wanner, O., & Gujer, W. (2006). Biofilm reactors. IWA Publishing.
- Wittmer, H., Schröter-Schlaack, C., Dietrich, K., & Schniewind, I. (2014). Ökosystemleistungen, bewertung und inwertsetzung: Wie nützlich sind diese konzepte für die deutsche naturschutzpraxis ein fazit. *BfN-Skripten*, 359, 88–101.
- Wolff, T., & colleagues. (2021). Fluorescence microscopy for biofilm analysis in mbbr systems. Water Research, 198, 117210.
- Xu, Y., et al. (2024). Exploring diclofenac potassium adsorption on activated carbon: A multi-disciplinary approach. Science of the Total Environment, 858, 159742.
- Zając-Woźnialis, A., Kruszelnicka, I., Zembrzuska, J., Ginter-Kramarczyk, D., Ochowiak, M., & Krupińska, A. (2023). Efficiency of diclofenac removal using activated sludge in a dynamic system (sbr reactor) with variable parameters of ph, concentration, and sludge oxygenation. *Materials*, 16(4), 1422. https://doi.org/10.3390/ma16041422
- Zhang, X., et al. (2023). Diclofenac removal from wastewater using activated sludge and activated carbon. Science of the Total Environment, 847, 157582.
- Zhang, Y., Angelidaki, I., Johansen, J. E., & Christensen, K. V. (2005). Modelling of phosphorus removal from aqueous and wastewater samples using ferric iron. *Water Research*, 39(1), 94–102. https://doi.org/10.1016/j.watres.2004.09.018

Zhang, Z., Zhang, Y., Zhang, X., Zhang, X., & Zhang, X. (2022). Efficiency of various biofilm carriers and microbial interactions with substrate in moving bed-biofilm reactor for environmental wastewater treatment. *Bioresource Technology*, 357, 127314. https://doi.org/10.1016/j.biortech.2022.127314

Appendix A

Calculations

This annex provides all the calculations and the formula used over the experimental period.

A.1 Ammonium Dosage for Batch Tests

The initial ammonium concentration in batch tests was calculated based on the amount of NH₄Cl added:

$$C_{\text{NH}_4\text{-N}} = C_{\text{NH}_4\text{Cl}} \cdot \frac{M_{\text{N}}}{M_{\text{NH}_4\text{Cl}}} \tag{A.1.1}$$

where

 $C_{\text{NH}_4\text{-N}} = \text{initial ammonium-nitrogen concentration (mg L}^{-1}),$

 $C_{\text{NH}_4\text{Cl}} = \text{added ammonium chloride concentration (mg L}^{-1}),$

 $M_{\rm N} = {\rm molar \ mass \ of \ nitrogen},$

 $M_{\rm NH_4Cl} = {
m molar \ mass \ of \ ammonium \ chloride}.$

A.2 Nitrification for batch Tests

Nitrification kinetics in batch experiments were described by a linear relation:

$$C_{\text{NO}_3^-}(t) = C_0 + \frac{dC}{dt} \cdot t \tag{A.2.1}$$

where:

 $C_{\mathrm{NO_{3}^{-}}}(t)=\mathrm{nitrate}$ concentration at time t [mg N L^{-1}],

 $C_0 =$ initial nitrate concentration [mg N L⁻¹], dC

 $\frac{dC}{dt} = \text{volumetric nitrate production rate [mg N L^{-1} h^{-1}]},$ t = time [h].

The surface-related nitrification rate, R_v , normalized to the total carrier surface area, A_{tot} , was calculated as:

$$R_v = \frac{\frac{dC}{dt} \cdot V}{A_{\text{tot}}} \tag{A.2.2}$$

where:

 $R_v = \text{surface-related nitrification rate [mg N m}^{-2} \text{ h}^{-1}],$

 $\frac{d\dot{C}}{dt} = \text{volumetric nitrate production rate [mg N L^{-1} h^{-1}]}, \\ V = \text{reactor liquid volume [L]},$

 $A_{\text{tot}} = \text{total carrier surface area } [\text{m}^2].$

A.3Coagulant Dosage for the Pilot Plant

The required dose of iron chloride (FeCl₃) was calculated based on the molar ratio of iron to phosphorus (β) and the phosphorus concentration in the influent.

- Molar masses: $M_{\rm P} = 30.97~{\rm g\,mol^{-1}},\,M_{\rm Fe} = 55.84~{\rm g\,mol^{-1}},\,M_{\rm Cl} = 35.45~{\rm g\,mol^{-1}}$
- FeCl₃ molar mass: $M_{\rm FeCl_3} = 162.19 \ {\rm g \, mol^{-1}}$
- $\beta = 1.5 \text{ molFe molP}^{-1}$
- Flowrate: $Q = 36 \text{ L} \, d^{-1} \, \text{line}^{-1}$
- Influent P concentration: $C_{\rm P}=6.27~{\rm mg\,L^{-1}}=0.00627~{\rm g\,L^{-1}}$

The phosphorus molar inflow is:

$$\dot{n}_{\rm P} = \frac{C_{\rm P} \cdot Q}{M_{\rm P}} \approx 0.00729 \text{ mol d}^{-1} \, \text{line}^{-1}$$
(A.3.1)

The required iron molar dosage per line:

$$\dot{n}_{\rm Fe} = \beta \cdot \dot{n}_{\rm P} \approx 0.01094 \text{ mol d}^{-1} \, {\rm line}^{-1}$$
 (A.3.2)

The corresponding $FeCl_3$ mass dosage:

$$\dot{m}_{\text{FeCl}_3} = \dot{n}_{\text{Fe}} \cdot M_{\text{FeCl}_3} \approx 1.773 \text{ g d}^{-1} \text{ line}^{-1}$$
 (A.3.3)

With a FeCl₃ solution of 572 g L^{-1} (40% by mass, density 1430 g L^{-1}), the required volume per day per line is:

$$\dot{V}_{\text{FeCl}_3} = \frac{\dot{m}_{\text{FeCl}_3}}{C_{\text{FeCl}_3,\text{solution}}} \approx 3.10 \text{ mL d}^{-1} \text{ line}^{-1}$$
 (A.3.4)

Tracer Concentration **A.4**

A pulse of NaCl solution was used as tracer with a stock concentration of $C_{\text{stock}} = 8 \text{ g L}^{-1}$. A total mass of $m_{\text{NaCl}} = 38.4$ g was added to the reactor influent.

The volume of stock solution added is:

$$V_{\text{stock}} = \frac{m_{\text{NaCl}}}{C_{\text{stock}}} \tag{A.4.1}$$

The resulting NaCl concentration in the influent is:

$$C_{\text{influent}} = \frac{m_{\text{NaCl}}}{V_{\text{influent}}} \tag{A.4.2}$$

where V_{influent} is the total volume of influent receiving the tracer.

A.5 PH Adjustment Solutions

During batch tests and pilot plant experiments, the pH of solutions was adjusted using 2 M HCl or 2 M NaOH. The volume of acid or base required for pH adjustment can be calculated using the molar balance approach:

$$V_{\text{titrant}} = \frac{\Delta[\text{H}^+] \cdot V_{\text{solution}}}{C_{\text{titrant}}}$$
(A.5.1)

where:

 $V_{\text{titrant}} = \text{volume of HCl or NaOH to add (L)}$

 $\Delta[H^+]$ = change in hydrogen ion concentration required (mol/L)

 $V_{\text{solution}} = \text{volume of solution to adjust (L)}$

 $C_{\rm titrant} = {\rm concentration~of~titrant~(mol/L)}$

The hydrogen ion concentration is related to pH as:

$$[H^+] = 10^{-pH}$$
 (A.5.2)

Thus, the difference in [H⁺] between the initial and target pH is:

$$\Delta[H^+] = 10^{-pH_{\text{final}}} - 10^{-pH_{\text{initial}}}$$
 (A.5.3)

Example: To adjust 1 L of solution from pH 7.2 to pH 7.0 using 2 M HCl:

$$\begin{split} [\mathrm{H}^+]_{\mathrm{initial}} &= 10^{-7.2} = 6.31 \times 10^{-8} \ \mathrm{M} \\ [\mathrm{H}^+]_{\mathrm{final}} &= 10^{-7.0} = 1.00 \times 10^{-7} \ \mathrm{M} \\ \Delta [\mathrm{H}^+] &= 1.00 \times 10^{-7} - 6.31 \times 10^{-8} = 3.69 \times 10^{-8} \ \mathrm{M} \\ V_{\mathrm{HCl}} &= \frac{3.69 \times 10^{-8} \cdot 1}{2} = 1.845 \times 10^{-8} \ \mathrm{L} \approx 0.018 \ \mu \mathrm{L} \end{split}$$

In practice, small volumes are added dropwise under stirring until the desired pH is achieved.

A.6 Diclofenac Dosage in Batch Tests and Pilot Plant

The diclofenac concentrations were calculated differently for batch tests and continuous-flow operation:

Batch Tests

1. Required diclofenac mass for a target concentration in total volume:

$$m_{\text{req}} = C_{\text{target}} \cdot V_{\text{total}}$$
 (A.6.1)

2. Conversion to sodium diclofenac (if salt is weighed):

$$m_{\rm salt} = m_{\rm req} \cdot \frac{M_{\rm NaDCF}}{M_{\rm DCF}}$$
 (A.6.2)

3. Stock solution preparation:

$$C_{\text{stock}} = \frac{m_{\text{stock}}}{V_{\text{stock}}} \tag{A.6.3}$$

4. Stock volume to add (total and per reactor/line):

$$V_{\text{add,total}} = \frac{m_{\text{req}}}{C_{\text{stock}}}, \quad V_{\text{add,per}} = \frac{V_{\text{add,total}}}{n_{\text{units}}}$$
 (A.6.4)

5. Initial concentration after bolus dosing:

$$C_0 = \frac{m_{\text{bolus}}}{V_{\text{reactor}}} \tag{A.6.5}$$

Continuous-Flow Operation

1. Steady-state concentration from continuous dosing (mass flow rate \dot{m} into total flow Q):

$$C_{\rm ss} = \frac{\dot{m}}{Q} \tag{A.6.6}$$

2. Continuous dosing from a concentrated stream:

$$C_{\rm ss} = \frac{C_{\rm dose} \cdot Q_{\rm dose}}{Q_{\rm main} + Q_{\rm dose}} \tag{A.6.7}$$

3. Equivalent continuous concentration by repeated boluses (frequency f):

$$C_{\rm ss} = \frac{m_{\rm bolus} \cdot f}{Q} \tag{A.6.8}$$

Additional Calculations

1. Conversion of mass-based to molar concentrations:

$$C_{\text{mol}} = \frac{C_{\text{mass}}}{M_{\text{DCF}}} \tag{A.6.9}$$

2. Solubility check:

$$C_{\text{stock}} \le S_{\text{sol}}$$
 (A.6.10)

3. Minimum volume requirement for multiple tests:

$$V_{\text{min,total}} = n_{\text{tests}} \cdot V_{\text{min,test}}$$
 (A.6.11)

where:

 $C_{\text{target}} = \text{target concentration } [\mu g/L];$

 $V_{\text{total}} = \text{total dosed volume [mL]};$

 $m_{\text{req}} = \text{required diclofenac mass [mg]};$

 $M_{\text{DCF}} = \text{molar mass of diclofenac [g/mol]};$

 $M_{\text{NaDCF}} = \text{molar mass of sodium diclofenac [g/mol]};$

 $m_{\rm salt} = {\rm mass~of~Na\text{-}DCF~[mg]};$

 $m_{\rm stock} = {\rm mass \ for \ stock \ [mg]};$

 $V_{\text{stock}} = \text{stock volume [mL]};$

 $C_{\text{stock}} = \text{stock concentration [mg/L]};$

 $V_{\text{add.total}} = \text{total added stock volume [mL]};$

 $V_{\text{add,per}} = \text{per-unit added stock volume [mL]};$

 $V_{\text{reactor}} = \text{reactor volume [L]};$

 $m_{\text{bolus}} = \text{bolus mass [mg]};$

 $C_0 = \text{initial batch concentration } [\mu g/L];$

 $\dot{m} = \text{continuous dosing rate [mg/day]};$

 $Q, Q_{\text{main}}, Q_{\text{dose}} = \text{flow rates [L/h]};$

 $C_{\text{dose}} = \text{concentration of dosing stream [mg/L]};$

 $C_{\rm ss} = {\rm steady\text{-}state\ concentration\ [\mu g/L]};$

 $f = \text{bolus frequency } [d^{-1}];$

 $C_{\text{mass}} = \text{mass-based concentration } [\text{mg/L}];$

 $C_{\text{mol}} = \text{molar concentration } [\mu M];$

 $S_{\rm sol} = \text{solubility limit [mg/L]};$

 $n_{\text{tests}} = \text{number of tests}$ [-]:

 $V_{\text{min,test}} = \text{minimum volume per test [mL]};$

 $V_{\rm min,total} = {
m total} \ {
m minimum} \ {
m volume} \ [{
m mL}].$

A.7 Area-Normalized Diclofenac Biodegradation

The area-normalized biodegradation constant accounts for the total carrier surface area available in each reactor, enabling direct comparison of diclofenac removal across reactors with different carrier numbers or sizes:

$$K_{\text{biol,area}} = \frac{K_{\text{biol}}}{A_{\text{tot}}}$$
 (A.7.1)

 $K_{\text{biol}} = \text{measured biodegradation constant } [L \cdot g_{\text{TSS}}^{-1} \cdot \text{day}^{-1}],$

 $K_{\rm biol,area} = {\rm area-normalized~biodegradation~constant~[L \cdot g_{\rm TSS}^{-1} \cdot m^{-2} \cdot {\rm day}^{-1}]},$

 $A_{\text{tot}} = \text{total carrier surface area in the reactor } [\text{m}^2].$

The total carrier surface area was calculated as:

$$A_{\text{tot}} = V_{\text{reactor}} \cdot a_{\text{carrier}} \tag{A.7.2}$$

where:

$$\begin{split} V_{\rm reactor} &= {\rm reactor~liquid~volume~[m^3]}, \\ a_{\rm carrier} &= {\rm specific~surface~area~of~the~carrier~[m^2~m^{-3}]}. \end{split}$$

This approach expresses diclofenac removal per unit biofilm surface area, allowing comparison between reactors independent of reactor volume or the number of carriers.

Appendix B

Project Planning

This annex provides a detailed overview of the project's planning and organization, which were crucial for the successful execution of the experimental work. The planning was developed to ensure that all tasks, from the initial literature review to the final thesis defense, were completed in a timely and logical sequence. This structured approach was essential for managing the complexity of the experimental phases, coordinating the work of all collaborators, and ensuring the availability of required resources.

Project Timeline

The project timeline, meticulously developed at the outset of the research, served as a crucial tool for managing experimental phases and coordinating the work of all collaborators. This living document, accessible to all team members, allowed progress to be monitored in real-time, delays to be identified early, and adjustments to be made when needed. It also clarified dependencies between tasks—for example, the installation of the waste pump system had to be completed before plant operation could begin. Figure B.0.1 illustrates the detailed Gantt chart that was used to track progress from initial planning to the final defense of the thesis.

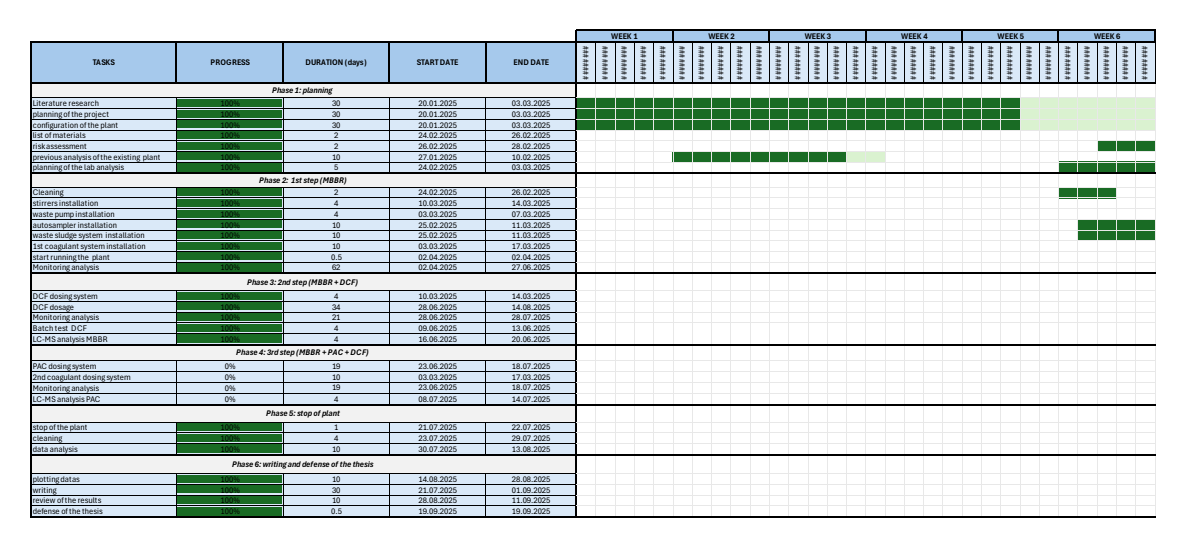


Figure B.0.1: Gantt chart of the project timeline.

Materials and Equipment

A comprehensive list of materials and equipment was created to ensure that all items required for the experimental setup were available. The inventory distinguished between items already present in the lab, those that needed to be ordered, and those still missing. Figure B.0.2 provides a summary of the key materials and their status.

Laboratory Analysis Plan

A structured plan for laboratory analyses was established for each phase of the experiment. This plan defined the parameters to be monitored, the sampling frequency, and the number of samples to be collected. Figure B.0.3 provides a detailed breakdown of the analysis across all experimental phases.

Together, the project timeline, equipment inventory, and analysis plan provided a transparent and structured framework. This approach ensured efficient collaboration, clarified task dependencies, and fostered accountability among all contributors, ultimately supporting the successful completion of the project.

palatic connectors Sameter (1.5, 2.6, 3.6) Tubes 12 To order Connectors							
Ist step (MBBR) Section Section							
Tat Stop (MBBR) Institute Comings Stock-blays, 4 conducted Comings Stoc							
Test step (MBR) A diplote Control Standard Sta							
Secretary Company of the Company of							in some
carriers process of supplied and annex of s							
Secretary Section Chips Accordance (Control Chips Accordance) What sudge tables (Secretary Chips Accordance) What sudge tabl	material	size/flow	decription	n. of picies		price	links to order
word subge tubes dans 77, length, at least general subge tubes dans 77, length, at least general subge tubes dans your public subges dans yo	carriers	circle shape, 4 cm diameter	Biofilm Chip M carriers (Anox-Kaldnes)	500		for free	www.js-umwelttechnik.ch
### district field 10m 10m			,		sludge system		
Section of the control of the contro			platic tubes				
and searching regions 1 Servicione 1 Servi							
anameter pursus 1 - 1 - 1 - 1 - 1 - 1 - 1 - 1 - 1 - 1	waste studge pumps	0.1 to 1000 mi/min	QD0860	3			wmts.com/siteassets/catalog/products/corporate/watson-marlow-pumps/cased-pumps/7206/liter
Sampling Labors 1977 Procession State Connections for this Unders 1977 Procession State Connections of the Connection State C	autosampler pumps	1-59mL/min		3			https://www.ercatech.ch/wp-content/uploads/RegioICC-dt lr.pdf
Destine for surpring 11 dissortines 6 aircardy in place 1 aircard in place 2 aircard in place 3 aircard in p	samplingtubes	???					
Section Process Companies Companie							
Stopp 1 2 2 2 2 2 2 2 2 2							
Comparison Com		11	glass bottles				
Cologitate pump D.2.Un Dump, pumpsed: MSCA 1 already in place (now used for waste studge) B.4. S.4. Prof. Duck Closed rate 1 Storage room U1 Storage roo	rioge				coagulant system (1 and 2)		1
patic connectors plant (connectors) diameter (1, 2, 2, 5, 1mm)	coagulant pump	0.2 l/h	pump, pump head: MS/CA	i			
Delicition connectors Summer (1, 2, 2, 3, m) Ease 12 10 order		5L		1	storage room U1		
Time relay Time relay	platic connectors	diameter (1.5, 2.25,3 mm)		12	to order		https://www.huberlab.ch/huberlab/en/CHF/Assortment/Medicine-%26-Healthcare/Surgery/Hose- connectors/Hose-connectors-micro/n/cat 24526
Inmater pump cassette / Loose the dameter (1 remit), pump you can title and possesses				6	to order		https://www.cariroth.com/ch/de/schlaeuche-fuer-allgemeine-anwendungen/schlauch-rotilabo-
choose the dument of millor, that you can sit is onto the later lock connectory and 1.8 mills of the later lock connectors and 1.8 mills of the later lock				6	to order		https://ch.wwr.com/store/item/EU7102538/masterflex-ismatec-ersatzkartuschen-und-adapter-
Time relay / coagulant 1 to order Infinite Time we comed childred Infinite State (Coagulant Infinite Time we comed childred Infinite Time (Coagulant Infinite Time (Coagu		mmID, that you can fit it onto the luer lock connector) and 1.8 mmID	in PTC are = 3.17 mm	6	to order??		https://ch.vwr.com/store/product/de/88705786/masterflex-ismatec-pump-tubing-3-stop-tygon-
Cable		1		1	to order		https://www.conrad.ch/de/p/finder-83-91-0-240-0000-83-91-0-240-0000-zeitrelais-
Coapelant 1	Cable	1	to control the pump	1	to order		https://www.conrad.ch/de/p/phoenix-contact-seriell-parallel-anschlusskabel-1x-d-sub-buchse- 15pol-1x-d-sub-stecker-15pol-2-00-m-weiss-673801.html
material size decription is officially system Solidade 1	coagulant	1L	FeCl3	1	storage room U1		
material size decription is officially system Solidade 1							
Material Size decription N. of picles State price What to order						_	
Comment					2nd step (MBBR + DC	'F)	
1	material	size	decription	n. of picies	state	price	links to order
1					DCF dosing system		
Street	tank	51		1	in lab	1	
Table 177	stirrer	,		1	already in place		pumps//200/interature/interature-datasneer.290/
diciofenas solution 10 ug/L Pertatalizationare selecte 0.2 L/h Pertatalizationare selecte bits mitter 1 already in lab / todervolument/pr. prod. strates_gene_bits_ene_bits_mitter pump Fordervolument-Classic Batchest 2 OF already in lab / todervolument/pr. prod. strates_gene_bits_ene_bits_mitter id=75549681256754pt_seq=uniform id=75549681256754pt_seq=uni			platic tubes				
Peristatisjumge- Heine bis mittere 1 already in lab / fordervolumen- Lissaic pump	diclofenac solution		to prepare from powder			1	
ainstones Sanchines 2 DEF			bis mittlere	1	already in lab	1	https://www.labmaterial.ch/products/peristaltikpumpe-kleine-bis-mittlere- fordervolumen?pr_prod_strat=e5_desc≺_rec_id=2e8e1d56c≺_rec_pid=6762540105913≺_ret_
airsdones airsdo	pump		Forgervolumen - Classic		Batch test 2 DCF		iu=/oo4968120625≺_seq=uniform
atready in lab 3rd step (MBBR + PAC + DCF) material size decription n of picles state picce links to order FAC desire system tank 10 L glass system, steedy bull by Jan 1 1315 floor stronge room	airstones						
Size decription n. of picies State DCF					already in lab		
material size decription n. of picles state price links to order **PAC dissing system** **Tank*** **Initial*** **Initial*** **Initial*** **Initial*** **Initial*** **Initial** **I							
material size decription n. of picles state price links to order **PAC dissing system** **Tank*** **Initial*** **Initial*** **Initial*** **Initial*** **Initial*** **Initial** **I							
tank 10 L glass system, already built 1 13th floor storage room by Jan							
tank 10 L glass system, already built 1 13th floor storage room by Jan	material	size	decription	n. of picies	state PAC dosing system	price	links to order
connectors 1 with 3 ways 1 to check		10 L	by Jan		13th floor storage room		
	connectors		1 with 3 ways		to check		
stirrer 1 already in place (motor in lab)	stirrer	-		1	already in place (motor in lab)		
Tubes noted (2 mesch) 3 to order?		in total (3 m each)					
pumps 777 3 to-order? PMC Stet SAUE 1 storage room tab U1			0115				
PAC 5kg SAUF 1 storage room lab U1	PAC	bkg	SAUF	1	storage room (ab U1		1

Figure B.0.2: Inventory of materials and equipment.

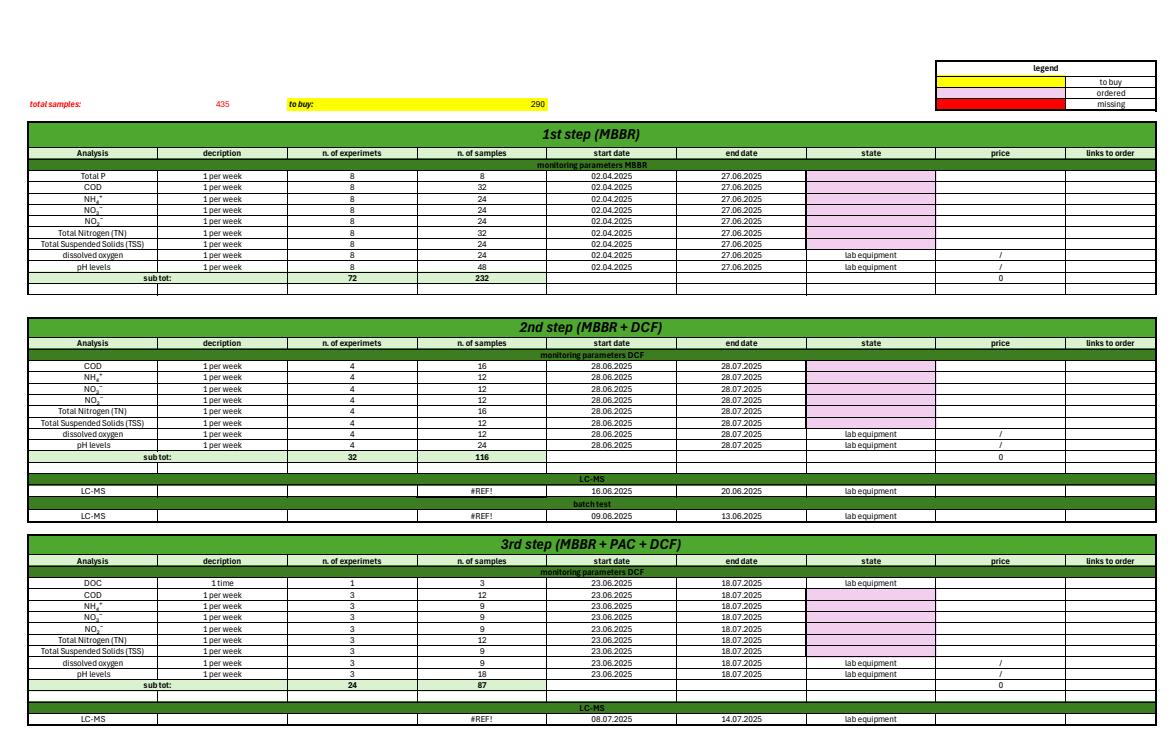


Figure B.0.3: Laboratory analysis plan.

Appendix C

Operational Challenges During Pilot Plant Operation

During the operation of the pilot plant, several issues occurred that affected system performance. The main issues are summarized below:

- Stop of the main pump before the start of operations: A delay of approximately two weeks occurred because the main pump feeding the WWTP in the PTC was stopped before the pilot plant could start.
- Main plant stoppage: Temporary shutdown of the main plant in the PTC, to which the pilot plant is connected, caused a stop of the inflow and a drop in pH inside the pilot plant reactors due to the ongoing coagulant dosage.
- Clogs in the plant and clarifiers: Blockages occurred in various sections of the pilot plant, including the clarifiers, affecting flow and sedimentation.
- Recirculation stops due to clogged pumps: Pump clogs interrupted recirculation, leading to floating sludge accumulation in the clarifiers.
- **Stirrer stoppages:** Temporary stoppage of stirrers in reactors Type 1 resulted in poor mixing in sludge-containing reactors.
- Overflow from MBBR: Formation of clogs or stuck carriers on the effluent side occasionally caused overflows from the Moving Bed Biofilm Reactors (MBBRs).

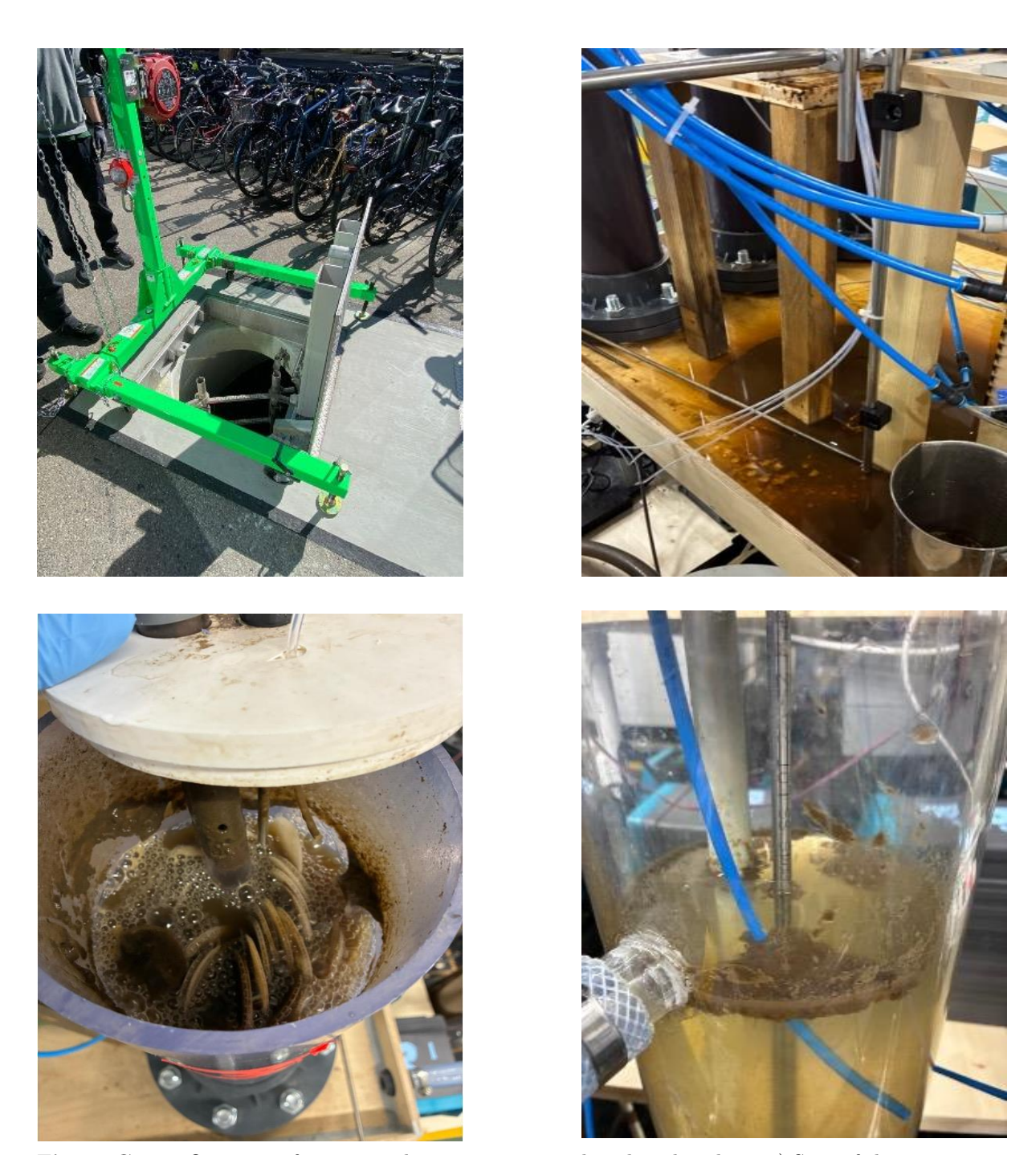


Figure C.0.1: Overview of operational issues encountered in the pilot plant: a) Stop of the main pump before start-up; b) Temporary shutdown of the main plant causing pH drop; c) Clogs and stuck carriers in the MBBR and sludge; d) Floating sludge accumulation in the clarifiers.

Appendix D

Standard Operating Procedure (SOP) for LC-MS Analysis

The following Standard Operating Procedure (SOP) describes the analytical method used for the quantification of diclofenac in water samples using liquid chromatography coupled with mass spectrometry (LC-MS). This SOP provides detailed instructions on sample preparation, instrument settings, calibration, and quality control to ensure reliable and reproducible measurements.



Standard Operating Procedure (SOP) for Diclofenac HPLC-MS Analysis



Autors:

Albin Sofjani

Matteo Rizzato

Table of Contents

Abstract	3
Chemicals and Equipment	3
Method Parameters	
Preparation of Diclofenac-Mix	5
Preparation ISTD-Diclofenac 0.2 mg/L	
Preparation of Recovery Measurement	
Samples Preparation of Analysis	5
Preparation of Calibration Solutions	6
Worklist	7
Storage	8

Abstract

Objective and Scope

This SOP describes the correct steps for the analysis of Diclofenac using an HPLC-MS in the nanogram range, including sample preparation.

Safety and Hygiene Requirements

Always work with personal protective equipment (gloves, lab coat, safety glasses). Work only in well-ventilated areas or under a fume hood. Review the safety data sheets (SDS) for all chemicals before use.

Chemicals and Equipment

- Solvents: Nanopure water, acetonitrile (LC-MS grade), formic acid. Equipment:
- Piston pipettes
- HandyStep Touch S (Brand) for volumes below 100 μL
- Glass vials from WICOM and caps from Agilent for LC
- Glass volumetric flasks and stoppers
- Pastette plastic pipettes
- Stock solutions of analyte from NeoChema (stored in refrigerator)
- HPLC-MS system (see designation in logbook)

Method Parameter

Table 1.0

<u>Parameter</u>	<u>Value</u>
LC	From Agilent 1200 binary pump G1312B, 1260 Infinity ALS
	G1329B, 1260 Infinity TCC thermostated column compartment
	G1316A,1260 Infinity HiP Degasser G4225A
Analytical column	Acquity UPLC HSS T3 1.8 μm, 3.0 x 100 mm
Column temperatur	40 °C
Injection volume	90 μL
Mobile phase	A) 95% Water (Nanopur system) and 5 % Acetonitril (LC-MS
	grade) with 0.1 % Formic acid (LC-MS grade)
	B) 95 % Acetonitril (LC-MS grade) and 5 % Water (Nanopur
Gradient flow rate	system) with 0.1 % Formic acid (LC-MS grad) 0.6 mL/min
Gradient	Time (min) % B (Eluent)
Gradient	0.0 0
	1.5 0
	10.0 98
	15 98
Stop time	As pump
Post time	8 min
Injection volume	50 μL
	MS Instrument Conditions
	MS/MS with Agilent AJS-ESI source
<u>Parameter</u>	<u>Value</u>
Source parameter	
Gas temperature	350 °C
Gas flow	10 L/min
Nebulizer	50 psi
Valve to MS	1.5 to 12.0 min
Delta EMV (+)	400
Delta EMV (-)	400
Sheath gas flow	12 L/min
Capillary voltage (Neg)	2500 V
Capillary voltage (Pos)	3500 V
Cycle time	300 ms
Total MRMs	39
Max concurrent MRMs	11
Min/Max dwell	24 ms/146 ms
All data were processed with Agi	lent MassHunter Workstation Quantitative Analysis for QQQ (Version
10.2)	

Preparation of Diclofenac-Mix

Example for preparing 0.10 mg/L and 0.01 mg/L stock mix:

- 1. Pipette 100 µL of analyte stock solution (10 mg/L, from NeoChema) into a 10 mL volumetric flask.
- 2. Fill up to 10 mL with nanopure water.
- 3. Mix thoroughly using a vortex (final concentration 0.1 mg/L).
- 4. Dilute 1 mL of this solution in 10 mL nanopure water to achieve 0.01 mg/L.
- 5. Label container with name, solution name (e.g., "Diclofenac 0.10 mg/L"), and date.
- 6. Store at 4 °C.

Preparation of ISTD-Diclofenac 0.2 mg/L

- 1. Dissolve solid Diclofenac 13C6 in ACN/H2O to a concentration of 100 mg/L.
- 2. Mix thoroughly (e.g., using a vortex).
- 3. Label container: Manufacturer, name of solution (e.g., "ISTD-Diclofenac 0.2 mg/L"), and date.
- 4. Store at 4 °C.

Preparation of Recovery Measurement

A recovery sample is used to verify accuracy and reliability of the method, ensuring the analyte is fully recovered.

- 1. A concentration from the mid-range of the calibration curve (e.g., 400 ng/L) is selected.
- 2. Prepare Kal 6 (see Table 1.1), but replace water with the sample.
- 3. Inject this solution after the sample is run in the worklist.

Sample Preparation for Analysis

- 1. Use a 15 mL Falcon tube.
- 2. Add 25 µL of ISTD mix, then 4.5 mL nanopure water, and 0.5 mL of sample.
- 3. Homogenize using a vortex and transfer into vials.
- 4. Dilution is chosen to match the calibration range; adjust as needed.

All pipettes and glassware must be pre-rinsed with the solvent (or sample, if sufficient volume is available). Small volumes (<1 mL) must be pipetted using an electronic pipette. For every new pipette tip, the first draw should be discarded to ensure correct volume dosing ("calibration by use"). Only then should the target volume be dispensed into the respective tube.

Preparation of the Calibration Solutions

To prepare the 10 calibration solutions, 15 mL plastic tubes (Falcon tubes) are used.

The exact volumes of each component are based on the predefined calibration scheme (see Table 1.1).

Instructions:

Small volumes (<1 mL) are pipetted with an electronic pipette.

For every new pipette tip, discard the first draw to ensure accurate volume measurement ("calibration by use").

Then dispense the required volume into the appropriate tube.

For the addition of nanopure water, a 10 mL piston pipette is used.

This pipette must be calibrated before use, and water is added precisely according to the protocol.

After all components have been added, close the tubes, label them clearly, and homogenize them (gently shake or vortex if needed).

Table 1.2

Calibration Level	<mark>IS uL</mark> In μL	GAK AL-Solution 0.01 mg/L µL (*0.1 mg/L)	Water	Final concentration ng/L
Kal 1 (0 ng/L)	25	-	5	0
Kal 2 (20 ng/L)	25	10	4.990	20
Kal 3 (50 ng/L)	25	25	4.975	50
Kal 4 (100 ng/L)	25	50	4.950	100
Kal 5 (200 ng/L)	25	100	4.900	200
Kal 6 (400 ng/L)	25	200	4.800	400
Kal 7 (1'000 ng/L)	25	500	4.500	1'000
Kal 8 (5'000 ng/L)	25	*250	4.750	5'000
Kal 9 (10'000 ng/L)	25	*500	4.500	10'000
Kal 10 (20'000 ng/L)	25	*1'000	4.000	20'000

All pipettes and glassware must be pre-rinsed with the solvent (or sample, if sufficient volume is available). Small volumes (<1 mL) must be pipetted using an electronic pipette. For every new pipette tip, the first draw should be discarded to ensure correct volume dosing ("calibration by use"). Only then should the target volume be dispensed into the respective tube.

Worklist

The creation of the worklist follows a fixed scheme to ensure consistent data quality and minimal carry-over.

The following sequence must be followed:

1. System flush & start control

Start the worklist with nanopure water (2 × injections) to flush the system and check the background. Then, Calibrator 6 is injected (from the middle of the calibration series, e.g., Cal 1–10). This serves as a check to ensure that concentrations and signal intensities are within the expected range.

2. Calibration series

If Calibrator 6 is within the target range, the full calibration series is injected (Cal 1 to Cal 10). This is followed by another injection of nanopure water to flush out potential residues of the high calibration standards.

3. Sample sets

The samples are labeled in sets using the same date (e.g., 20250510_A, 20250510_B, 20250510_C, and 20250510_0).

Within each set, measurement is carried out in the following order:

 $_A \rightarrow _B \rightarrow _C \rightarrow _0$, where $_0$ contains the highest concentration.

The order $A \to B \to C$ is deliberately chosen as it starts with lower concentrations to minimize the risk of carry-over.

4. Intermediate rinsing

Between each set, an injection of nanopure water is carried out to clean the system and avoid carryover.

5. Regular system check

After every 20–25 injections, Calibrator 6 is injected again to check the stability and reproducibility of the measurement.

6. Recovery

• Immediately after each sample, a recovery sample is injected to verify the analytical accuracy of the determination.

Storage

All prepared solutions with degradation risk must be stored in a refrigerator or freezer. Calibration solutions remain stable for up to 9 days. Samples are filtered with these filtertypes:

PP: Polypropylene filters

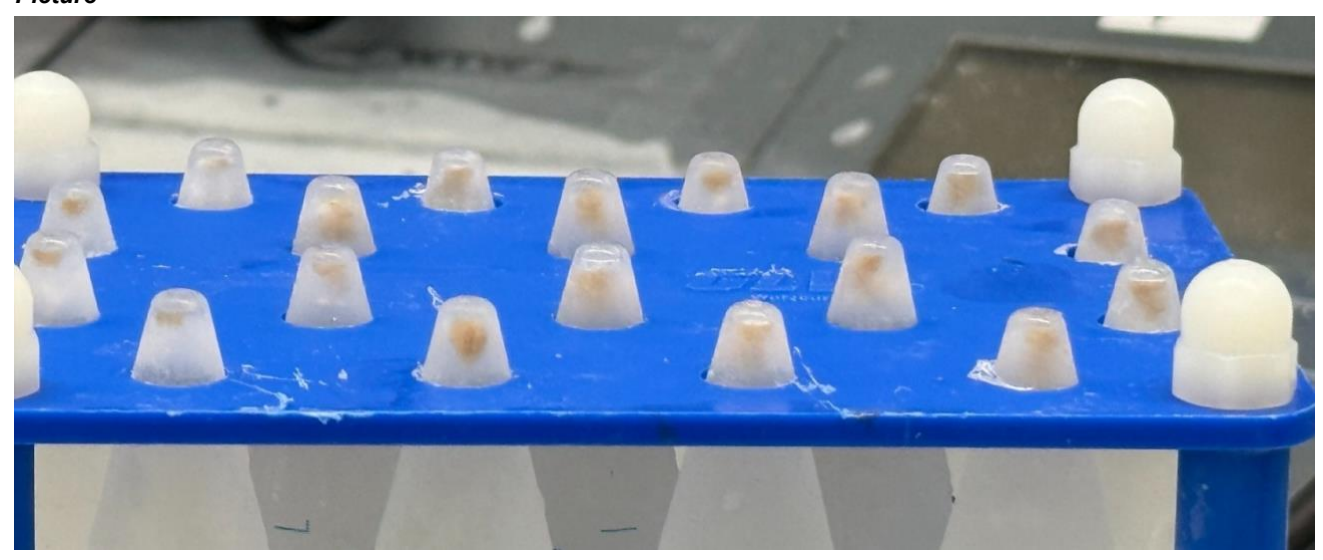
NY: Nylon filters

PVEF: Polyvinyl filters

and stored at -20°C.

Attention! After freezing, brown phase forms at tube tip — homogenize using vor-tex after thawing.

Picture



Appendix E

Risk Assessment

The following document provides a detailed risk assessment related to the handling of chemicals, operation of pilot plant equipment, and general laboratory safety considerations relevant to this study.

Risk Analysis: Hybrid Moving Bed Bioreactor (MBBR) in Conjunction with Activated Carbon Adsorption for increased Diclofenac Removal from Municipal Wastewater

Student:

Matteo Rizzato

Supervisors:

Michael Thomann (FHNW) Bartosz Kawecki (FHNW)

> Institut für Ecopreneurship Hochschule für Life Sciences der FHNW

> > Muttenz, 10.03.2025

Lab experiment: Msc Thesis

Function	Name	Date & Signature	
MSc student	Matteo Rizzato	Breat	
Supervisor	Bartosz Kawecki	1 Apr 2025 Simple electronic signature	Bartosz Kawecki
Supervisor	Michael Thomann	M. Thomas	7 Apr 2025 Sireple electronic signeture Signed on Sarbble.com
Lab responsible	Patrik Eckert	3 Apr 2025 Simple electronic algraphere Signed on Skribble.com	Patrik Eckert
Safety officer	Andreas Zogg	Andreas Zogg	7. Apr. 2025 Elefachs elektronische Signatur Signiert ouf Skribblacom

8 Apr 2005
SES Simple electronic signature
Signed on Skribble.com

Document history

Date	Version	Ву	Affected Sections / Reason	New	Added	Updated
25.11.2024	0	Valeria Gardin	Risk Assessment Hybrid MBBR_ Valeria Gardin_ 03.12.2024_ VO2.PE_signed copy.pdf (https://fhnw365- my.sharepoint.com/:w:/g/personal/matteo_rizzato_ students_fhnw_ch/ERybbWDFYYBFvAdQhvza OlkBw_lfET3wb-Pyk27dH3Z-Tg?e=au3DtE)	x		
10.03.2025	1	Matteo Rizzato	 implementation of the pilot plant with: coagulant system (reactors type 1 and type 3) stirrers (reactor type 1) DCF dosing system (reactor type 1) PAC dosing system (reactor type 3) Autosampler system (effluent/ influent) waste sludge system (reactor type 1) electrical components (start/stop system of the PP) Reason: optimize the existing pilot plant, to reach higher elimination rate of diclofenac. Additional risk due to use of chemicals and PAC 		x	x

Contents

- 1. Introduction
- 2. Process Description
 - 2.1 Equipment
 - 2.2 Overview of Installed Pumps
 - 2.3 Objective of the Study
 - 2.4 Setup Description
 - 2.5 Process Flow Diagram
- 3. Analytical Methods
- 4. Conditions for Safe Operation
- 5. Process Safety
- 6. Hazard Identification
 - 6.1 Product-Specific Hazard Identification
 - 6.2 Biological Hazards
- 7. Annex: Risk Matrix
- 8. References

1. Introduction

This risk assessment evaluates the safety and potential hazards associated with operating a Hybrid Moving Bed Bioreactor (MBBR) in conjunction with a Powdered Activated Carbon (PAC) adsorption system designed to enhance diclofenac removal from municipal wastewater. The study is conducted at the FHNW facility using a pilot plant located in the PTC.

2. Process description

2.1. Equipment

The pilot plant comprises three lines, each with four parallel stages:

- 3x Activated Sludge Reactors (4.8 L each).
- 3x Activated Sludge Reactors (3.6 L each).
- 3x Moving Bed Bioreactors (MBBRs) (9 L each).
- 3x Clarifiers (sedimentation process) (7.4 L each).

At those four stages are added other components:

- 1x coagulant dosing system with a 5 L tank.
- 1x diclofenac dosing system using a 1 L bottle.
- 1x powdered activated carbon dosing system with a 10 L tank.
- 1x autosampler system equipped with 4 bottles, each holding 1 L.

2.2. Overview of Installed Pumps

Table 1: Installed Pumps

Type of pump	Flow rate [L/h]	Remarks
9x Watson Marlow Qdos60	0.1-2000 ml/min	Waste sludge/ Sludge recirculation/ Influent
1x Ismatec BVP 6 lines	0.001 – 68 ml/min	Coagulant dosing system (FeCl₃)
1x Ismatec Reglo ICC 3 lines	0.001 – 68 ml/min	Diclofenac dosing system
1x Ismatec Reglo ICC 2 lines	0.001 – 68 ml/min	Autosampler (effluent)
1x Masterflex Ismatec Reglo	0.001 – 68 ml/min	Autosampler (influent/effluent)
ICC Digital Pump 2 lines		
2x Prominent beta 4	0.1 - 12.33 ml /min	PAC dosage system
1x Prominent Solenoid	0.1 – 34 ml/min	PAC dosage system
Metering Pump gamma/ X,		
GMXa		

2.3. Objective of the Study

This study evaluates a pilot-scale wastewater treatment plant (WWTP) utilizing Moving Bed Biofilm Reactor (MBBR) technology to enhance the removal of diclofenac, a non-steroidal anti-inflammatory drug (NSAID) with ecotoxic effects. The primary objective is to determine whether clean biofilm carriers—identical to those used at the ARA Bad Ragaz facility—can rapidly develop biofilms and achieve a certain removal efficiency, as reported by Jewell et al. (2016). The optimization strategy involves testing three different sludge retention times (SRTs) to assess their impact on diclofenac elimination. Once a specific removal rate is achieved, powdered activated carbon (PAC) will be directly dosed into the MBBR stage. The findings of this study aim to support

the integration of hybrid MBBR technology with activated carbon adsorption to meet stringent regulatory standards for diclofenac removal.

2.4. Setup Description

The pilot plant (figure 3) operates continuously (24h / 7 days per week) for at least six months (until 24/07/2025), treating wastewater sourced from the FHNW facility. Influent is drawn from the clear water tank (0020BB01) (PID2_FHNW_Muttenz_CH_Rev.4.5) through three tubes and pumped into the activated sludge (AS) reactors using peristaltic pumps (Watson Marlow Qdos60), one for each process train (Figure 7). Each train processes an influent flow of 2.9 L/h, with sludge recirculation at 1.7 L/h and waste sludge at 0.36 L/h (Line 1), 0.12 L/h (Line 2), and 0.022 L/h (Line 3). The residual effluent passes through the clarifier and discharges directly into the floor drain (Figure 3). The entire system is equipped with a containment structure in case of leaks or overflow, which is directly connected to the main sewage system. The electrical system is connected to a secure socket that automatically turns off all the pumps in case of an overflow of the plant. (figure 13, 14)

Feed pumps, waste sludge pumps and sludge recirculation pumps are located within a containment basin under the support table (Figure 8). The pumps are placed 20 cm above the floor to prevent issues in case of overflow or leakage. Waste sludge is collected in a bucket beneath the pilot plant and connected to the floor drain (Type 5) (figure 3).

The system consists of Activated Sludge reactors (Type 1-2), MBBRs (Type 3), and secondary clarifiers (Type 4) (figure 3). The reactors (Types 1-2-3) are mounted on a table with a wooden collection trough draining into the floor drain. Reactor Type 1 is continuously mixed at 3 rpm by a mechanical stirrer to ensure better mixing between the chemicals dosed and the influent wastewater. The clarifiers (Type 4) are placed in separate troughs, each equipped with a sewer drain. In the clarifiers, sludge settles at the bottom, separating from the clear water. To prevent sludge accumulation, each clarifier is equipped with a motorized scraper mounted on the lid, powered by a 9V socket. The electrical components, including motor connections, are housed in a secured box behind the table.

Aeration (figure 3) is provided by aquarium air stones delivering compressed air a maximum pressure of 2 bar. Airflow is precisely regulated using valves housed in a wooden box beneath the first reactor line (Figure 5). Process effluent is discharged directly into the sewer system (Figure 3).

The reactors (figure 3) receive different chemicals (through a dosing System) to evaluate their performance. Each reactor receives specific chemicals as follows:

- Reactor Type 1 receives coagulant and DCF.
- Reactor Type 3 receives coagulant and PAC.
- Each treatment line is dosed separately to maintain precise control over the dosing system.

The coagulant used is iron chloride (FeCl₃), with a total of 50 mL per day dosed across the two reactors (Type 1-3). Specifically, 25 mL per day is dosed into Reactor Type 1, and 25 mL per day is dosed into Reactor Type 3. The total 50 mL of coagulant is distributed across six dosing points: three dosing points in each reactor. The coagulant is mixed with a magnetic stirrer for uniformity and dosed using a six-way Ismatec BVP pump. The coagulant is stored at room temperature in a 5-liter HD-PE container, which is suitable for containing acids. (Figure 9)

PAC (Powder Activated Carbon) is pre-mixed continuously in a 10-liter glass tank with clean water using mechanical mixing (figure 3). The PAC mixture is dosed into Reactor Type 3, and the volume of PAC dosed is determined based on the DOC (Dissolved Organic Compounds) level in the MBBR system. The PAC is pumped using two Prominent Beta 4 pumps and one Prominent Solenoid

Metering Pump (Gamma/X, GMXa), ensuring accurate dosing for each treatment line in Reactor 3.(Figure 3)

Diclofenac ($C_{18}H_{16}CI_2N_4O_2$) is dosed in solution at 100 mL per day, with a target concentration of 20 µg/L per treatment line. The dosing of DCF is performed using a three-way Ismatec ICC Reglo pump. Reactor Type 1 receives the DCF, and the solution is stored in a glass bottle kept at 4°C in the refrigerator to maintain its stability. The 100 mL of DCF is evenly distributed across the three reactors to ensure each treatment line receives the target concentration. (Figure 10, 11)

Additionally, four autosamplers have been installed (figure3), controlled by two pumps: one Ismatec Reglo ICC pump with 2 lines and one Masterflex Ismatec Reglo ICC Digital Pump with 2 lines. Three points of autosampling are carried out in Reactor 4 (at the surface to capture the effluent), and one is placed in the influent (primary clarifier of the PTC). The samples are collected continuously for 24 hours, controlled by a timer socket that takes a sample every 15 minutes. Each sample is stored in a glass bottle in a refrigerator at 4°C. The autosampling is performed once a week. (Figure 10, 11)

2.5. Process Flow Diagram

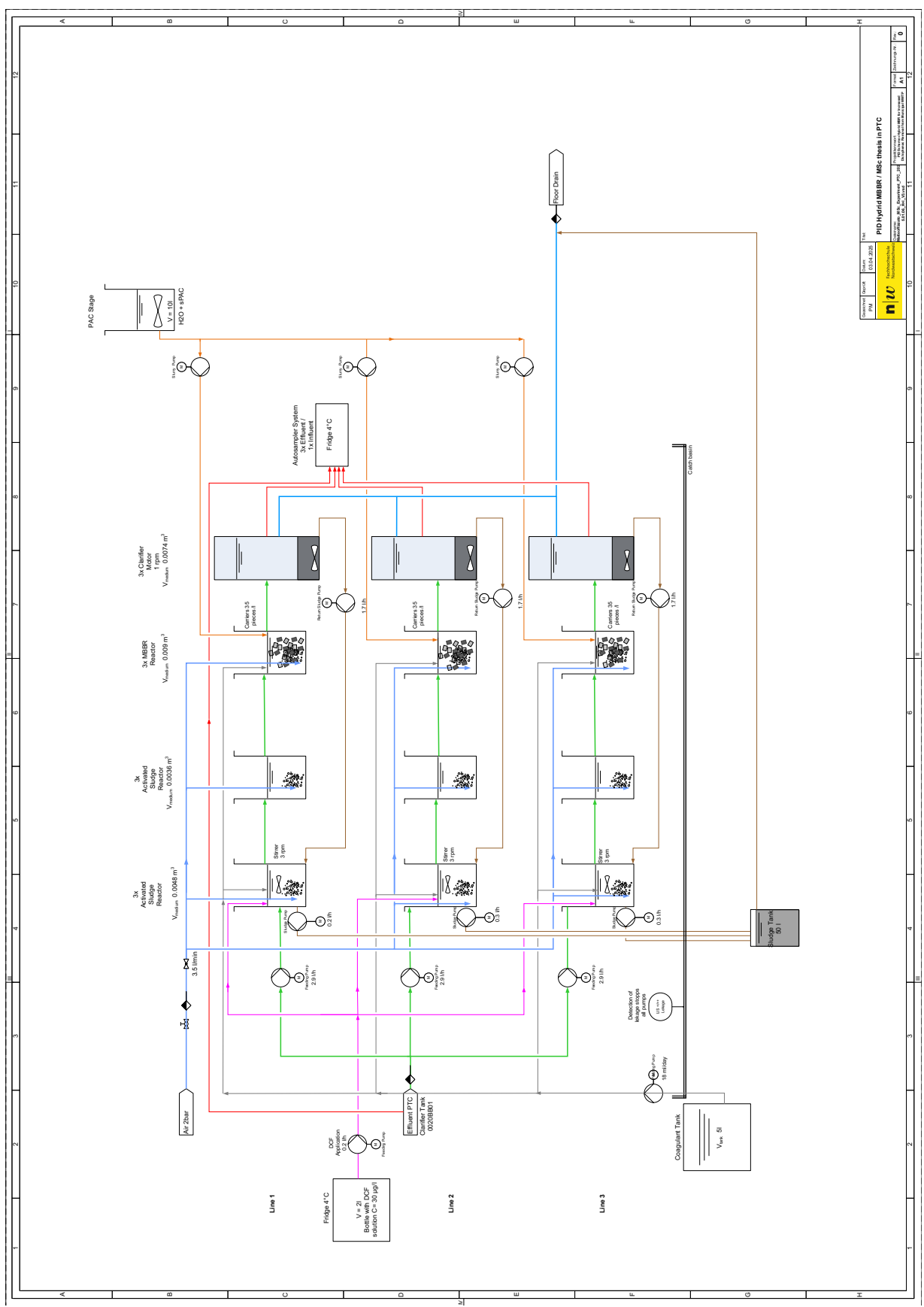


Figure 3: PID of the Pilot Plant



Figure 4: overview of the pilot plant



Figure 5: aeration system



Figure 8: safety containers and pumps support

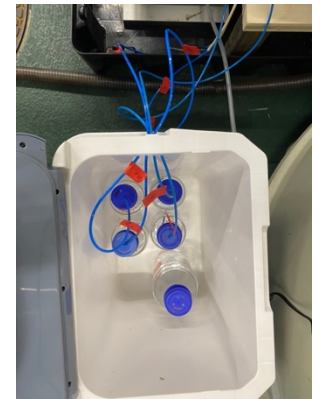


Figure 10: fridge (samples + Diclofenac)



Figure 6: stirrers on sludge reactor Type 1



Figure 7: Watson Marlow Qdos60 pumps



Figure 9: coagulant system (Ismatec BVP)



Figure 11: autosampler dosing system + diclofenac dosing system (Ismatec ICC)

3. Analytical Methods

 Table 2: analytical methods

Measurement Type	Description	Methods Used
Overall DCF Removal	Evaluate the pilot plant's overall	Solid-phase extraction (SPE), LC-MS
	effectiveness in removing diclofenac by sampling water at the inlet and outlet. (Figure 12, point 1, 5)	for quantification of DCF concentrations. HLS internal Method (DCF_positiv_20250121.m, Aquity UPLC HSS T3, 3.0x100mm, 1.8um, 186004680)
Batch Incubation Experiments	Determine specific DCF removal rates by biofilm carriers in isolated vessels. Compare the degradation capacities with the pilot plant results.	DCF spiked in vessels, periodic water sampling, SPE, LC-MS for concentration analysis. HLS internal Method (DCF_positiv_20250121.m, Aquity UPLC HSS T3, 3.0x100mm, 1.8um, 186004680)
TSS Monitoring	Regularly assess Total Suspended Solids (TSS) in activated sludge reactor (Point 3, figure 12) to maintain system balance.	Standard protocol based on guidelines (Eugene W. Rice, n.d.)
Total P	Regularly assess total Phosphorous in the influent (Point 1, Figure 12) with Harch Lange test.	ISO 6878_2004, DIN EN 6878 / D11 (https://cdn.hach.com/7FYZVWYB/at /pb792mgm8xggbftctjj5k9rr/DOC142 5220283.pdf)
Total and dissolved COD	Regularly assess total Phosphorous in the influent and in the effluent (Point 1-5, Figure12) with Harch Lange test.	ISO 6060-1989, DIN 38409-H41-H44 (https://cdn.hach.com/7FYZVWYB/at /pb792mgm8xggbftctjj5k9rr/DOC142 5220283.pdf)
Total N	Regularly assess total Phosphorous in the influent and in the effluent (Point 1-5, Figure 12) with Harch Lange test.	EN ISO 11905-1, ISO23697-1 (https://cdn.hach.com/7FYZVWYB/at /pb792mgm8xggbftctjj5k9rr/DOC142 5220283.pdf)
PH	Regularly assess PH the activated sludge reactor and in the MBBR (Point 2-4, Figure 12).	Standard protocol based on guidelines (Eugene W. Rice, n.d.)
Dissolved Oxigen	Regularly assess Dissolved Oxygen in the activated sludge reactor and in the MBBR (Point 2- 4, Figure 12).	Standard protocol based on guidelines (Eugene W. Rice, n.d.)
DOC	Regularly assess Dissolved Organic Compounds in the MBBR (Point 4, Figure 12).	Standard protocol based on guidelines (Eugene W. Rice, n.d.)
NH ₄ ⁺	Regularly assess Ammonia levels in the Effluent (Point 5, Figure 12) with Merk Millpore test.	The method is analogous to EPA 350.1, APHA 4500-NH3 F, ISO 7150-1, and DIN 38406-5. (https://www.merckmillipore.com/CH/en/product/Ammonium-Test, MDA_CHEM-114752?ReferrerURL=https%3A%2F%2Fduckduckgo.com%2F)
NO ₃ -	Regularly assess Nitrate Levels in the Effluent (Point 5, Figure12) with Merk Millpore test.	The method is analogous to DIN 38405-9.(https://www.merckmillipore.com/C H/en/product/Nitrate-Test,MDA_CHEM-109713)
NO ₂ -	Regularly assess Nitrite Levels in the Effluent (Point 5, Figure 12) with Merk Millpore test.	The method is analogous to EPA 354.1, APHA 4500-NO2- B, and DIN EN 26 777.(https://www.merckmillipore.com/CH/en/product/Nitrite-Test,MDA_CHEM-114776)

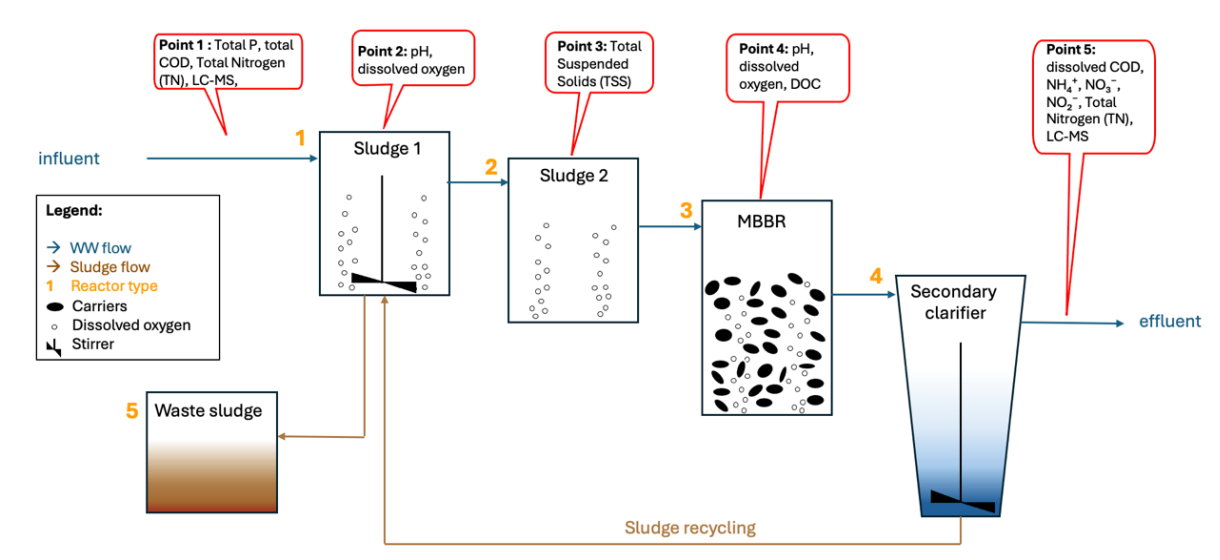


Figure 12: Sampling points in the pilot plant

4. Conditions for Safe Operation

4.1. Training and preparations of the persons performing the experiments

- 1. All operators must read this risk analysis and check whether the measures listed in the 'chapter 1 LVO Matteo Rizzato_Kommentare PE' have been implemented. The operator is responsible for the implementation of all organizational measures listed in the chapter "To Do List".
- 2. The operator must practice the following emergency stop procedure with an already instructed employee before operating the equipment:
 - a. switch off the pilot plant (Figure 14), including aeration (Figure 5)
 - b. inform colleagues and supervisors
 - **c.** attach sign
 - d. write name and telephone number, use "on going experiment" template
 - e. leave the laboratory and wait for instructions from supervisor





Figure 13: Safety socket



Figure 14: on/off switches of WWTP (yellow circle)

5.Process Safety

Table 3: Process Safety

Hazard number	Scenario (Brief description of hazard incl. cause and effect)	R	lisk	Measures	Risk	
		P	C		P	C
1.1	Too high pressure in the water pipes connected to the reactors: Pressure exceeds limit of components leading to bursting followed by leakage of feed solution, e.g., in case of clogging	В	IV	 All pipes have open ends. Pumps use peristaltic technology, generating low pressure. Pipes are regularly inspected (daily), cleaned (biweekly), and replaced (monthly) to prevent leaks/clogging. Flow rates range from a minimum of 3.5 L/min (to prevent bacterial death) to a maximum of 10 L/min. All pipes and connected reactors are placed in a containment tray, which is directly connected to the sewage system to drain water in case of leakage due to high pressure. Mandatory safety equipment includes gloves, an FFP2 mask, safety glasses, and a lab coat when operating the plant. 	В	V
1.2	Pump malfunction: Leakage or wrong pump operation resulting in spillage	В	IV	 The pilot plant is positioned in a containment tray capable of holding potential overflows. If the outflow pump fails, the reactor may overflow. Since the lid is not sealed, the system can spill its contents. In the event of an overflow, the containment tray drains into the sewage system. Daily inspections of the pilot plant and biweekly pipe cleaning help prevent pump malfunctions. The PVC pipes used are suitable for wastewater and can withstand pressures up to 10 bar. Waste sludge is removed from Reactor Type 1 at the following rates: 0.36 L/h (Line 1), 0.12 L/h (Line 2), and 0.022 L/h (Line 3). It is stored in a 15 L bucket connected to the main drain, preventing excess sludge accumulation inside the system (Figure 3). A water level detection sensor is connected to the power socket shared with the inlet pumps. If water leakage is detected, the sensor cuts power to the pumps, stopping inflow (1.5 L/h per line) and preventing additional overflows (Figure 3). Mandatory safety equipment includes gloves, an FFP2 mask, safety glasses, and a lab coat when operating the plant 	В	V

Hazard number	Scenario (Brief description of	R	isk		Measures	R	isk
number	hazard incl. cause and effect)						
		P	C			P	C
1.3	Release of bacteria and other germs from the wastewater: Exposure to pathogens when handling wastewater (IPC)	В	IV	•	tolerable. If the smell becomes intolerable after the first overnight operation, close the reactor and connect the off-gas lines to the main ventilation system. Hepatitis B vaccination is required in case of potential contact with biological hazardous material. Mandatory safety equipment includes gloves, an FFP2 mask, safety glasses, and a lab coat when operating the plant.	В	V
1.4	Leaking fluids (acidic FeCl3 14%): Release of acidic FeCl3, which is acute toxic (oral), etching and can cause eye damage and skin irritation	В	IV	•	(biweekly), and replaced (monthly) to prevent leaks. Only chemical-resistant. Tygon pipes, suitable for FeCl ₃ ,and peristaltic pump suitable are used. The pilot plant is situated in a collecting trough with a floor drain available.	В	٧
1.5	Leacking fluids (diclofenac solution): can cause skin irritation, respiratory issues if inhaled, and potential toxicity through prolonged exposure.	В	IV		(daily), cleaned (biweekly), and replaced (monthly). Safety equipment (glasses, lab coat, gloves, masks) is mandatory when operating the plant. The pilot plant is situated in a collecting trough with a floor drain available.	В	٧
1.6	Leacking fluids (Slurry PAC + water solution): potential respiratory irritation if inhaled, skin and eye irritation, and sedimentation issues affecting dosing consistency.	В	IV	•	(daily), cleaned (biweekly), and replaced (monthly). Safety equipment (glasses, lab coat, gloves, masks) is mandatory when operating the plant. The pilot plant is situated in a collecting trough with a floor drain available. Only low concentrations (approximately 0.1 to 1 mg/L) are present in the pilot plant. Solutions must be prepared exclusively in a fume hood.		
1.7	Electricity: Electric shock for collaborators, fire	В	IV	•	All plug strips are elevated from the floor in case of leakeges.		

6. Hazard Identification

6.1 Product-Specific Hazard Identification

Iron Chloride (FeCl₃):

- Corrosive (H290, H314) Causes severe skin burns and eye damage.
- Irritant (H335) May cause respiratory irritation.
- Environmental Hazard (H400) Very toxic to aquatic life.

Diclofenac (DCF):

- **Health Hazard (H302, H361, H373)** Harmful if swallowed, suspected of damaging fertility or the unborn child, and may cause organ damage through prolonged exposure.
- Environmental Hazard (H400, H410) Very toxic to aquatic life with long-lasting effects.

Powdered Activated Carbon (PAC):

- Irritant (H335, H319, H315) May cause respiratory irritation, eye irritation, and skin irritation.
- **Dust Hazard** Fine particles can be an inhalation risk, leading to respiratory discomfort.
- **Explosion Risk** When airborne in high concentrations, PAC dust can be combustible.

6.2 Biological Hazards

The biological hazards of wastewater include the presence of **pathogenic microorganisms** such as:

- **Bacteria** E. coli, Salmonella, Vibrio cholerae, and other harmful bacteria can cause gastrointestinal infections, respiratory diseases, and skin infections.
- **Viruses** Enteric viruses like norovirus and hepatitis A can spread through contaminated water, causing illnesses like gastroenteritis and liver diseases.
- Parasites Protozoa (e.g., Giardia, Entamoeba histolytica) and helminths (e.g., tapeworms) can be transmitted through contaminated water, leading to gastrointestinal issues and other infections.
- **Fungi** Certain fungi may thrive in wastewater, posing a risk of respiratory issues and skin infections, particularly in immunocompromised individuals.

7. Annex: Risk Matrix

LVO Hybrid MBBR; 02.12.2024; VO2.PE

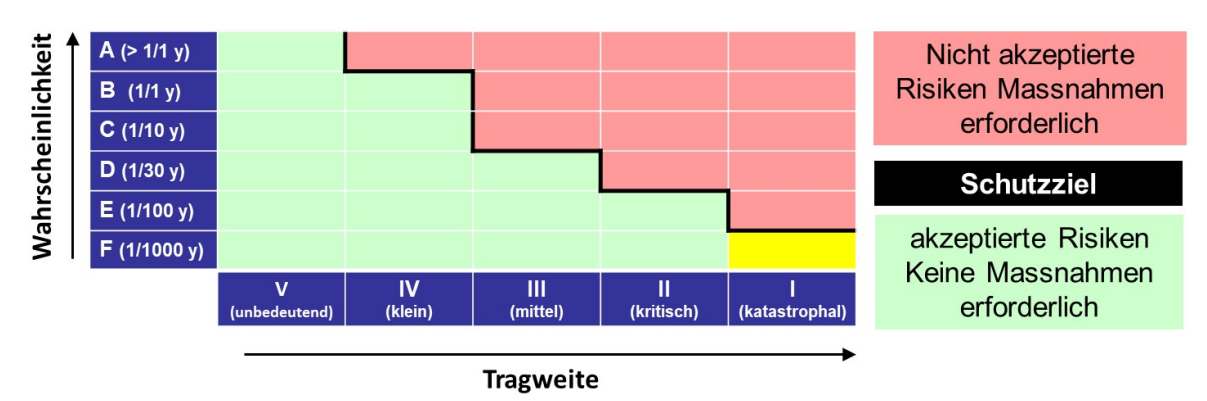
Assessment of consequences at FHNW-HLS level:

	V (unbedeutend)	IV (klein)	III (mittel)	ll (kritisch)	l (katastrophal)
Personenschaden	Keine Auswirkung	Keine Auswirkung	Leichtverletzte (erste Hilfe, Arbeitsausfall <= 3 Tage	Schwerverletzte (medizinische Behandlung; Arbeitsausfall > 3 Tage)	Tote / bleibende Behinderung oder Gesundheitsschäden, Evakuierung des Gebäudes und der Umgebung
Umweltschaden	Marginale Stofffreisetzung	Sofffreisetzung am Standort der Anlage (regulärer Entsorgungsweg)	Stofffreisetzung im Gebäude bzw. Gebäudeabschnitt	Stofffreisetzung ausserhalb des Gebäudes: Reversible Kurzzeitschäden	Stofffreisetzung ausserhalb des Gebäudes: Irreversible Langzeitschäden (z.B. Fischsterben)
Finanzieller Sachschaden	< 500 CHF	< 5000 CHF	< 25 kCHF	< 500 kCHF	> 1 Mio. CHF
Betriebsunterbruch	< 1 Tag	< 1 Woche	< 1 Monat	< 3 Monate	> 3 Monate
Image-Schaden	Kenntnis innerhalb der Arbeitsgruppe	Kenntnis innerhalb der Arbeitsgruppe	Kenntnis innerhalb der HLS	Regionale Berichterstattung	Überregionale Berichterstattung

Assessment of probability at FHNW-HLS level:

Α	В	С	D	E	F
> 1 pro Jahr	1 pro Jahr	1 pro 10 Jahre	1 pro 30 Jahre	1 pro 100 Jahre	1 pro 1000 Jahre

Protection goal at FHNW-HLS:



8. References

Eugene W. Rice, R. B. B. (n.d.). Standard Methods for the Examination of Water and Wastewater (23rd ed.).

Metcalf & Eddy. (2014). Wastewater engineering: Treatment and resource recovery (fifth edition). PID2_FHNW_Muttenz_CH_Rev.4.5

Swiss Federal Council. (1983). Environmental Protection Act (Umweltschutzgesetz, USG). (https://www.admin.ch.)

Swiss Federal Council. (1986). Chemical Risk Reduction Ordinance (ChemRRV). (https://www.admin.ch.)

Swiss Federal Council. (2014). Laboratories Ordinance. (https://www.admin.ch.)

HLS method: DCF_positiv_20250121.m C:\MassHunter\Methods\DCF_positiv_20250121.m Aquity UPLC HSS T3, 3.0x100mm, 1.8um, 186004680

Merk Millpore (https://www.merckmillipore.com/CH/en) Harch Lange (https://www.hach.com)

LVO Matteo Rizzato_Kommentare PE (https://fhnw365 my.sharepoint.com/:w:/r/personal/matteo_rizzato_students_fhnw_ch/Documents/LVO%20Matteo %20Rizzato_Kommentare%20PE.docx?d=w96a96ad6e81e45e0aced50fa830c5541&csf=1&web =1&e=LfoYz4)

Appendix F

Laboratory and Operational Logbook (LVO)

The LVO document summarizes the local regulatory requirements and safety protocols that must be followed when operating the pilot plant and conducting experiments with hazardous substances.

Lab procedure for experiments in Laboratory / Miniplant area

Hybrid Moving Bed Bioreactor (MBBR) in Conjunction with Activated Carbon Adsorption for increased Diclofenac Removal from Municipal Wastewater

Matteo Rizzato
Supervisors:
Michael Thomann (FHNW)
Bartosz Kawecki (FHNW)

Student:

Institut für Ecopreneurship
Hochschule für Life Sciences der FHNW

Muttenz, 10.03.2025

Lab experiment: Msc Thesis

Function	Name	Date & Signature	
MSc student	Matteo Rizzato	Breakt	
Supervisor	Bartosz Kawecki	1 Apr 2025 Sirgie electronic signature	Bartosz Kawecki
Supervisor	Michael Thomann	M. Thomas	2 Apr 2025 Simple electronic algorithm Signed on Skribble.com
Lab responsible	Patrik Eckert	3 Apr 2025 Simple electronic algreture Signed on Skribblo.com	Patrik Eckert

1. Apr. 2025
Einfoche elektronische Signatu
Signiert auf Skribble.com

Document history

Date	Version	Ву	Affected Sections / Reason	New	Added	Updated
25.11.2024	0	Valeria Gardin	Risk Assessment Hybrid MBBR_ Valeria Gardin_ 03.12.2024_ VO2.PE_signed copy.pdf (https://fhnw365- my.sharepoint.com/:w:/g/personal/matteo_rizzato _students_fhnw_ch/ERybbWDFYYBFvAdQhvza OlkBw_lfET3wb-Pyk27dH3Z-Tg?e=au3DtE)	x		
10.03.2025	1	Matteo Rizzato	 coagulant system (reactors type 1 and type 3) stirrers (reactor type 1) DCF dosing system (reactor type 1) PAC dosing system (reactor type 3) Autosampler system (effluent/ influent) waste sludge system (reactor type 1) electrical components (start/stop system of the PP) Reason: optimize the existing pilot plant, in order to reach higher elimination rate of diclofenac. Additional risk due to use of chemicals and PAC 		x	x

Contents

- 1. Error! Not a valid bookmark self-reference.
 - 1.1 Procedures
 - **1.2** Operational parameter
- 2. Analytical Methods
- 3. Process safety
- 4. Waste management
- 5. References

1. Process flow

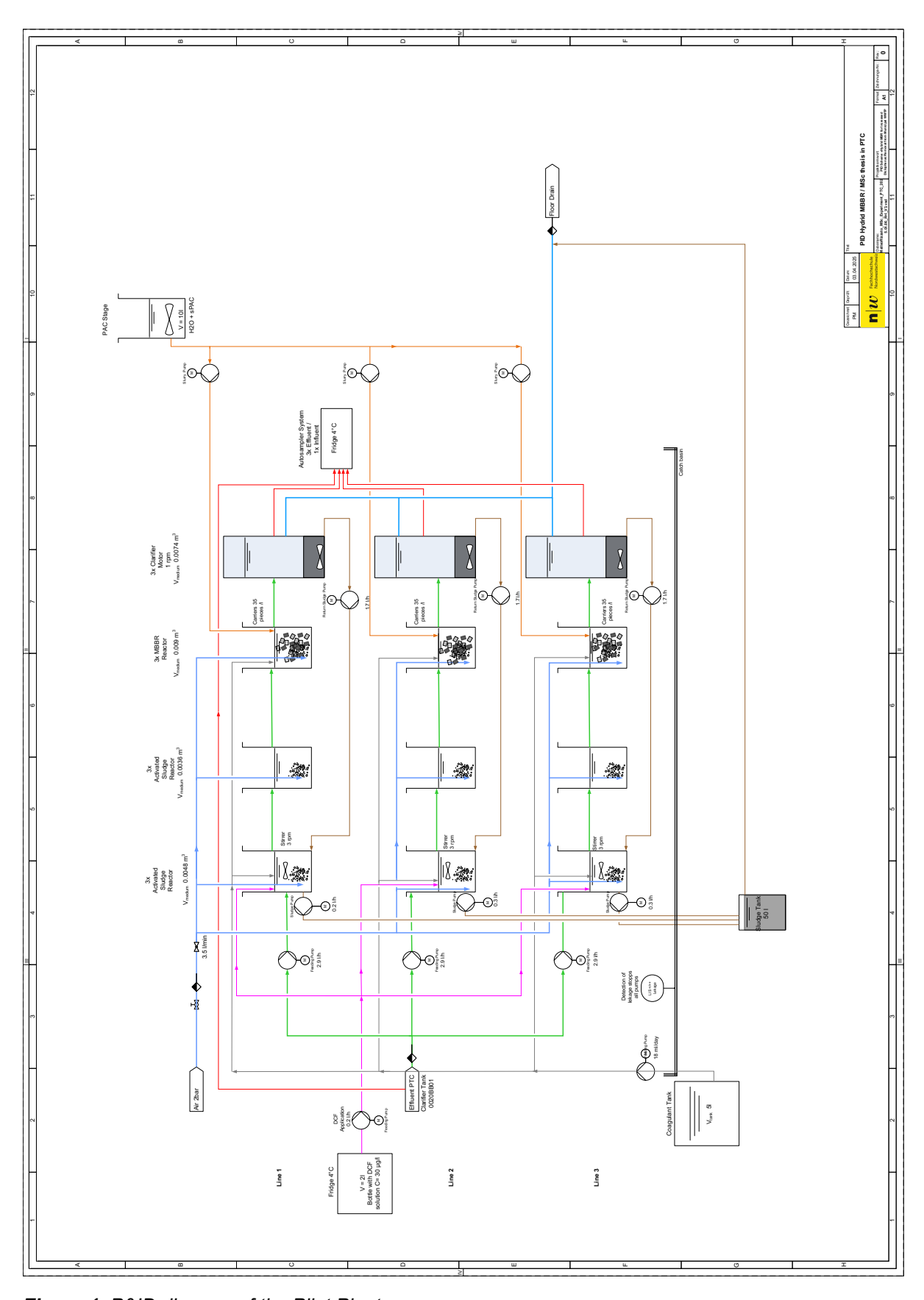


Figure 1: P&ID diagram of the Pilot Plant

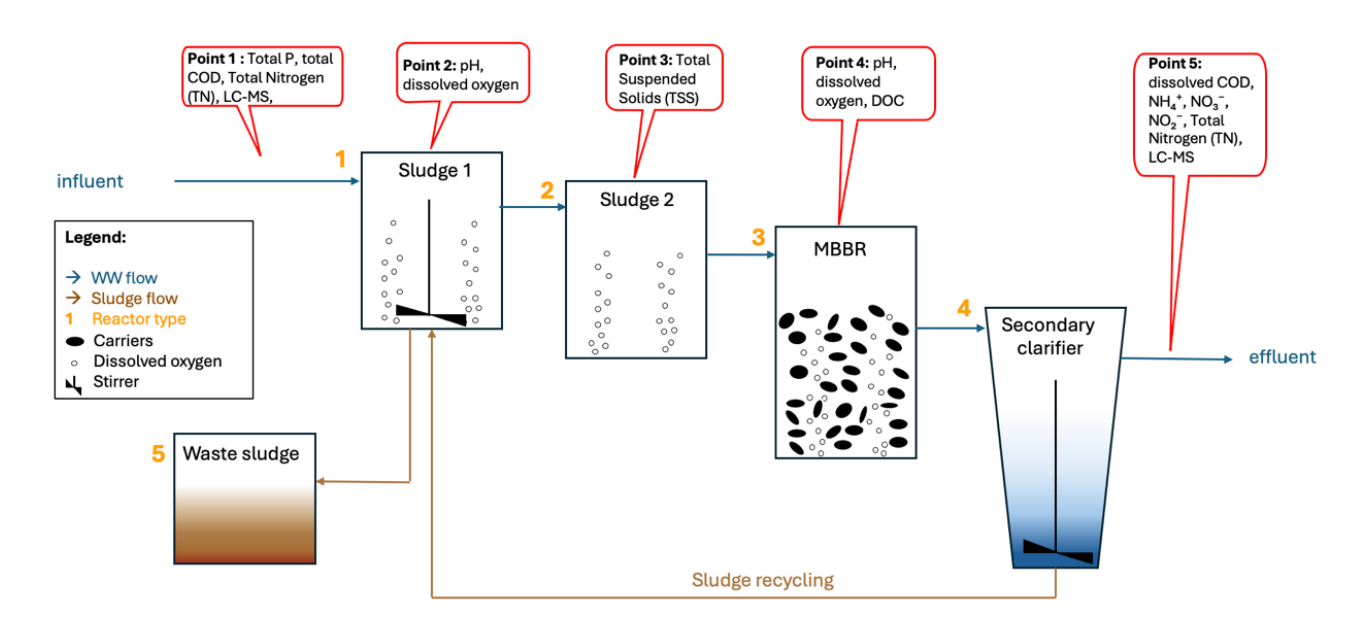


Figure 2: Stage diagram of the pilot plant with related sampling points and reactor types

1.1. Procedures

Table 1: list of procedures

Part	Description
а	Preparation of unit
b	Filling of reservoirs
с	Main process
d	Emptying and cleaning of unit and reservoirs
е	Disposal of wastes

Part	Step	Description	Visum/Date	
	Preparation of unit Use checklist (chapter 5, RA_MatteoRizzato)			
а	1	 Conduct a visual inspection of the pilot plant (Figure 1) to check all components and understand their functions. Repair or rebuild any damaged reactors (Figure 2) and replace any clogged or particle-filled tubing (Chapter 5, RA). Test the electrical control system, focusing on the Raspberry Pi and the main control socket (Chapter 4, RA). Verify air flow rates (Chapter 2, Subsection 2.4, RA) and set the pressure to 2 bar (Figure 5, RA). Test and adjust pump speeds to ensure proper flow throughout the pilot plant (Chapter 2, Subsection 2.2, and Table 1, RA) Check the stirrers at 3 rpm to confirm proper operation (figure 6, RA). Use always safety equipment: safety glasses, lab coat, gloves, Face shield while working on the Pilotplant (PP). 		
а	2	 Water Tightness Test: Connect the system to a clean water reservoir and operate it for approximately 24 hours at 4.5 L/h. Ensure there are no leaks. Pump Inspection: Check all pumps and verify the volume pumped per hour (Figures 7, 9, and 11, RA). 		
а	3	 Connect water tanks, including feed and waste containers. Install and secure piping to ensure proper flow. Set up catch basins to contain any potential spills. 		
	Filling of reservoirs			
b	1	• Fill reservoirs with activated sludge, sourced from the second membrane reactor of the PTC. ((EC/D – 2.6481) PID2_FHNW_Muttenz_CH_Rev.4.5).		
b	2	 Monitor sludge levels and ensure there is no foaming. Inspect reactor types 1, 2, and 4. Verify inflow pumps, air distribution, and stirrers to ensure steady operation of the pilot plant according chapter 1.2. 		

Main process			
С	1	Pump wastewater from the clear water tank (0020BB01) of the PTC. Set parameters in consultation with the supervisor. (e.g., Total Inflow: 4.5 L/h, SRT:2 days, airflow: 2 bar, stirrers velocity: 3rpm, coagulant dosage, DCF dosage, PAC dosage based on your needs).	
С	2	 Perform in-process control (IPC): Manually check pressure and flow rates during sampling. Monitor micropollutant concentrations in the effluent using the autosampler system or take the samples directly from the reactors, Use labeled, clean syringes and glass bottles (muffled) for analysis and testing the samples every week (figure 2 and chapter 2). Pipes must be regularly inspected (daily), cleaned (biweekly), and replaced (monthly) to prevent leaks. Maintain MBBR (Type 3) pressure flow rate at 3.5 L/min Collect samples from the influent (clear water tank) and effluent (second clarifier- Type 4). Prevent any splashing when opening the reactors for sampling. Use appropriate techniques and protective measures to minimize spills. Use labeled, clean syringes and glass bottles for analysis. Muffeld glass bottles have to be used for Micropollutant analytics. 	
С	3	 If excess sludge or foaming occurs: open safety valves on the first line of activated sludge reactors to release surplus sludge (Reactors Type 1, 2). Remove waste sludge from the reactors (Type 1) at a rate of 0.2 L/h (4.4 L/d) and store it in a 15L bucket, which is also connected to the main sewer system for handling excess sludge (Type 5). Use safety equipment: safety glasses, lab coat, gloves, Face shield while running the PP. In case of foaming adapt the aeration. Note deviation and inform supervisor 	
С	4	Stop the experiment (chapter 4, RA), when necessary,), in case of water leakage detection the installed sensor will stop automatically the plant (figure 13 RA) or the feed solution is depleted.	
		Emptying and cleaning of unit and reservoirs	
d	1	 Stop the pumping of feed solution (figure 1). Stop the airflow (figure 5, RA). Use safety equipment: safety glasses, lab coat, gloves, Face shield while stopping the PP. 	
d	2	 Disconnect the feed tank and flush the system by pumping clean water to empty the lines. Clean the pipes and the reactors. After cleaning, turn off the PP (figure 14, RA). 	

Disposal of waste Use check-list (chapter 4: Waste management)			
е	1	Dispose of liquid waste according to its type: Discharge into the sewer if allowed under wastewater regulations/ Health, Safety & Environment (HSE) (chapter 4). Use separate containers for regulated waste disposal (chapter 4, following Health, Safety & Environment (HSE) actual version) Dispose of laboratory waste in sealed containers (HDPE / LENSO) after consulting the supervisor or lab head.	

1.2. Operational parameters

Table 3: Process Parameters

Parameter	Value
HRT ^a (figure 2)	8 h
Influent Flow (figure 1)	2.9 L/h
Reactors Volume per line (type 1 + type 2 + type 3) (figure 2)	17.4 L
Tot. Reactors Volume (type 1 + type 2 + type 3 + type 4) (figure 2)	74.5L
COD _{influent} Concentration ^b (figure 2)	400 mgCOD
BOD _{influent} to COD _{influent} ratio (figure 2)	0.5
BOD _{influent} Concentration ^c (figure 2)	200 mgBOD
BOD _{influent} loading (figure 2)	0.600 kgBOD/m³/d
RAS ^d Ratio (figure 2)	0.6
RAS ^d Flow (figure 2)	1.7 L/h

^aHRT: Hydraulic Retention Time

^bCOD: Chemical Oxygen Demand

°BOD: Biochemical/Biological Oxygen Demand

^dRAS: Return Activated Sludge

(Metcalf & Eddy, 2014)

2. Analytical Methods

Table 4: Analytical Methods

Measurement Type	Description	Methods Used
Overall DCF Removal	Evaluate the pilot plant's overall effectiveness in removing diclofenac by sampling water at the inlet and outlet. (Figure 1)	Solid-phase extraction (SPE), LC-MS for quantification of DCF concentrations. HLS internal Method (DCF_positiv_20250121.m, Aquity UPLC HSS T3, 3.0x100mm, 1.8um, 186004680)
Batch Incubation Experiments	Determine specific DCF removal rates by biofilm carriers in isolated vessels. Compare the degradation capacities with the pilot plant results.	DCF spiked in vessels, periodic water sampling, SPE, LC-MS for concentration analysis. HLS internal Method (DCF_positiv_20250121.m, Aquity UPLC HSS T3, 3.0x100mm, 1.8um, 186004680)
TSS Monitoring	Regularly assess Total Suspended Solids (TSS) in activated sludge reactor (Point 3, figure 2) to maintain system balance.	Standard protocol based on guidelines (Eugene W. Rice, n.d.)
Total P	Regularly assess total Phosphorous in the influent (Point 1, Figure 2) with Harch Lange test.	ISO 6878_2004, DIN EN 6878 / D11 (https://cdn.hach.com/7FYZVWYB /at/pb792mgm8xggbftctjj5k9rr/DO C1425220283.pdf)
Total and dissolved COD	Regularly assess total Phosphorous in the influent and in the effluent (Point 1-5, Figure 2) with Harch Lange test.	ISO 6060-1989, DIN 38409-H41- H44 (https://cdn.hach.com/7FYZVWYB /at/pb792mgm8xggbftctjj5k9rr/DO C1425220283.pdf)
Total N	Regularly assess total Phosphorous in the influent and in the effluent (Point 1-5, Figure 2) with Harch Lange test.	EN ISO 11905-1, ISO23697-1 (https://cdn.hach.com/7FYZVWYB /at/pb792mgm8xggbftctjj5k9rr/DO C1425220283.pdf)
РН	Regularly assess PH the activated sludge reactor and in the MBBR (Point 2-4, Figure 2).	Standard protocol based on guidelines (Eugene W. Rice, n.d.)
Dissolved Oxigen	Regularly assess Dissolved Oxygen in the activated sludge reactor and in the MBBR (Point 2- 4, Figure 2).	Standard protocol based on guidelines (Eugene W. Rice, n.d.)
DOC	Regularly assess Dissolved Organic Compounds in the MBBR (Point 4, Figure 2).	Standard protocol based on guidelines (Eugene W. Rice, n.d.)

Measurement Type	Description	Methods Used
NH₄ ⁺	Regularly assess Ammonia levels in the Effluent (Point 5, Figure 2) with Merk Millpore test.	The method is analogous to EPA 350.1, APHA 4500-NH3 F, ISO 7150-1, and DIN 38406-5. (https://www.merckmillipore.com/C H/en/product/Ammonium-Test,MDA_CHEM-114752?ReferrerURL=https%3A% 2F%2Fduckduckgo.com%2F)
NO ₃ -	Regularly assess Nitrate Levels in the Effluent (Point 5, Figure 2) with Merk Millpore test.	The method is analogous to DIN 38405-9. (https://www.merckmillipore.com/C H/en/product/Nitrate-Test,MDA_CHEM-109713)
NO ₂ -	Regularly assess Nitrite Levels in the Effluent (Point 5, Figure 2) with Merk Millpore test.	The method is analogous to EPA 354.1, APHA 4500-NO2- B, and DIN EN 26 777. (https://www.merckmillipore.com/C H/en/product/Nitrite-Test,MDA_CHEM-114776)

3. Process safety

Table 5: Process safety

Parameter	Мах	Risk	Measures to check	Visum / Date
Pressure	2 bar	Pressure exceeds limit of components leading to bursting followed by leakage of feed solution, e.g. in case of a clogging	 All pipes have open ends. Pumps use peristaltic technology, generating low pressure. Pipes are regularly inspected (daily), cleaned (biweekly), and replaced (monthly) to prevent leaks or pressure problems. Flow rates range from a minimum of 3.5 L/min (to prevent bacterial death) to a maximum of 10 L/min. All pipes and connected reactors are placed in a containment tray, which is directly connected to the sewage system to drain water in case of leakage due to high pressure. Mandatory safety equipment includes gloves, an FFP2 mask, safety glasses, and a lab coat when operating the plant. 	
Volume flow	209 L/d	Leakage or Wrong pump operated	 The pilot plant is positioned in a containment tray capable of holding potential overflows. If the outflow pump fails, the reactor may overflow. Since the lid is not sealed, the system can spill its contents. In the event of an overflow, the containment tray drains into the sewage system. Daily inspections of the pilot plant and biweekly pipe cleaning help prevent pump malfunctions. The PVC pipes used are suitable for wastewater and can withstand pressures up to 10 bar. Waste sludge is removed from Reactor Type 1 at the following rates: 0.36 L/h (Line 1), 0.12 L/h (Line 2), 	

	/day	prolonged exposure potential respiratory irritation if	 Solutions must be prepared exclusively in a fume hood. Pipes and containers are regularly inspected (daily), cleaned (biweekly), and replaced (monthly). Safety equipment (glasses, lab coat, gloves, masks) is mandatory when operating the plant. 	
IIIIII	ug/day	can cause skin irritation, respiratory issues if inhaled, and potential toxicity through	 Pipes and containers are regularly inspected (daily), cleaned (biweekly), and replaced (monthly). Safety equipment (glasses, lab coat, gloves, masks) is mandatory when operating the plant. The pilot plant is situated in a collecting trough with a floor drain available. Only low concentrations (approximately 0.1 to 1 mg/L) are present in the pilot plant. 	
	mi/day	Release of acidic FeCl3, which is acute toxic (oral), etching and can cause eye damage and skin irritation	 connected to the main drain, preventing excess sludge accumulation inside the system (Figure 3). A water level detection sensor is connected to the power socket shared with the inlet pumps. If water leakage is detected, the sensor cuts power to the pumps, stopping inflow (1.5 L/h per line) and preventing additional overflows (Figure 3). Mandatory safety equipment includes gloves, an FFP2 mask, safety glasses, and a lab coat when operating the plant Pipes are regularly inspected (daily), cleaned (biweekly), and replaced (monthly) to prevent leaks. Only chemical-resistant Tygon pipes, suitable for FeCl₃, are used. The pilot plant is situated in a collecting trough with a floor drain available. Only low concentrations of chemicals are present in the plant. Solutions must be prepared exclusively in a fume hood. Safety equipment is mandatory in the laboratory (glasses, lab coat, gloves, masks) when operating on the plant. 	

			 connect the off-gas lines to the main ventilation system. Hepatitis B vaccination is required in case of potential contact. Mandatory safety equipment includes gloves, an FFP2 mask, safety glasses, and a lab coat when operating the plant. In case of bacterial or germ release, all water is directly discharged into the floor drain. 	
Electricity	10A	Electric shock for collaborators, fire	 No open electric contacts in the pilot plant. All plug strips are elevated from the floor in case of leakeges. In case of short circuit: Sockets are protected with FI. 	

4. Waste management

Wastes must be disposed according to current regulations (Health, Safety & Environment (HSE)).

5. References

Eugene W. Rice, R. B. B. (n.d.). Standard Methods for the Examination of Water and Wastewater (23rd ed.).

Metcalf & Eddy. (2014). Wastewater engineering: Treatment and resource recovery (fifth edition).

PID2_FHNW_Muttenz_CH_Rev.4.5

Swiss Federal Council. (1983). Environmental Protection Act (Umweltschutzgesetz, USG). (https://www.admin.ch.)

Swiss Federal Council. (1986). Chemical Risk Reduction Ordinance (ChemRRV). (https://www.admin.ch.)

Swiss Federal Council. (2014). Laboratories Ordinance. (https://www.admin.ch.)

HLS method: DCF_positiv_20250121.m C:\MassHunter\Methods\DCF_positiv_20250121.m Aquity UPLC HSS T3, 3.0x100mm, 1.8um, 186004680

Merk Millpore (https://www.merckmillipore.com/CH/en)

Harch Lange (https://www.hach.com)

RA: risk assessment - Msc thesis Matteo Rizzato_Kom PEdocx (https://fhnw365-my.sharepoint.com/:w:/r/personal/matteo_rizzato_students_fhnw_ch/Documents/risk%20assessment%20%20Msc%20thesis%20Matteo%20Rizzato_Kom%20PEdocx.docx?d=wf465df508c43413e8eefc49507fcc33f&csf=1&web=1&e=mlfPWs)